

This is to certify that the

thesis entitled

SODIUM 5'-GUANOSINE MONOPHOSPHATE AGGREGATION: STOICHIOMETRY, MODES OF SPECIFIC SODIUM ION COMPLEXATION, AND BINDING TO ETHIDIUM

presented by

CHRISTOPHER L. MARSHALL

has been accepted towards fulfillment of the requirements for

Ph.D. degree in Chemistry

Major professo

Date 00 14, 1980

O-7639



OVERDUE FINES: 25¢ per day per item

RETURNING LIBRARY MATERIALS: Place in book return to remove charge from circulation records

SODIUM 5'-GUANOSINE MONOPHOSPHATE AGGREGATION: STOICHIOMETRY, MODES OF SPECIFIC SODIUM ION COMPLEXATION, AND BINDING TO ETHIDIUM

Ву

Christopher L. Marshall

A DISSERTATION

Submitted to
Michigan State University
in partial fulfillment of the requirements
for the degree of

DOCTOR OF PHILOSOPHY

Department of Chemistry

ABSTRACT

SODIUM 5'-GUANOSINE MONOPHOSPHATE AGGREGATION: STOICHIOMETRY, MODES OF SPECIFIC SODIUM ION COMPLEXATION, AND BINDING TO ETHIDIUM

By

Christopher L. Marshall

The dianion of guanosine-5'-monophosphate (5'-GMP⁼) forms regular structures in aqueous solution that are slow to exchange on the ¹H NMR time scale. The self-assembly process is dramatically dependent on the nature of the alkali metal counterion, which is believed to direct structure formation through a size-selective coordination mechanism. Previous work has not been successful in determining the exact metal ion and nucleotide stoichiometries of the aggregated units, in part because the metal to nucleotide ratio in the pure salts is fixed at 2:1.

The discovery that the tetramethyl ammonium ion (TMA⁺) acts as neither a structure directing nor inhibiting ion has facilitated the study of 5'-GMP⁼ self-assembly at varying ratios of metal to nucleotide. The objective of this thesis was to determine the stoichiometry of the Na⁺/5'-GMP⁼ aggregates. The present study examined the concentration dependence of Na⁺/5'-GMP⁼ self-aggregates at

constant free Na⁺ ion concentration using ¹H NMR. Several equilibrium models were investigated as possible fits to the experimental data using a computer curve-fitting routine. The models selected were: (1) monomer in equilibrium with aggregated n-mer, (2) monomer in equilibrium with stacked tetramers, (3) monomer in equilibrium with tetramer and tetramer in equilibrium with stacked tetramer, and (4) tetramer in equilibrium with stacked tetramer. On the basis of closeness of fit to the experimental data and symmetry arguments, an equilibrium involving monomer 5'-GMP⁼ aggregating to form two stacked tetramer units is preferred.

A second series of experiments examined the Na⁺ dependence of the aggregation process. An equation which assumes an octameric nucleotide stoichiometry was fit to the experimental data. Closest fit of this equation to the experimental data was for the Na⁺ stoichiometry with a value $x = 4.1(\pm 0.1)$ which results in an over-all stoichiometry for the self-structures of Na₄(5'-GMP)¹²⁻₈.

Model building studies in conjunction with symmetry considerations show that the stacking of two tetramers can explain the three line H(8) ¹H NMR spectrum characteristic of the ordered form. The directional character of the hydrogen bonding of the tetramer allows two distinctly different stacking patterns upon octamer formation.

Stacking of two tetramers with the same hydrogen bond directionality creates an octamer with C_4 symmetry which is believed responsible for the appearance of the outer $\mathrm{H}(8)$ structure lines. The inner $\mathrm{H}(8)$ structure line is believed to arise from one of the diastereomers with D_4 symmetry created from the stacking of two tetrameric plates with opposite hydrogen bond directionality.

Specific Na⁺ coordination and interplatelet hydrogen bonding are also believed to be important factors in the stabilization of the structures. The four Na⁺ ions are most likely coordinated in two different positions. Two Na⁺ ions are placed in the cavity defined by the four O(6) donors of the tetramer unit. A water molecule may also be coordinated to the Na⁺ at this position. The remaining two Na⁺ ions are believed to be chelated by phosphates on the top and bottom tetramer units. Between four (OH(2')-OP or OH(3')-OP) and eight (NH(2)-OP) interplate hydrogen bonds are possible.

The intercalation drug ethidium bromide (EtdBr) was found to interact very strongly with structured forms of both Na₂5'-GMP and K₂5'-GMP. Evidence provided by ¹H NMR chemical shift changes indicates that the octamers of Na₂5'-GMP form a strong 2:1 (EtdBr:octamer) structure and a slightly weaker 1:1 complex. The stacking of two and one drug molecules respectively to the exterior aromatic faces

is postulated. The stoichiometry of the structure:drug complex supports the over-all stoichiometry of the aggregated nucleotides.

The drug appears to break up the proposed hexadecameric structures of K_25 '-GMP and to stack in a 2:1 and 1:1 fashion with the octameric fragments. As in the sodium case, the 2:1 complex is stronger than the 1:1 complex.

To Susan

ACKNOWLEDGEMENTS

It is hard in a page to properly thank all of those who have been of help over the past few years of graduate school. Those listed below were especially helpful throughout; for those not mentioned, a general thank you is extended.

First, I would like to thank the M.S.U. Chemistry
Department for both financial support and the use of the
facilities. Financial support received through the
National Institutes of Health is gratefully acknowledged.
I would also like to thank Dr. Carl H. Brubaker for acting
as my second reader. Assistance received from Dr. James
L. Dye and Mr. John Leckey with the KINFIT program, Ms.
Kathryn Nyland with figures, and Dr. Thomas Atkinson with
computer graphics is noted. Dr. Alexander I. Popov is
thanked for both serving on my guidance committee and for
his assistance with the ethidium structure fitting.

The help and love of my parents, Kay and Lyle Marshall, and my wife's parents, Betty and Bob Bolda, has always been a source of guidance for me. Their encouragement of my graduate career helped make the going a little easier.

Dr. Thomas J. Pinnavaia has been a continual source of guidance, wisdom, and encouragement, for which I am

sincerely thankful. He is an able and patient teacher to whom I shall always be indebted. I would also like to thank Mr. Rasik Raythatha, Mr. Richard Barr, Mr. Steven Christiano, and Dr. Elene Bouhoutsos-Brown whose collaboration and fruitful discussions (often late into the night) were extremely helpful. Dr. Bouhoutsos-Brown is also thanked for providing the spectra used in the sodium ion stoichiometry study.

It is not a simple task to thank my wife for all the help that she has always been to me. Susan not only did the typing and graphics that made this thesis possible; her love and encouragement always provided the driving force to go on when I felt down. Her faith, patience, and love for me cannot be compared to any other source of help.

TABLE OF CONTENTS

	Page
INTRODUCTION	
General	1
Guanine Nucleotides	6
Intercalation Drugs	13
Statement of Research Aims	17
EXPERIMENTAL	
A. Materials, Techniques, and Preparation	19
B. Instrumentation	20
Nuclear Magnetic Resonance Spectroscopy	20
Ultraviolet/Visible Absorption Spectroscopy	21
Computation	21
C. Theoretical	22
GMP Stoichiometry	22
Na ⁺ Stoichiometry	28
Drug Binding Constants	30
RESULTS	
A. Stoichiometry of 5'-GMP Aggregation: Na ⁺ Salt	35
B. Model Building Investigation of Octameric Structures	45
C. Metal Ton Stoichiometry: Na Salt	62

D.	Interaction of Intercalation Compounds with Structured Na ₂ 5'-GMP and K ₂ 5'-GMP	67
E.	Interaction of Ethidium Bromide with Structured and Unstructured Forms of Na ₂ 5'-GMP	69
F.	Interaction of Ethidium Bromide with Structured and Unstructured Forms of K ₂ 5'-GMP	82
DISCUS	SION	
A.	Present Study	91
В.	Other Proposed Structures	100
c.	Stability of the Base Overlap	111
D.	Drug Intercalation	114
CONCLU	SION	121
BIBLIO	GRAPHY	124

LIST OF TABLES

		Page
Table 1.	Fraction of Structure of 5'-GMP with Changing Total Nucleotide Concentration	38
Table 2.	Results of Stoichiometry Fitting of 5'-GMP= in NaCl	41
Table 3.	Results of Curve Fitting Equation Equation (la) to the Data in Table 1 with n Held to a Constant Value	46
Table 4.	Number of Isomers and H(8) Lines Expected for Three Exchange Regions	58
Table 5.	Torsional Angles and Notations for 5'-Nucleotides	59
Table 6.	Results of the Model Building Study of the Octameric Forms of 5'-GMP	61
Table 7.	Fraction of Structure of 5'-GMP with Changing 5'-GMP / Na+	64

LIST OF FIGURES

		Page
Figure 1.	 a) Structure and numbering sequence for pyrimidine and purine. b) Structure and numbering sequence for β-D-ribose (RNA) and 2-deoxy-β-D-ribose (DNA). 	2
Figure 2.	Ring current effects in aromatic systems.	5
Figure 3.	 a) Structure of 5'-guanylic acid (5'-GMP). b) Structure of 3'-guanylic acid (3'-GMP). 	8
Figure 4.	Proposed structure of the hydrogen bonded tetramer in the Na ₂ (5'-GMP) solution and NaH(3'-GMP) gel (R = ribose-phosphate group).33,37	9
Figure 5.	Schematic diagram of the proposed size selective coordination sites in the structuring of a neutral aqueous solution of 5'-GMP. a) Coordination into the center of the tetrameric plate by Na+ (r = 0.99Å). b) Coordination between the plates by K+ and Rb+ (r = 1.51Å and 1.60Å respectively). Note that Li+ (r = 0.59Å for 4-coordination, 0.74Å for 6-coordination) would be too small to substitute for Na+ and that Cs+ (r = 1.78Å) is too large to replace K+ or Rb+. (Ionic radii from ref. 51)	12

Figure 6. Schematic of the mode of inter-14 calation binding to nucleic acids. a) Normal double stranded polynucleotide with ribose-phosphate backbone (striped) and hydrogen bonded base pairs. b) Same sketch as in a) with three drug molecules (shaded region) intercalated. Figure 7. Chemical structures of a) actino-15 mycin D; b) ethidium bromide; c) daunorubicin (also called daunomycin) and andrianmycin; and d) platinum (II) 2,2',2"-terpyridyl chloride. 36 Figure 8. Effect on the H(8) NMR of adding (TMA)₂5'-GMP into 0.85M NaCl in D₂O at 15^OC. Structure lines are labelled A, B, and D, and the monomer line is labelled C. Figure 9. Plots of the computed curves for 44 equation (la) when a) n and K' are both varied, and b) K' is varied and n is held constant at either 8, 12, or 16. Experimental conditions are the same as in Table 1. Error bars represent the experimental points. Errors in n and K' are reported at the 95% confidence level. Figure 10. Schematic diagram of a) normal stacking 48 and b) the two enantiomeric reversed stacking modes of the octamers of 5'-GMP. 51 Figure 11. Overlap pattern of the guanine bases for the two enantiomeric forms in the normal stacking mode of two tetramers. The dark tetramer is the top layer and the light tetramer is the bottom layer. a) $C_4(CW, CW, +30^\circ)$; b) $C_4(CW, CW, -30^\circ)$. a) is the enantiomer of b) in the absence of the chiral ribose-phosphate group.

Figure	12.	Overlap pattern of the guanine bases for two of the diastereomeric forms in the reversed stacking mode of two tetramers. The dark tetramer is the top layer and the light tetramer is the bottom layer. a) D_4 (CW,CCW,+30°); b) D_4 (CW,CCW,+60°).	54
Figure	13.	Overlap pattern of the guanine bases for the remaining two diastereomeric forms in the reversed stacking modes of two tetramers. The dark tetramer is the top layer and the light tetramer is the bottom layer. a) $D_4(CCW,CW,-60^\circ)$; b) $D_4(CCW,CW,-30^\circ)$. In the absence of the chiral ribose phosphate group, Figure 13a is the enantiomer of Figure 12b, and Figure 13b is the enantiomer of Figure 12a.	56
Figure	14.	Plots of the best fits for equation (5a) with a) the values of x and K allowed to vary and b) x held constand at 6 and K allowed to vary. Experimental conditions are the same as in Table 7. Error bars represent the experimental points. Errors in x and K are reported at the 95% confidence level.	66
Figure	15.	Structure of hematoporphyrin.	67
Figure	16.	Effect on the ¹ H NMR of adding Na ₂ 5'-GMP into 0.034M EtdBr at 5°C. Nucleotide H(8) resonances are denoted by shading.	71
Figure	17.	Effect of the fraction of Na_25 GMP structured in the presence (\square) and in the absence (Δ) of EtdBr. Experimental conditions are the same as in Figure 16.	76
Figure	18.	Plot of the chemical shift of the EtdBr methyl resonance as a function of the structured Na ₂ 5'-GMP/Drug ratio. Extrapolation of the linear portions of the curve included.	77

Figure	19.	Plot of the best fit curve for equations (6a) and (6c). δ_{Obs} is the observed chemical shift in ppm of the EtdBr methyl resonance and Mg/D is the ratio of the structured Na ₂ 5'-GMP to total drug. X's represent experimental points. Errors in K's and δ 's are standard deviations.	80
Figure	20.	Plots of the best fits for equations (6a) and (6c) in which K_1 is held constant at a) 6.4 x 10^3 and b) 6.4 x 10^7 and only K_2 , δ_1 and δ_2 are allowed to vary. Legends are the same as in Figure 19. Errors in K_2 and δ 's are standard deviations.	81
Figure	21.	Plot of the best fit for equations (6a) and (6c) in which δ_1 and δ_2 are held constant at 0.63 and 0.87 ppm and K_1 and K_2 are allowed to vary. Legends the same as in Figure 19. Errors in K_1 and K_2 are standard deviations.	83
Figure	22.	Effect on the ¹ H NMR of adding K25'-GMP into 0.29M EtdBr at 5°C. Nucleotide H(8) resonances denoted by shading.	85
Figure	23.	Plot of the chemical shift of the EtdBr methyl resonance as a function of the structured K ₂ 5'-GMP/Drug ratio. Extrapolation of the linear portions of the curve included.	88
Figure	24.	Plots of the best fits for a) equations (6a) and (6c) and b) equations (10) and (11). $\delta_{\rm obs}$ is the observed chemical shift in ppm of the EtdBr methyl resonance and a) Mg/D or b) M ₁₆ /D is the ratio of structured K ₂ 5'-GMP to total drug. Errors are standard deviations.	90
Figure	25.	Schematic diagram of the proposed structure for the self-assembled forms of Na ₂ 5'-GMP.	101

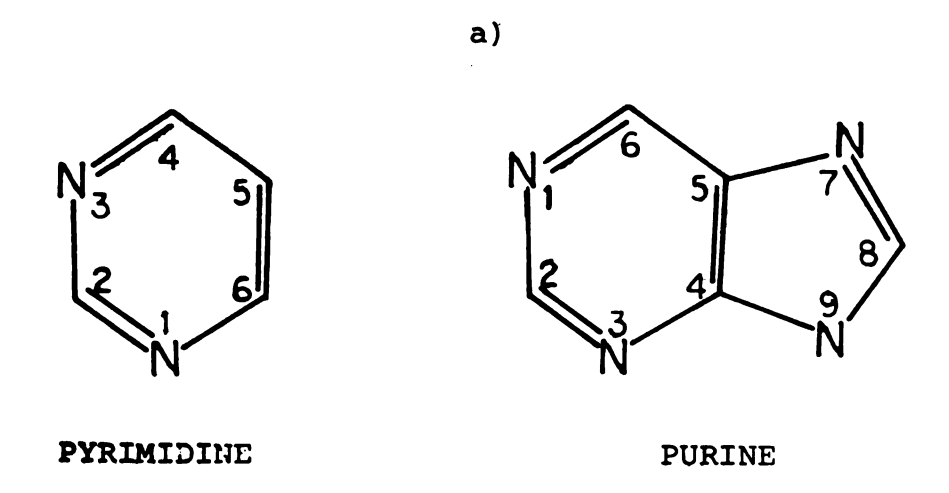
Figure	26.	Structures proposed by Borzo and Laszlo ⁴⁶ to explain the ¹ H NMR spectrum of the self-assembled forms of Na ₂ 5'-GMP. Open circles represent phosphate groups pointing down while closed circles represent phosphate groups pointing up. Na ⁺ ions represented by striped circles (from ref. 46).	103
Figure	27.	Structure proposed by Detellier and Laszlo ⁹⁸ to explain the NMR results for the K ⁺ /Na ⁺ -5'-GMP ⁼ self-structure. Only two of the four chelated Na ⁺ ions are illustrated (from ref. 98).	107
Figure	28.	Expected upfield shift (in ppm) of a nucleus 3.5A above or below the aromatic plane due to the ring current and diamagnetic susceptibility effects (from ref. 82).	113
Figure	29.	Schematic diagram of the proposed equilibrium involved in the formation of a 2:1 and 1:1 complex between the intercalation drug EtdBr and the octameric forms of Na ₂ 5'-GMP.	117
Figure	30.	Schematic diagram of the proposed equilibrium involved in the formation of a 2:1 and 1:1 complex between the intercalation drug EtdBr and structured forms of K 5'-CMP	120

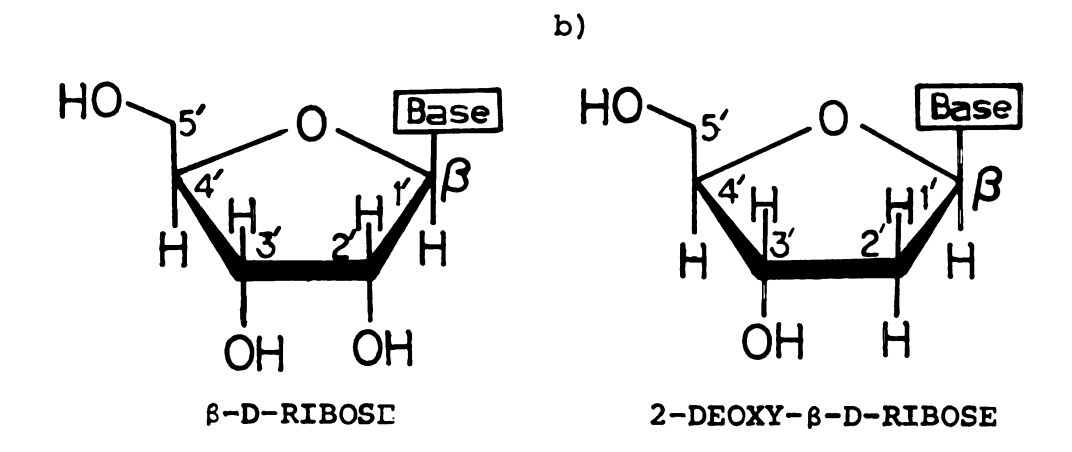
INTRODUCTION

General

Since the discovery of nucleic acids in the late nineteenth century the study of their chemical and biochemical properties has become a highly active area of research. 1978 alone, over 2,000 separate listings were indexed under the general heading of "nucleic acids." As the building blocks in the formation of ribonucleic acids (RNA's) and deoxyribonucleic acids (DNA's), mononucleotides are of fundamental importance in the molecular mechanisms by which genetic information is stored, replicated, and transcribed throughout the cell. They have also been shown to participate in intermediary metabolism, to act as factors during certain enzymatic processes, and to take part in energy transforming reactions in biological systems. Naturally occurring mononucleotides are composed of three characteristic components: 1) a nitrogenous aromatic base, 2) a five carbon ribose sugar, and 3) a phosphoric acid group. 3

The nitrogenous bases are aromatic heterocyclic compounds which are classified as either pyrimidines (six membered rings) or purines (pyrimidines with fused imidazole rings) (Figure 1a). The two major naturally





 a) Structure and numbering sequence for pyrimidine and purine.
 b) Structure and numbering sequence for β-D-ribose (RNA) and 2-deoxy-β-D-ribose Figure 1.

(DNA).

occurring purines, adenine (6-aminopurine) and guanine (2-amino-6-oxypurine) occur in both ribonucleic acids and deoxy-ribonucleic acids. There are three major naturally occurring pyrimidines: thymine (5-methyl-2,4-dioxypyri-midine), which occurs only in DNA, uracil (2,4-dioxypyri-midine), which occurs only in RNA, and cytosine (2-oxy-4-aminopyrimidine), which occurs in both forms of cellular polynucleotides.

Nucleosides are N-glycosides of the pyrimidine or purine, in which carbon 1 of a β -D-ribose sugar is linked to N(1) of a pyrimidine or N(9) of a purine (Figure 1b). In RNA the sugar is a simple β -D-ribose whereas in DNA the sugar is 2-deoxy- β -D-ribose. Naturally occurring nucleosides always have the glycosidic linkage in the β epimeric form and the pentose is always found in the cyclic furanose form. The most common ribonucleosides; adenosine, guanosine, cytidine, thymidine, and uridine are more water soluble than their parent bases.

Nucleotides are phosphoric acid esters of nucleosides in which one or more mono-, di-, or tri-phosphoric acids are esterified to hydroxyl groups of the pentose. Although these phosphate groups may be attached at the 2', 3', or 5' hydroxyl positions, the 5'-isomers are by far the most abundant in the cell. Mononucleotides (nucleotides containing only a single base) are strong acids with two dissociable protons on the phosphoric acid group having

pK_a values of approximately 1.0 and 6.2. Therefore, at neutral pH the free mononucleotide is completely dissociated.

Mononucleotides are able to form hydrogen bonded complexes between complementary base pairs as first proposed by Watson and Crick for the double stranded helix formation of DNA. This base pairing is highly specific and has been studied for nucleosides in non-aqueous solvents by infrared spectroscopy. In both aqueous and non-aqueous solution, NMR of nucleosides has also shown evidence for complementary hydrogen bonded base pairing by the observation of chemical shift changes in both amino and aromatic ring protons. The hydrogen bonded amino protons exhibit both concentration and temperature dependent downfield chemical shifts in comparison to those of the monomer.

While hydrogen bonding between base pairs is significant, base stacking effects have also been shown to provide ordered stabilization. 14 Stacking is the vertical aligning of the planar aromatic bases one atop the other. The stabilizing effect of base stacking is usually described in terms of hydrophobic forces, 14 special van der Waals interactions, 15 π -electron polarizability, 15 dipoledipole induced forces, 16 or electrostatically stabilized ionic (charge transfer) complexes. 15

It is important to note that base stacking has been observed only in aqueous solutions. ¹⁷ This dependence on the solvent indicates that the hydrophobic description of base stacking is appropriate. It is suggested ¹⁷ that stacking is a demonstration of the ordering of water molecules around the dissolved solute allowing short-ranged, attractive forces within the bases to become operative. ¹⁸

Proton magnetic resonance (1 H NMR) is very useful for determining the stacking tendencies of various aromatic molecules. Because of the mobile π electrons in an aromatic system, a large diamagnetic current is induced in the plane of the ring by an external magnetic field. This induced ring current gives rise to a small secondary magnetic field which reinforces the primary field at positions outside and in the plane of the ring. However, at positions directly above and below the plane of the ring, the primary field is reduced (Figure 2). Therefore, the

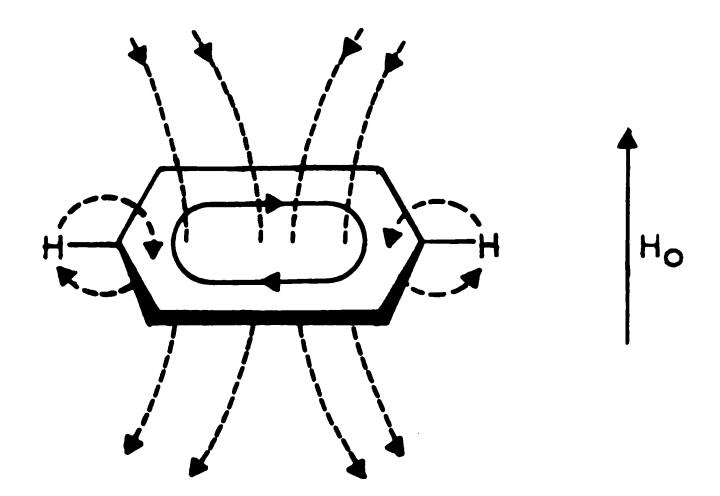


Figure 2. Ring current effects in aromatic systems.

chemical shifts of protons for molecules which stack vertically above the aromatic plane should appear shielded from their normal positions. This interaction should easily be distinguished from hydrogen bonding which induces a downfield shift.

Chan, et al. 19 have shown that the chemical shifts of aromatic protons of purine and 6-methylpurine in aqueous solution move significantly to higher field as the concentration is increased. However the same solutes in either dimethyl sulfoxide or dimethylformamide exhibit aromatic chemical shifts which are virtually independent of concentration. This change was therefore attributed to hydrophobic stacking of the aromatic rings. Ts'o and his coworkers showed a similar upfield shift of aromatic protons as a function of concentration for aqueous solutions of nucleic acid bases, 20,21 nucleosides, 20,21 and mononucleotides. 22 They found that base stacking was stronger for purine bases than for pyrimidine bases and the ring current effects of the latter are not very substantial. Furthermore, they reported that the nucleosides had a far greater tendency to form vertical stacks than the corresponding mononucleotides which carry some negative charge on the phosphate moiety.

Guanine Nucleotides

Derivatives of the mononucleotide, guanylic acid, have shown the unique ability to spontaneously form

regular ordered structures in aqueous solution. This ability has not been observed to date for any other mononucleotide component.

As early as 1910, Bang, in work involved with isolating and characterizing quanine nucleic acids, reported that acidic solutions of guanylic acid formed clear gels. 23 This phenomenon has been observed in aqueous solutions of both the nucleoside and the mononucleotide derivatives. Several authors have investigated by infrared spectroscopy, 24-26 optical rotatory dispersion (ORD), 27,28 circular dichroism (CD), 27,28 Raman spectroscopy, 29-31 calorimetry, 32 and x-ray fiber diffraction 33-36 the structure of these gels, which are formed at pH ≤ 5. Investigation of the fibrillar structures upon drying of the gels indicates that, at pH = 5, two different hydrogen bonded selfstructured forms exist. One of these structures, represented by fibers of sodium 5'-guanosine monophosphate (NaH(5'-GMP)) (Figure 3a) at pH = 5, consists of a long chain, single stranded continuous helix with 15 nucleotide units for every four helical turns. 36 On the other hand, Na₂ (5'-GMP) fibers grown from concentrated solution at neutral pH in the presence of NaCl consist of hydrogen bonded planar tetramer units stacked in a helical array (Figure 4). 37 The stacked planar tetramer structure has also been found for NaH(3'-GMP) fibers (Figures 3b and 4). 33 In both the helical and the stacked tetramer

Figure 3. a) Structure of 5'-guanylic acid (5'-GMP). b) Structure of 3'-guanylic acid (3'-GMP).

proposed structures, nitrogen (1) and nitrogen (2) are hydrogen bond donors, while oxygen (6) and nitrogen (7) act as hydrogen bond acceptors.

In 1972, Miles and Frazier reported IR evidence that 5'-GMP in neutral or slightly alkaline solution (pH $^{\alpha}$ 8) can exist in a regular ordered form. ³⁸ In this pH range, both acidic protons on the phosphate group are dissociated (pK $_{a_2}$ = 6.1). ³⁹ They reported that in going from the unstructured to the structured form, three major IR changes occur. First, the carbonyl stretch at 1665 cm⁻¹

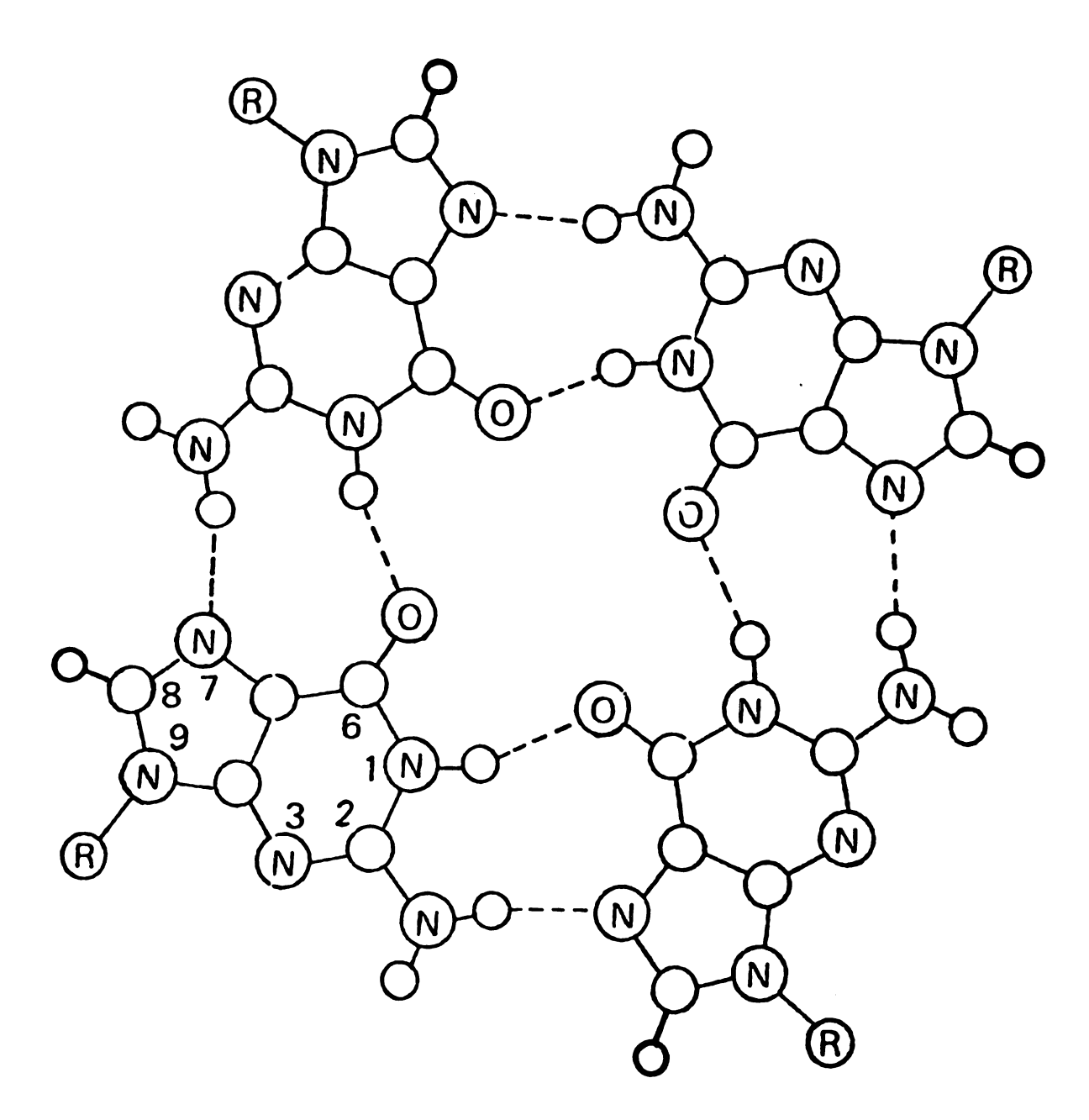


Figure 4. Proposed structure of the hydrogen bonded tetramer in the Na₂(5'-GMP) solution and NaH(3'-GMP) gel (R = ribose-phosphate group). 33,37

moves to 1672 cm⁻¹ and intensifies. Second, the C(4)=C(5) ring vibration at 1580 cm⁻¹ decreases in intensity and shifts to 1593 cm⁻¹. Finally, a new ring vibration at 1540 cm⁻¹ was found to grow in. This IR pattern differs from that of the structured form of NaH(5'-GMP). The neutral solution also shows no evidence for gelation as is observed in the acidic solution. Based on the similarities between the IR spectra of 3'-GMP in acidic media²⁴ and 5'-GMP in neutral or slightly alkaline media, 38 Miles and Frazier postulated that the structure for 5'-GMP in this medium is based on the same stacked planar tetramer units (Figure 4). Zimmerman's 1976 x-ray fiber diffraction study³⁷ supported this assumption of stacked planar tetramer units. His work indicated that the planar tetramer units were stacked on a common axis at a distance of 3.4A with each unit rotated 30° with respect to the preceding unit.

A ¹H NMR study of Na₂(5'-GMP) by Pinnavaia, Miles, and Becker ⁴⁰ showed that the structures of Na₂(5'-GMP) were slow to exchange and had an energy barrier to exchange with monomers of greater than 15 kcal·mol⁻¹. Previously all H-bonded mononucleotides, including those with Watson-Crick complementarity, were reported as exhibiting only time average ¹H NMR spectra. Subsequent ¹H NMR work showed that structure formation is highly dependent upon the alkali metal counter-ion. ⁴¹⁻⁴³ These studies showed

that structure formation was based on a size selective coordination of the alkali metal cation. The thermal stability of the ordered forms decreased in the order K⁺ > Na⁺ = Rb⁺ >> Li⁺, Cs⁺. The proposal was made that the Na tion coordinates to the four carbonyl O(6) positions which form a hole in the center of the tetrameric plate (cf. Figure 4) (Figure 5). The ionic radii of Li⁺ and K⁺ would be too small and too large, respectively, to coordinate adequately in this position. A second coordination site, bounded by eight carbonyl oxygens, was proposed as existing halfway between two stacked tetrameric plates (cf. Figure 5). The size of this hole could adequately coordinate with either K or Rb but would be too large to coordinate Na properly and too small to coordinate Cs t without sacrificing base-stacking interactions. Due to similarities in IR spectra upon coordination, all structures were assumed to be based on stacked tetramer plates. This was the first reported case of selective alkali metal ion coordination by any nucleic acid component. Previously the role of alkali metal ions was relegated to neutralization of phosphate charge.

Since that time other groups have confirmed the alkali metal ion specificity in 5'-GMP⁴⁴⁻⁴⁷ and also in the polymeric nucleic acids, polyinosinic acid⁴⁸ and polyxanthylic acid.⁴⁹ Recent work by Bouhoutsos-Brown⁵⁰ sought to determine the metal ion and nucleotide stoichiometry of

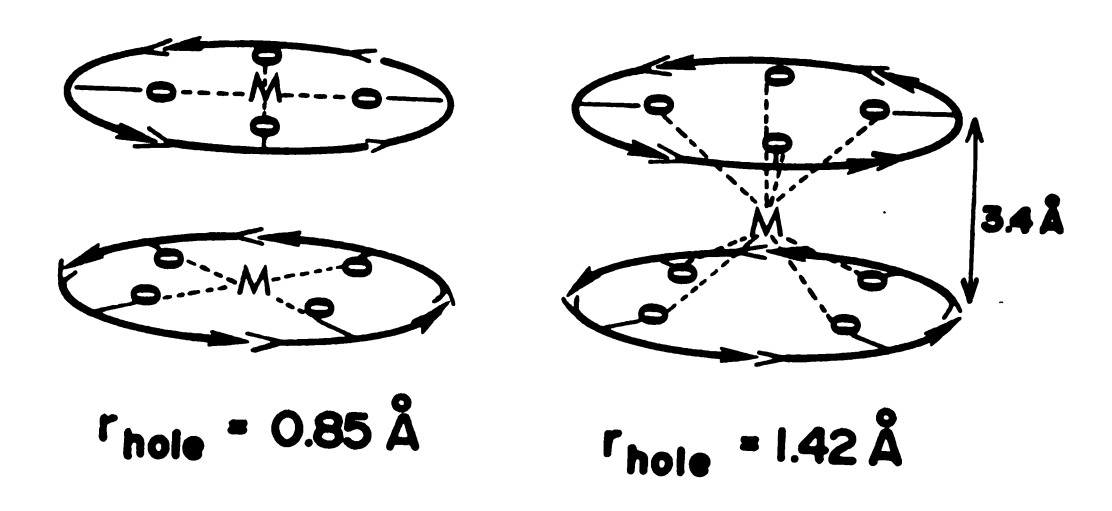


Figure 5. Schematic diagram of the proposed size selective coordination sites in the structuring of a neutral aqueous solution of 5'-GMP. a) Coordination into the center of the tetrameric plate by Na+ (r = 0.99A). b) Coordination between the plates by K+ and Rb+ (r = 1.51A and 1.60A, respectively). Note that Li+ (r = 0.59A for 4-coordination, 0.74A for 6-coordination) would be too small to substitute for Na+ and that Cs+ (r = 1.78A) is too large to replace K+ or Rb+. (Ionic radii from ref. 51)

the 5'-GMP self-structures. She postulated that the Na₂5'-GMP structure is octameric with respect to the nucleotide and requires six Na⁺ ions per octamer; one each in the centers of the two tetramer plates and the remaining four chelated between the top and bottom tetramers. Furthermore, she noted the existence of two structurally different self-assembled forms with either K⁺ or Rb⁺ as the counter-ion. These structures she termed "simple" (at ratios of 5'-GMP⁼/M⁺ \geq 1) and "complex" (5'-GMP⁼/M⁺ \geq 0.5) and proposed the stacking patterns with respect to the 5'-GMP to be octameric and hexadecameric respectively. It was also discovered that five other GMP derivatives (2'-GMP, 3'-GMP, 2',3'-cGMP, 3',5'-cGMP, and 5'-dGMP) were able to form metal ion specific self-assembled structures.

Intercalation Drugs

The determination of the structures of nucleic acids has been aided in recent years by the use of intercalation drugs. The word <u>intercalation</u> comes from the Greek and literally means "insert between." Thus an intercalating drug is one in which the planar portion of the drug molecule is inserted between the adjacent base pairs of a double-stranded region of a DNA or RNA helix (Figure 6). Figure 7 shows some of the more commonly employed intercalation drugs. All are antibiotics and some are known antitumor agents. The intercalation mode of binding was

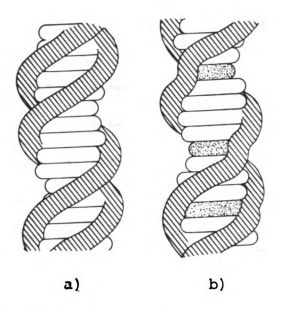


Figure 6. Schematic of the mode of intercalation binding to nucleic acids. a) Normal double stranded polynucleotide with ribose-phosphate backbone (striped) and hydrogen bonded base pairs. b) Same sketch as in a) with three drug molecules (shaded region) intercalated.

first proposed by Lerman⁵³ to explain the binding of the aminoacridines to DNA. The physiological activity of intercalating drugs is generally attributed to their ability either to produce mutations or to interfere with DNA or RNA polymerase.⁵² There is also a wide range of compounds in which only a portion of the molecule may intercalate (for example, the intercalation of aromatic amino acids is probably one of the modes involved in protein-nucleic acid recognition⁵⁴).

Ethidium bromide (EtdBr; Figure 7b) is biologically active, possessing trypanocidal, 55 antiviral 56 and

R = H DAUNORUBICIN R = OH ADRIAMYCIN

Figure 7. Chemical structures of a) actinomycin D;
b) ethidium bromide; c) daunorubicin (also called daunomycin) and andriamycin; and d)
platinum (II) 2,2',2''-terpyridyl chloride.

antibacterial⁵⁶ properties. EtdBr inhibits DNA synthesis in vivo; ⁵⁷ and, in vitro, EtdBr interferes with DNA-dependent DNA and RNA polymerases of Escherichia coli. ^{58,59} EtdBr-DNA complexes exhibit several properties which are indicative of intercalation. These include a diminished sedimentation coefficient, ⁶⁰ enhanced intrinsic viscosity, ⁶⁰ and a greatly augmented fluorescence. ^{61,62} Recent interest in EtdBr has centered on its special ability to unwind closed circular DNA. ⁶³⁻⁶⁶

Proton NMR has proven to be a useful tool in studying the interaction of intercalation drugs with short nucleic acid polymers. The purpose is to gain an understanding of the binding mode of the drug in polynucleotides. Krugh, et al. 67,68 and Chan and coworkers 69 have used dinucleoside monophosphates with intercalated EtdBr as models. Their findings were that as the drug is intercalated, the aromatic protons shift upfield due to the change in ring currents felt by the nucleus. The change for each individual line was not clear due to overlap with other drug lines and with nucleotide lines. However, the resonance of the side chain methyl group lies upfield of all other resonances and its change in chemical shift as a function of nucleotide concentration provided stoichiometric information. In all cases it was found that one EtdBr intercalates between two stacks of hydrogen bonded base pairs.

Statement of Research Aims

To date, the proposed structures of the ordered alkali metal salts of 5'-GMP⁼ in neutral solution have been based on intuition and indirect evidence. This is primarily due to the fact that most previous work was done at a fixed ratio between the nucleotide and the metal ions (M⁺/5'-GMP⁼ = 2). Direct evidence about the exact stoichiometry requires a method in which the metal and nucleotide concentrations may be varied independently. This must be accomplished, however, without adding ions which will act as competitors with the species of interest. What is required is a counter-cation which will allow the addition of 5'-GMP⁼ and will act neither as a structure directing ion nor as a structure inhibiting ion.

Bouhoutsos-Brown⁵⁰ has shown that the tetramethyl ammonium cation (TMA⁺) acts as neither a structure inhibitor nor director. This makes it an ideal "dummy ion" for use in directly determining the stoichiometry of the structures in solution.

The present study will use (TMA)₂5'-GMP as a source of nucleotide in order to vary the 5'-GMP⁼/M⁺ ratio. This should yield more quantitative information than has previously been available about the exact stoichiometries of both the metal and the nucleotide in the structures.

It is also hoped that intercalation compounds added into solutions of the structured nucleotide will interact strongly enough with the structured forms of 5'-GMP to allow collaborating evidence concerning the stoichiometries of the structured forms.

EXPERIMENTAL

A. Materials, Techniques, and Preparation

5'-guanosine monophosphate was purchased as the disodium salt monohydrate from Calbiochem, Inc. and as the free acid from Sigma Chemical Co. The free acid form was converted to the dipotassium salt or the ditetramethylammonium (TMA) salt by titration with KOH (Mallinkroft) or (TMA)OH (Matheson, Coleman and Bell). Dilute solutions (~0.01M) of the free acid were titrated to a pH of ~7.8 with the use of a Fisher model 370 pH meter fitted with a Markson model E-884 combination pH electrode. All distilled water was passed through an Illinois Water Treatment Company purification system to remove any paramagnetic ion impurities and organic residues. All nucleotide solutions were lyophilized three times from 99.8% D₂O (Stohler Isotope Chemicals or Norell Chemical Co., Inc.) then prepared to the proper concentrations. spectra were obtained from samples in 10mm tubes (Wilmad Glass Co., Inc.) and stoppered with silicone rubber serum Sodium $2,2,3,3,-d_A-3$ -trimethylsilylpropionate (TSP), purchased from Merck and Company was used as an internal reference (~0.1 wt%) for chemical shift

measurements. In solutions containing counter-ions other than sodium, the Na⁺ ions of the reference were replaced by passing the NaTSP solution through the appropriate Dowex 50W-X8 (100-200 mesh) cation exchange resin. The resin has an exchange capacity of 1.7 meq/mL The resin was prepared by the following wash sequence: (1) 10% HCl, (2) H₂O and EDTA, (3) 10% NaOH, (4) H₂O, (5) 1:1 H₂O-CH₃OH, (6) CH₃OH, (7) 1:1 CH₃OH-CH₂Cl₂, (8) CH₂Cl₂, (9) 1:1 CH₃OH-CH₂Cl₂, (10) CH₃OH, (11) 1:1 H₂O-CH₃OH, (12) 10% HCl, (13) H₂O and EDTA, (14) 1N solution of desired metal ion hydroxide and (15) H₂O.

Ethidium bromide (EtdBr), which was purchased from Sigma Chemical Company, was lyophilized three times from 99.8% D₂O to remove ethanol and water of crystallization.

Hematoporphyrin (Sigma Chemical Company) was titrated (pH = 8) with the appropriate metal hydroxide to obtain the salt form.

Platinum 2,2',2"-terpyridyl chloride was prepared according to the procedure of Intille. 70

Model building studies used CPK space filling models (Ealing Corporation). The models had a scale of 12.5 cm/nm.

B. Instrumentation

Nuclear Magnetic Resonance Spectroscopy--NMR spectra were obtained on either a Bruker WH-180 interfaced to a Nicolet 1180 computer with 16K of memory or a Bruker

WM-250 interfaced to an Aspect 2000 computer with 32K of memory. Probe temperatures were maintained to ${}^{\pm}1^{\circ}$ C by a Bruker temperature control unit coupled to a probe-mounted thermocouple calibrated at low temperature in liquid N₂ and high temperature in ice water.

Ultraviolet/Visible Absorption Spectroscopy—Concentrations of all 5'-GMP and EtdBr solutions were determined by UV/Vis absorption using a Beckman DU spectrometer equipped with a Gilford Photometer 252. Solution concentrations were determined by assuming that Beer's Law holds. The molar absorptivity of 5'-GMP at 252 nm is 13,700, 72 and the absorptivity for Etd at 480 nm is 5450. 66

Computation—Computer curve fitting was accomplished on a Control Data Corporation, Cyber 170 model 750 computer by using the KINFIT program developed by Dye. 73 This method uses Wentworth's 74 minimization procedure. Since the weighting procedure used in minimization and therefore the final estimates of the parameters and their standard deviations is dependent upon the errors in integration, a description of the technique used in integration and error estimation is presented.

NMR integrations of the H(8) region of the spectra were accomplished by cutting and weighing of photocopies of the individual spectra. Triplicate measurements were made and the average taken. Systematic errors were

determined by taking the average value obtained from integration by two separate investigators. Errors were also estimated from the threshold concentration of structure that can be observed and from the signal to noise ratio at the given concentration. All errors in the variable parameters that were used in curve fitting were the sum of random and systematic errors.

The assumption was made for determining the fraction of structure (see Figure 8 for characteristic spectra) that the third highest field resonance (labelled B) which lies under the monomer resonance (C) has an integral intensity equal to the average of resonances A and D. At higher concentrations where the monomer resonance (C) moves upfield, the integral intensity of structure line (B) is equal to that of either structure line (A) or (D). Integration of the structure peaks for K_2 5'-GMP/EtdBr solutions was accomplished by integrating the entire aromatic region (6.5-8.5 ppm) and the drug methyl resonance. The portion of the aromatic region due to the drug (10/3 x methyl integration) was then subtracted out to give the H(8) integration.

C. Theoretical

 $\underline{\mathsf{GMP}}^{=}$ Stoichiometry--The following is a summary of the equations used in the KINFIT curve fitting routine to determine the stoichiometry of 5'-GMP aggregation under conditions where the ratio of the metal to structured 5'-GMP concentration is large. C_{M} defines the concentration of

 $5'-GMP^{=}$ in disordered monomer form and C_S defines the concentration of $5'-GMP^{=}$ in the ordered form.

1. Formation of ordered n-mers, $\mathbf{M}_{\mathbf{n}}$, from monomers, $\mathbf{M}_{\mathbf{n}}$

$$nM \stackrel{?}{\leftarrow} M_n$$
 (la)

$$K = \frac{\left[M_{n}\right]}{\left[M\right]^{n}} \tag{1b}$$

$$\left[\mathbf{M}\right] = \left(\frac{\left[\mathbf{M}_{\mathbf{n}}\right]}{\mathbf{K}}\right)^{1/\mathbf{n}} \tag{1c}$$

Substituting with C_S and C_M :

$$\left[\mathbf{M}\right] = \mathbf{C}_{\mathbf{M}} \tag{1d}$$

$$\left[M_{n}\right] = \frac{C_{s}}{n} \tag{1e}$$

and

$$C_{M} = \left(\frac{C_{S}}{nK}\right)^{1/n} \tag{1f}$$

If $C_S = XX(1)$, $C_M = XX(2)$, 1/n = U(1), and nK = U(2), this equation can be expressed in FORTRAN language as:

$$XX(2) = (XX(1)/U(2)*U(1))**U(1)$$
 (1g)

2. Formation of stacked tetramers, $(M_4)_n$, from monomers, M:

$$4nM \stackrel{?}{\leftarrow} (M_4)_n$$
 (2a)

$$K = \frac{\left[\binom{M_4}{n}\right]}{\left[\binom{M}{4}\right]^{4n}} \tag{2b}$$

$$\left[\left(\mathbf{M}_{4} \right)_{n} \right] = \mathbf{K} \left[\mathbf{M} \right]^{4n} \tag{2c}$$

Substituting with C_S and C_M :

$$\left[\mathbf{M}\right] = \mathbf{C}_{\mathbf{M}} \tag{2d}$$

$$\left[\left(M_4 \right)_n \right] = \frac{C_s}{4n} \tag{2e}$$

and

$$C_{S} = 4nK(C_{M})^{4n}$$
 (2f)

If $C_S = XX(1)$, $C_M = XX(2)$, n = U(1), and K = U(2), this equation can be expressed in FORTRAN language as:

$$XX(1) = 4.*U(1)*U(2)*(XX(2)**(4.*U(1)))$$
 (2g)

3. Equilibria involving monomers (M), tetramers (M_4) and stacked tetramers $((M_4)_n)$. In this case C_M = total concentration for the disordered monomer and unstacked tetramer, and X = concentration of disordered monomer:

$$4M \not\equiv M_{\Delta}$$
 (3a)

$$nM_{4} \stackrel{?}{=} (M_{4})_{n} \tag{3b}$$

$$\kappa_1 = \frac{\left[M_4\right]}{\left[M\right]^4} \tag{3c}$$

$$K_2 = \frac{\left[\left(M_4 \right)_n \right]}{\left[M_4 \right]^n} \tag{3d}$$

$$\left[M_{4}\right] = \left(\frac{\left[\left(M_{4}\right)_{n}\right]}{K_{2}}\right)^{1/n} \tag{3e}$$

$$K' = K_1 K_2 = \frac{[(M_4)_n]}{[M]^4 [M_4]^{n-1}}$$
 (3f)

$$[(M_4)_n] = K'[M]^4[M_4]^{n-1}$$
(3g)

Substituting with C_S , C_M , and X:

$$\left[\mathsf{M}\right] = \mathsf{X} \tag{3h}$$

$$\left[M_{4}\right] = \frac{C_{M} - X}{4} \tag{3i}$$

$$\left[\left(M_4 \right)_n \right] = \frac{C_s}{4n} \tag{3j}$$

(3e) becomes:

$$x = C_{M} - 4\left(\frac{C_{S}}{4nK_{2}}\right)^{1/n}$$
 (3k)

and (3g) becomes:

$$C_S = K'(X^4) \left(\frac{C_M - X}{4}\right)^{n-1} (4n)$$
 (31)

If $C_S = XX(1)$, $C_M = XX(2)$, X = C1, N = U(1), K' = U(2), and $K_2 = U(3)$, then (3k) can be expressed in FORTRAN language as:

$$C1 = XX(2) - (4.*((XX(1)/((4.*U(1))*U(3)))**(1./U(1))))$$
(3m)

letting

$$C2 = ((XX(2) - C1)/4.)**(U(1) - 1.)$$
 (3n)

and

$$C3 = 4.*U(1)$$
 (30)

then, equation (31) in FORTRAN becomes

$$XX(1) = U(2)*((C1)**4)*C2*C3$$
 (3p)

4. Formation of stacked tetramer, $(M_4)_n$, from tetramer, M_4 :

$$nM_{4} \stackrel{\rightarrow}{\leftarrow} (M_{4})_{n} \tag{4a}$$

$$K = \frac{\left[\left(M_4 \right)_n \right]}{\left[M_4 \right]^n} \tag{4b}$$

$$\left[M_{4}\right] = \left(\frac{\left[\left(M_{4}\right)_{n}\right]}{K}\right)^{1/n} \tag{4c}$$

Substituting with C_S and C_M :

$$\left[\mathsf{M}_{4}\right] = \frac{\mathsf{C}_{\mathsf{M}}}{4} \tag{4d}$$

$$\left[\left(M_4 \right)_n \right] = \frac{C_S}{4n} \tag{4e}$$

and

$$C_{M} = 4 \left(\frac{C_{S}}{4nK}\right)^{1/n} \tag{4f}$$

If $C_S = XX(1)$, $C_M = XX(2)$, n = U(1), and K = U(2), this equation can be expressed in FORTRAN language as:

$$XX(2) = 4.*((XX(1)/(4.*U(1)*U(2)))**(1./U(1)))$$
 (4g)

 ${
m Na}^+$ Stoichiometry--The following is a summary of the equations used in the KINFIT curve fitting to determine the stoichiometry of the Na $^+$ in the 5'-GMP $^-$ aggregate. The number of 5'-GMP $^-$ units per aggregate was assumed to be eight. ${
m C}_{
m M}$ defines the concentration of 5'-GMP $^-$ in the disordered form and ${
m C}_{
m S}$ defines the concentration of 5'-GMP $^-$ in the ordered form. ${
m C}_{
m Na}^{
m t}$ is the total concentration of Na $^+$.

$$xNa^{+} + 8M^{2-} \stackrel{?}{\leftarrow} Na_{x}^{M}_{8}^{(16-x)-}$$
 (5a)

$$K = \frac{\left[Na_{x}^{M_{8}}^{(16-x)-}\right]}{\left[Na^{+}\right]^{x}\left[M^{2-}\right]^{8}}$$
 (5b)

$$\left[\operatorname{Na}_{\mathbf{x}}^{\mathbf{M}_{8}}^{(16-\mathbf{x})^{-}}\right] = K\left[\operatorname{Na}^{+}\right]^{\mathbf{x}}\left[\operatorname{M}^{2-}\right]^{8} \tag{5c}$$

Substituting with C_S , C_M , and C_{Na}^t :

$$\left[\mathsf{M}^{2}\right] = \mathsf{C}_{\mathsf{M}} \tag{5d}$$

$$\left[\operatorname{Na}_{\mathbf{x}}^{\mathsf{M}_{8}}^{(16-\mathbf{x})^{-}}\right] = \frac{\operatorname{C}_{\mathsf{S}}}{8} \tag{5e}$$

$$\left[\mathrm{Na}^{+}\right] = \mathrm{C}_{\mathrm{Na}}^{\mathrm{t}} - \mathbf{x} \left(\frac{\mathrm{C}_{\mathrm{S}}}{8}\right) \tag{5f}$$

and

$$c_{S} = 8K \left[c_{Na}^{t} - x \left(\frac{c_{S}}{8} \right) \right]^{x} (c_{M})^{8}$$
 (5g)

If $C_{Na}^{t} = XX(1)$, $C_{S} = XX(2)$, $C_{M} = XX(3)$, x = U(1), K = U(2), and $C1 = [Na^{+}]$, then equation (5g) can be expressed in FORTRAN language in the following way:

let

$$C1 = XX(1) - (U(1)*XX(2)/8.)$$
 (5h)

then

$$XX(2) = 8.*U(2)*((C1)**U(1))*(XX(3)**8)$$
 (5i)

Drug Binding Constants—The following is a summary of the equations used in the KINFIT curve fitting to determine the binding constants of the structured forms to the intercalation drug ethidium bromide using the procedure developed by Popov and coworkers. The number of 5'-GMP units per aggregate was assumed to be 8. An octamer (M₈) binding to two drug molecules (D) gives the following expressions,

$$M_8 + 2D \stackrel{?}{\downarrow} M_8 \cdot D_2$$
 (6a)

$$K_{1} = \frac{\left[M_{8} \cdot D_{2}\right]}{\left[M_{8}\right]\left[D\right]^{2}} \tag{6b}$$

 $M_8 \cdot D_2$ can react with more M_8 to give,

$$M_8 \cdot D_2 + M_8 \stackrel{K_2}{\neq} 2M_8 \cdot D \tag{6c}$$

$$K_2 = \frac{\left[M_8 \cdot D\right]^2}{\left[M_8 \cdot D_2\right]\left[M_8\right]} \tag{6d}$$

The total concentration of drug (C_D^t) and the total concentration of octamer $(C_{M_R}^t)$ can be defined as

$$c_{D}^{t} = [D] + 2[M_{8} \cdot D_{2}] + [M_{8} \cdot D]$$
 (6e)

$$c_{D}^{t} = [D] + 2K_{1}[M_{8}][D]^{2} + \sqrt{K_{1}K_{2}}[M_{8}][D]$$
 (6e')

$$0 = (2K_{1}[M_{8}])[D]^{2} + (1 + \sqrt{K_{1}K_{2}[M_{8}]})[D] - c_{D}^{t}$$
 (6e")

$$C_{M_8}^{t} = \left[M_8\right] + \left[M_8 \cdot D_2\right] + \left[M_8 \cdot D\right] \tag{6f}$$

$$c_{M_8}^{t} = \left[M_8\right] + K_1 \left[M_8\right] \left[D\right]^2 + \sqrt{K_1 K_2} \left[M_8\right] \left[D\right]$$
 (6f')

Therefore, the free drug concentration, [D], and the free octamer concentration, $[M_8]$, are defined as

$$\left[D\right] = \frac{-(1+\sqrt{K_{1}K_{2}}[M_{8}]) + \sqrt{(1+\sqrt{K_{1}K_{2}}[M_{8}])^{2}+4(2K_{1}[M_{8}])C_{D}^{t}}}{2(2K_{1}[M_{8}])}$$
(6g)

$$\begin{bmatrix} M_8 \end{bmatrix} = \frac{C_{M_8}^t}{1 + K_1 \begin{bmatrix} D \end{bmatrix}^2 + \sqrt{K_1 K_2} \begin{bmatrix} D \end{bmatrix}}$$
 (6h)

Defining X_1 as the mole fraction of drug in $M_8 \cdot D_2$ and δ_1 as its corresponding chemical shift, X_2 as the mole fraction of drug in $M_8 \cdot D$ and δ_2 as its corresponding chemical shift, and X_f as the mole fraction of free drug and δ_f as its corresponding chemical shift, the observed chemical shift (δ_{obs}) of the drug can be defined as

$$X_{1} = \frac{2K_{1} \left[M_{8}\right] \left[D\right]^{2}}{c_{D}^{t}}$$
 (6i)

$$x_{2} = \frac{\sqrt{K_{1}K_{2}[M_{8}][D]}}{C_{D}^{t}}$$
 (6i')

$$x_{f} = \frac{[D]}{c_{D}^{t}}$$
 (6i")

and

$$\delta_{\text{obs}} = \delta_{\text{f}} X_{\text{f}} + \delta_{1} X_{1} + \delta_{2} X_{2}$$
 (6j)

If $C_D^t = CONST(1)$, $\delta_f = CONST(2)$, $C_{M_8}^t = XX(1)$, [D] = COND, $\delta_{obs} = XX(2)$, $K_1 = U(1)$, $K_2 = U(2)$, $\delta_1 = U(3)$, $\delta_2 = U(4)$, $B = \sqrt{K_1 K_2} [D]$, $B1 = 1 + K_1 [D]^2$, and $C(N) = [M_8]$, equation (6h) can be written in FORTRAN language as

$$B = ((U(1)*U(2))**2)*COND$$
 (6k)

$$B1 = 1. + (U(1)*(COND**2))$$
 (6k')

$$C(N) = XX(1)/(B + B1)$$
 (6k")

With D = $2K_1[M_8]$ and Dl = 1 + $\sqrt{K_1K_2[M_8]}$ equation (6g) written in FORTRAN becomes

$$D = (2.*U(1)*C(N))$$
 (61)

$$D1 = 1. + (SQRT(U(1)*U(2)))*C(N)$$
 (61')

$$C1 = -D1 + SQRT((D1**2) + (4.*D*CONST(1)))$$
 (61")

$$COND = C1/(2.*D)$$
 (61"')

Based on the technique of reference 75, an estimate of [D] is made and used in equations (6k) - (6k") to solve for $[M_8]$. This value is used in equations (61) - (61") to

solve for a new value of [D] which is resubstituted into the first set of equations. This loop is continued until self-consistent values of [M₈] and [D] are obtained. KINFIT then uses these values to solve equation (6j). If $X_f = F$, $X_1 = COMP1$, $X_2 = COMP2$, and $\delta_{obs} = SOBS$, then equations (6i) - (6j) in FORTRAN become

$$F = COND/CONST(1)$$
 (6m)

$$COMP1 = (2.*U(1)*C(N)*(COND**2))/CONST(1)$$
 (6m')

$$COMP2 = ((SQRT(U(1)*U(2)))*C(N)*COND)/CONST(1)$$
 (6m")

$$SOBS = (CONST(2)*F) + (U(2)*COMP1) + (U(3)*COMP2)$$
 (6n)

RESULTS

A. Stoichiometry of 5'-GMP Aggregation: Na Salt

In order to determine the stoichiometry of 5'-GMP aggregation, it is necessary to investigate a system in which the metal ion concentration is constant. For the general reaction,

$$xNa^{+} + n5' - GMP^{=} \stackrel{K}{\leftarrow} Na_{x} (5' - GMP)_{n}^{(2n-x)}$$
 (7)

if the concentration of Na^+ is large with respect to the concentrations of either the dissociated nucleotide monomer or aggregated structure, then the Na^+ concentration and ionic strength can be assumed to remain nearly constant. In this case, we can define an apparent equilibrium constant, K^+ , as

$$K' = K \left[Na^{+} \right] = \frac{\left[Na_{x} \left(5' - GMP \right)_{n}^{\left(2n - x \right) - \right]}}{\left[5' - GMP^{-} \right]^{n}}$$
(8)

Figure 8 shows the effect on the H(8) region of the NMR spectrum of adding TMA_2^5 '-GMP into a $0.85\underline{M}$ solution of NaCl in D_2^0 . The tetramethyl ammonium ion (TMA^+) has been

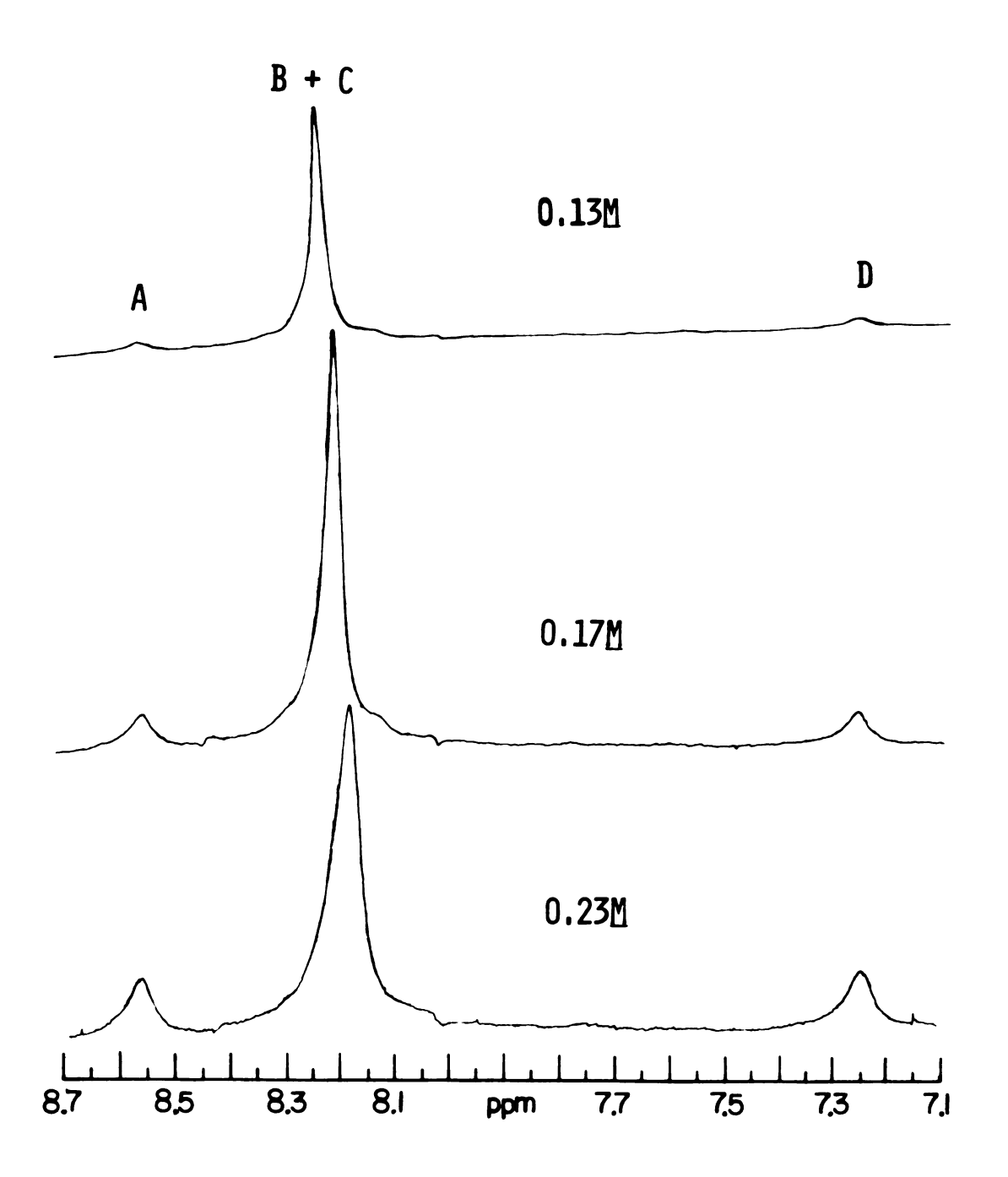


Figure 8. Effect on the H(8) NMR of adding (TMA) 5'-GMP into 0.85M NaCl in D2O at 15°C. Structure lines are labelled A, B, and D, and the monomer line is labelled C.

shown by Bouhoutsos-Brown 50 to be a structurally inert cation with regard to Na⁺/5'-GMP⁼ self-assembly. As the concentration of 5'-GMP increases, an increase in the total concentration of structure is observed. ances are assigned to the monomer 5'-GMP (labelled C), the two observable structure lines (labelled \underline{A} and \underline{D}), and a third structure line (labelled B) which lies under the monomer resonance. At high concentrations of 5'-GMP, the C peak moves upfield making the third structure peak, B, visible. At all concentrations where it is possible to integrate the B peak, the integral intensities of all three structure lines (A, B, and D) are identical within ± 3% experimental uncertainty. In this study, therefore, at concentrations where the B line is not observable due to overlap with the monomer resonance, its intensity is assumed to be the average of the intensities of the A and D peaks.

Table 1 lists the fraction of structured $5'-GMP^{=}$ as the total nucleotide concentration is varied from $0.13\underline{M}$ to $0.23\underline{M}$ while the Na⁺ concentration is held constant at $0.85\underline{M}$. Under these conditions the total Na⁺ to total $5'-GMP^{=}$ ratio varied from ~ 6.5 to ~ 3.7. The Na⁺ concentration is much larger than the concentration of structured $5'-GMP^{=}$ (11 $\leq [Na^{+}]_{total}/[5'-GMP^{=}]_{structured} \leq 85$).

An attempt was made to fit these results to a series of different equilibrium equations (for a complete summary,

Table 1. Fraction of Structure of 5'-GMP with Changing Total Nucleotide Concentrationa

		Na ⁺]total
$\begin{bmatrix} 5' - GMP^{=} \end{bmatrix} total^{\frac{b}{2}}$	Fstructured	5'-GMP structured
0.13(±0.003)	0.078(±0.048)	85
0.14(±0.003)	0.134(±0.049)	45
0.15(±0.003)	0.164(±0.018)	35
0.16(±0.003)	0.180(±0.020)	30
0.17(±0.003)	0.220 (±0.018)	23
0.18(±0.004)	0.236(±0.017)	20
0.19(±0.004)	0.272(±0.019)	16
0.20(±0.004)	0.287 (±0.020)	15
0.21(±0.004)	0.299 (±0.025)	14
0.22(±0.004)	0.322(±0.019)	12
0.23 (±0.005)	0.328 (±0.024)	11

a. 0.85M NaCl in D₂O; 15(±1) C; errors are the sums of the systematic and random errors of two independent integrations of H(8) resonances. The 5'-GMP was introduced as the TMA+ salt.

b. Concentration in moles/liter.

see Experimental section). The most general form that such an equilibrium could take would be that of disordered monomers of $5'-GMP^=$ (M) associating to form structured n-mers (M_n) such that

$$nM \neq M_n$$
 (la)

If the basic structural building block is assumed to be a tetramer, then a more specific equilibrium can be written as

$$4nM \stackrel{?}{\leftarrow} (M_4)_n$$
 (2a)

Equation (2a) can be written in terms of a two-step equilibrium process such that monomer (M) first forms tetramer (M_4) which then proceeds to form the stacked tetramers $((M_4)_n)$. The resulting expressions are

$$4M \stackrel{\rightarrow}{\leftarrow} M_{\Lambda}$$
 (3a)

$$nM_4 \stackrel{?}{\leftarrow} (M_4)_n \tag{3b}$$

Chantot and Guschlbauer 76 using UV spectroscopy have reported observing free tetramer (M₄) for the gels of the acidic nucleotides, KH(5'-GMP) and KH(3'-GMP) (pH \simeq 5.5).

Lee and Chan⁷⁷ have determined by 1 H nmr a tetramer formation constant of 2.5 x $10^7 \, \underline{\text{M}}^{-3}$ for NaH(5'-GMP). If a similar value is applicable for Na₂(5'-GMP) at concentrations where structure formation occurs, nearly all of the monomer is expected to be in the tetrameric form. The $\underline{\text{C}}$ resonance ($\underline{\text{cf}}$. Figure 8) would therefore be all tetramer and a fourth equilibrium expression,

$$nM_4 \stackrel{?}{\leftarrow} (M_4)_n \tag{4a}$$

can be written.

Table 2 shows the results of fitting values of n and K' in the above equations using the data from Table 1.

It is clear from an inspection of the results of the curve fitting that equations (3a) and (3b), describing tetramer formation from monomer and subsequent stacking of tetramers, cannot be fitted to the data. The standard deviation estimates (95% confidence) of the best values are large. The K' values are too large to fit with the available range of data. In addition, (3a) and (3b) allow for negative values of n, a physical impossibility.

For reasons that will be discussed later, the n and K' values obtained for equations (la) or (2a) are preferable to those obtained for equation (4a).

Looking at the results for n-mer formation from monomer (equation (la)) it appears that between 4.9 and

Results of Stoichiometry Fitting of 5'-GMP in NaCla Table 2.

ro i terror		٤	×
Eduacton		**	4
u	(1a)	6.5(±1.6)	$2.7(\pm 9.1) \times 10^3$
$4nM \stackrel{?}{=} (M_4)_n$	(2a)	1.5(±0.3)	9.2(±22.) x 10 ²
4M ≠ M ₄	(3a)		$1.7 (\pm 1400000) \times 10^{-3}$
$nM_4 \stackrel{?}{\leftarrow} (M_4)_n$	(3p)	L. 6 (±3.3)	$9.8(\pm580000) \times 10^{7}$
$n_{M_4} \stackrel{+}{\leftarrow} (M_4)_n$	(4a)	6.5(±1.5)	5.8(±29.) × 10 ⁶

 $\begin{bmatrix} Na^+ \end{bmatrix} = 0.85M; \begin{bmatrix} 5' - GMP^= \end{bmatrix} = 0.13 - 0.23M; 15(\pm 1.)^OC;$ errors are estimated at the 95% confidence level.

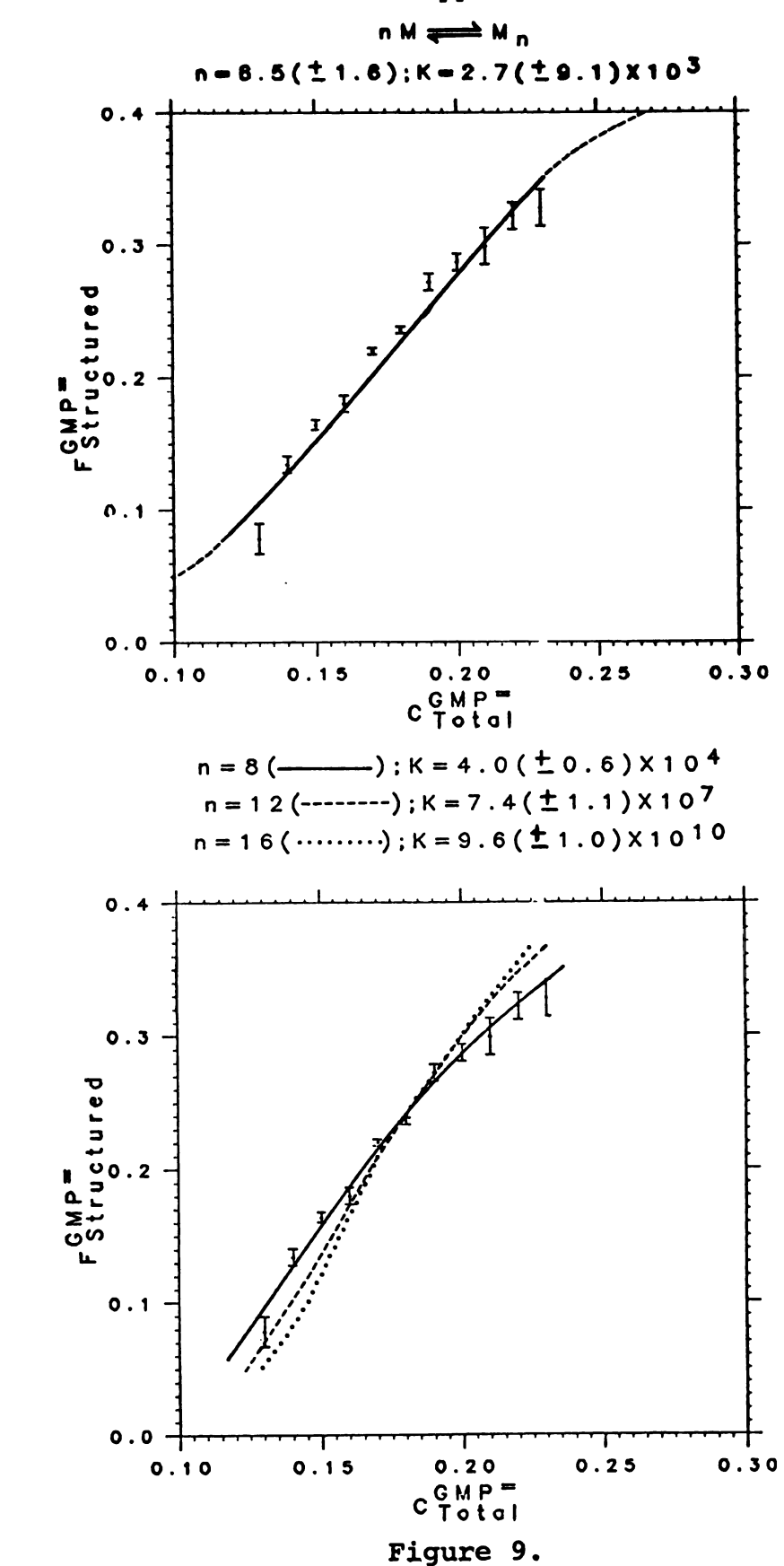
ر ا 8.1 5'-GMP units are contained in a structured unit within experimental uncertainty. No single-stranded helical
structure containing between five and eight 5'-GMP units
can explain a three line H(8) spectrum. If structure formation is assumed to be based on tetramer units, this range
of values of n would indicate between 1.2 and 2.0 tetrameric 5'-GMP sper structured form. Equation (2a) yields
a value between 1.2 and 1.8 tetramers per structured form.
Taking only integer values within this range allows the
structures to be composed of either one or two tetramers
of 5'-GMP. As will be shown later, an octamer consisting
of two stacked tetramers can explain the observed H(8)
spectrum.

A single tetramer unit has a C_4 axis perpendicular to the aromatic plane (<u>cf</u>. Figure 4). All four H(8) positions are therefore equivalent and cannot give rise to the three-line H(8) nmr spectrum observed for the ordered nucleotide.

Based on the above observations, it is believed that eight nucleotide units combine to form the aggregate in the ordered form of the sodium salt. A later section shall discuss how an octameric 5'-GMP⁼ structure can exhibit the three H(8) resonances by ¹H NMR. Figure 9a shows a plot of the best fit curve for (la) over the experimental data.

Besides the octameric form of the Na₂5'-GMP, other stoichiometries have been proposed in the literature.

Figure 9. Plots of the computed curves for equation (la) when a) n and K' are both varied, and b) K' is varied and n is held constant at either 8, 12, or 16. Experimental conditions are the same as in Table 1. Error bars represent the experimental points. Errors in n and K' are reported at the 95% confidence level.



Pinnavaia, Miles, and Becker⁴⁰ have suggested the possibility that the three tetramer plates stack to form a dodecamer. Laszlo and his coworkers,⁷⁸ in their most recent model, have introduced the possibility of stacking four tetramers to form a hexadecamer.

In an attempt to compare the validity of the dodecamer and hexadecamer models with the present octameric model, equation (la) was refitted to the data. This time, however, instead of allowing n to vary, its value was held constant at values of either 8, 12, or 16 and only the value of K was allowed to vary.

Table 3 summarizes the results of the curve-fitting of equation (la) at a constant value of n.

Figure 9b shows plots of the computed curves for the best values of K' for octamer, dodecamer, and hexadecamer formation. It is apparent from a comparison of the computed curves and the experimental data that the value of n = 8 provides a closer fit to the observed points.

Therefore, all further work shall be based on the assumption that sodium 5'-GMP forms octameric structures in aqueous solutions.

B. Model Building Investigation of Octameric Structures

Having proposed an octameric unit for the structured form of Na₂5'-GMP it is necessary to establish how the simple stacking of two tetramers can yield a three line

Table 3. Results of Curve Fitting
Equation (la) to the Data
in Table 1 with n Held to
a Constant Value.

$$nM \stackrel{K}{\stackrel{+}{\leftarrow}} M_n$$
 (la)

n	К'
8	4.0(±0.6) x 10 ⁴
12	$7.4(\pm 1.1) \times 10^7$
16	$9.6(\pm 1.0) \times 10^{10}$

a. The experimental conditions are the same as in Table 1. Errors are at the 95% confidence level.

H(8) NMR spectrum. In order to address this question, a model building study was undertaken. In addition to answering questions concerning symmetry, it was also hoped that additional stabilizing factors (e.g., additional hydrogen bonding) for octamer formation could be found.

For the stacking of tetrameric plates of 5'-GMP, the symmetry of the stacking is very important. The hydrogen bonding scheme for 5'-GMP has a pair of hydrogen bond donor atoms, N(1) and N(2), nearly orthogonal to a pair of hydrogen bond acceptors, O(6) and N(7) (cf. Figure 4). Arrows bent at right angles, the heads representing hydrogen bond donor atoms and the tails representing hydrogen bond acceptor atoms, can be used to illustrate a tetramer unit of 5'-GMP (I).

Ī

Due to the directional character of this type of bonding, the tetramer unit is prochiral independent of the ribose group. When a pair of tetramers stack, stacking can occur in either normal (head-to-tail) or reversed (head-to-head) arrangements (Figure 10). A twist angle, θ , is defined as the angle caused by the projection of a line joining the center of a tetramer unit and O(6) with a similar line on

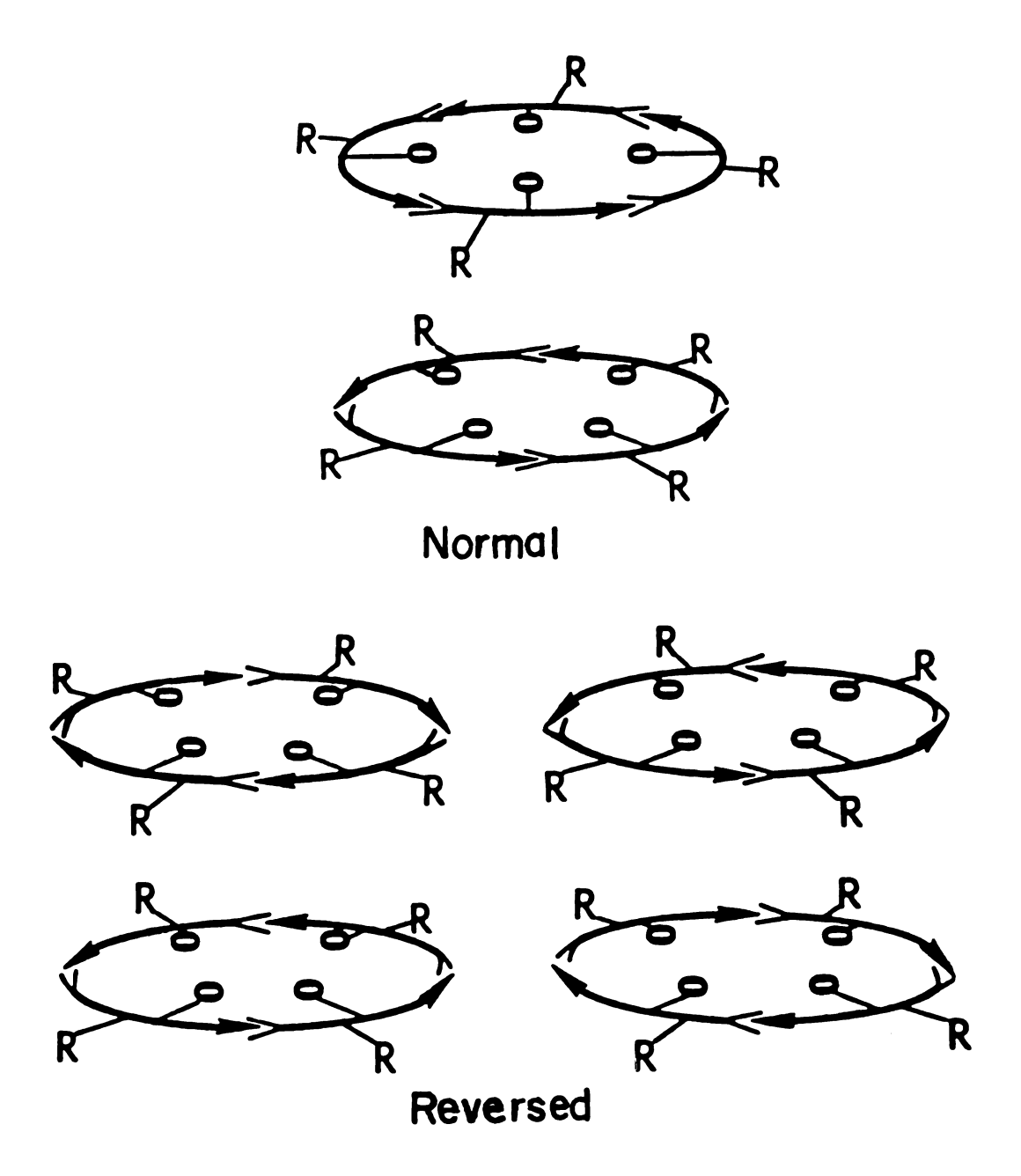


Figure 10. Schematic diagram of a) normal stacking mode and b) the two enantiomeric reversed stacking modes of the octamers of 5'-GMP.

the tetramer plate below it. The comparison is made between carbonyls of overlapping base units. θ is defined as positive if the bottom plate twists clockwise with respect to the top plate and negative for a counterclockwise twist.

Taking into account the symmetry of the possible stacking patterns, one may predict the number of H(8) lines expected for each structure. The normal stacking pattern (Figure 11), in the absence of the chiral ribose phosphate group, exists in three different symmetry states depending upon the value of θ . For $\theta = 0^{\circ}$, the symmetry is C_{Ab} and therefore the unit is achiral. When $\theta = 45^{\circ}$, the symmetry is S_8 and the unit is again achiral. However, at 0° < θ < 45° , the unit has C_{A} symmetry and, therefore, is chiral. If only the values of θ equal to $+30^{\circ}$ and -30° are considered (for reasons which will be described later), it is found that the structure with $\theta = +30^{\circ}$ is the enantiomer of the structure with $\theta = -30^{\circ}$ (designated $C_{\Delta}(CW, CW, +30^{\circ})$ and $C_A(CW,CW,-30^{\circ})$ respectively). The addition of the chiral ribose phosphate group causes the normal stacking pattern to adopt C_A symmetry, regardless of the value of θ . For $\theta = +30^{\circ}$ and -30° there are therefore two diastereomers $(C_4(CW,CW,+30^{\circ})-ribose phosphate and C_4(CW,CW,-30^{\circ})-ribose$ phosphate respectively). When $\theta = 0^{\circ}$ or 45° , these diastereomers isomerize into a single species.

Since the point group for normal stacking is C_4 , regardless of the value of θ , the top and bottom units are

Figure 11. Overlap pattern of the guanine bases for the two enantiomeric forms in the normal stacking mode of two tetramers. The dark tetramer is the top layer and the light tetramer is the bottom layer. a) $C_4(CW,CW,+30^\circ)$; b) $C_4(CW,CW,-30^\circ)$.

a) is the enantiomer of b) in the absence of the chiral ribose-phosphate group.

,

inequivalent and two H(8) environments should be observed for each value of θ . Consequently, for $\theta = +30^{\circ}$ and $\theta = -30^{\circ}$ a total of four H(8) lines are predicted for normal stacking. This would be the expected maximum at the slow exchange limit. If the twisting of the plates from $\theta = +30^{\circ}$ to $\theta = -30^{\circ}$ is fast on the NMR time scale, isomerization reduces the number of H(8) lines to two.

Figures 12 and 13 show the overlap of the purine bases for the reversed stacking modes. For the reversed stacking modes in the absence of the ribose phosphate, the symmetry is $D_{\boldsymbol{A}}$ for all values of θ . This chiral stacking pattern will give two enantiomers for a given value of θ . One is formed by the hydrogen bonds going clockwise on the top tetramer and counterclockwise on the bottom tetramer (D_4 (CW,CCW)) and the other has the hydrogen bond direction counterclockwise on top and clockwise on the bottom $(D_A(CCW,CW))$. With the attachment of the chiral ribose phosphate group the symmetry remains $\mathbf{D_4}$ and causes the enantiomeric forms to become diastereomeric. Since in D_A symmetry the tetramer plates are equivalent, each diastereomer should yield only one H(8) environment for a given value of θ . Considering only $\theta = +30^{\circ}$ and $\theta =$ -30° gives a total of four H(8) lines expected at the slow exchange limit. Rapid twisting would collapse this into a two line spectrum.

Figure 12. Overlap pattern of the guanine bases for two of the diastereomeric forms in the reversed stacking mode of two tetramers. The dark tetramer is the top layer and the light tetramer is the bottom layer.

a) D₄(CW,CCW,+30°); b) D₄(CW,CCW,+60°).

Figure 13. Overlap pattern of the guanine bases for the remaining two diastereomeric forms in the reversed stacking mode of two tetramers. The dark tetramer is the top layer and the light tetramer is the bottom layer. a) D4(CCW,CW,-60°); b) D4(CCW,CW,-30°). In the absence of the chiral ribose phosphate group, Figure 13a is the enantiomer of Figure 12b, and Figure 13b is the enantiomer of Figure 12a.

Table 4 summarizes the isomers discussed along with the number of H(8) lines expected for each exchange region. It should be pointed out that for all isomers, rapid twisting with isomerization of θ is not hindered by the ribose phosphate group.

This summary supports the assumption that the four line H(8) spectrum for Na₂5'-GMP is due to the stacking of tetramers to form octameric structures. On Figure 8, the second highest field line (labelled C) is assigned to the unassociated monomer. The lowest and highest field resonances (A and D) have been reported 40 as having equal intensities and T_1 values at all concentrations and temperatures studied and relax at the same rate upon addition of paramagnetic Mn^{2+} or Cu^{2+} . These two lines are therefore assumed to arise from two inequivalent H(8) environments on the same structured octamer. Only the normal stacking pattern has inequivalent H(8) positions on the same structure, therefore lines A and D are assigned to this stacking mode. Since only two lines with these characteristics exist (instead of four) it is assumed that the twisting mechanism is fast on the NMR time scale (cf. Table 4).

The second lowest field line (\underline{B} , Figure 8) has a different \underline{T}_1 than lines \underline{A} and \underline{D} and relaxes at a much faster rate upon addition of paramagnetic ions. ⁴⁰ It therefore arises from an octameric structure in which H(8) environments on the top and bottom tetramer plates are equivalent.

Table 4. Number of Isomers and H(8) Lines Expected for Three Exchange Regions

Conditions	Normal Stacking	Reversed Stacking	Total
Slow twisting with $\theta = +30^{\circ}$ and $\theta = -30^{\circ}$ equally preferred. Slow stack separation.	<pre>Isomers: 2 H(8) lines: 4 C_4(CW, CW, +30^O) C_4(CW, CW, -30^O)</pre>	Isomers: 4 H(8) lines: 4 D ₄ (CW, CCW, +30 ⁰) D ₄ (CW, CCW, +60 ⁰) D ₄ (CCW, CW, -30 ⁰) D ₄ (CCW, CW, -60 ⁰)	Isomers: 6 H(8) lines: 8
Fast twisting with isomerization of θ . Slow stack separation.	Isomers: 1 H(8) lines: 2 C ₄ (CW, CW, +30 ^O)	<pre>Isomers: 2 H(8) lines: 2 D₄(CW,CCW,+30⁰) D₄(CW,CCW,+60⁰) D₄(CCW,CW,-30⁰) D₄(CCW,CW,-30⁰) D₄(CCW,CW,-60⁰)</pre>	Isomers: 3 H(8) lines: 4
Fast twisting. Fast stack separation.	$c_4 (CW, CW, +30^{\circ}) + D_4 (CW)$ $c_4 (CW, CW, -30^{\circ}) D_4 (CW)$	$c_{4}(cw,cw,+30^{\circ}) + D_{4}(cw,ccw,+30^{\circ}) + D_{4}(ccw,cw,-30^{\circ})$ $c_{4}(cw,cw,-30^{\circ}) + D_{4}(cw,ccw,+60^{\circ}) + D_{4}(ccw,cw,-60^{\circ})$	<pre>Isomers: 1 H(8) lines: 1 (time averaged with tetramer (monomer))</pre>

Correspondingly this line is assigned to one of the inequivalent reversed stacking modes possessing D_A symmetry.

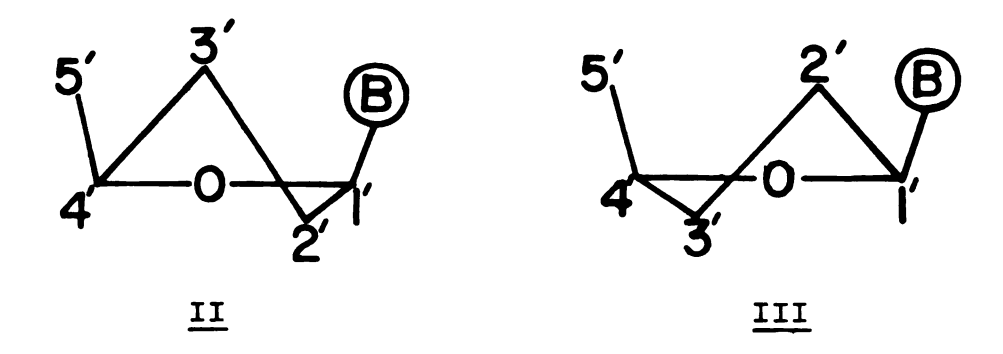
A number of crystal structures have been done on a wide variety of nucleic acid constituents and have been reviewed previously. They illustrate that the bond angles for the ribose moiety are normally confined to limited values independent of the nucleotide. Table 5 defines the four critical bond angles along with listing their most probable values. Along with these angles, there are two predominant conformations for the ribose sugar: C(3')-endo (II) for the ribonucleic acids and C(2')-endo (III) for the deoxyribonucleic acids.

Table 5. Torsional Angles and Notations for 5'-Nucleotidesa

Torsion Anglesb	Notation	Most Probable Angle
O(1')-C(1')-N(9)-C(8)	х	36° ± 19°
C(3')-C(4')-C(5')-O(5')	Ψ	53° ± 7°
C(4')-C(5')-O(5')-P	ф	187° ± 24°
C(5')-O(5')-P-O(3')	ω	69° ± 4° 294° ± 13°

a. From reference 80.

 $[\]overline{b}$. All angles A-B-C-D are measured clockwise from A to D when viewed along B-C. An eclipsing D is 0° .



In the technique employed, two tetramer units built with CPK space filling models were set up with the most common bond angles (cf. Table 5) and with C(3')-endo conformations of the ribose moiety. Both the normal and reversed stacking patterns were investigated. The twist angle, 0, was set at either +30° or -30° (±30° or ±60°) corresponding to Zimmerman's model building work with fourstranded poly(G)³⁶ in which planar tetrameric guanine units are present. The same helical parameters were also found by Zimmerman for fibers of Na₂5'-GMP grown from excess NaCl.³⁷ The bond angles were then adjusted by the smallest amount possible in order to give octameric structures with hydrogen bonds between the tetramer plates.

Table 6 shows the results of the model building studies. The parameter $\Delta \delta_{H(8)}$ is the intermolecular shielding (in ppm) for an H(8) nucleus 3.4 Å above or below the ring plane due to the sum of the contributions of the ring current and of the atomic diamagnetic susceptibility anisotropies as calculated by Giessner-Prettre and Pullman. See Several important points should be noted

Results of the Model Building Study of the Octameric Forms of 5'-GMP Table 6.

Θ	×	∌∙	•	3	(mdd) (8) $^{\mathrm{Q}}$	Ribose Conformations	Hydrogen Bonds
Normal Stacking C ₄ (CW, CW, +30 ^O) C ₄ (CW, CW, -30 ^O)	200	20° 60° 18	20° 60° 181° 20° 60° 181°	o 69	0000	C(3')-endo	Four OH(3')+ OP bonds Four OH(2')+ OP bonds
Reversed Stacking D_{4} (CCW, CW, -30°) 20° 60° 18° D_{4} (CCW, CW, -60°) 20° 60° 18°	20° 20° 20°	09	181 ⁰ 181 ⁰	069	0.5200.52	C(3')-endo	Eight NH(2)→ OP bonds Eight NH(2)→ OP bonds
Reversed Stacking $D_{4}(CW,CCW,+30^{\rm O}) 20^{\rm O} 60^{\rm O} 18$ $D_{4}(CW,CCW,+60^{\rm O}) 20^{\rm O} 60^{\rm O} 18$	20°	009	181 ⁰ 181 ⁰	o69	0.2 0.2 0.2	C(3')-endo C(3')-endo	Four OH(2')→ O(3') bonds Four OH(2')→ OP bonds

from this table. First, it is significant that in all eight octamer structures studied, the nucleotide has to undergo little variation from its "normal" bond angles in order to gain at least four and in two cases eight additional hydrogen bonds between the top and bottom tetramer plates. Second, it should also be noted that this variance is self-consistent for all eight structures.

C. Metal Ion Stoichiometry: Na Salt

Having established the nucleotide stoichiometry at eight for the solution ordering of Na₂5'-GMP, we now direct our attention to the number of metal ions required per structured unit. The equilibrium expression can be written as

$$xNa^{+} + 8M^{2-} \stackrel{?}{\leftarrow} Na_{x}M_{8}^{(16-x)-}$$
 (5a)

with the equilibrium constant, K, defined as

$$K = \frac{\left[Na_{x}^{M_{8}^{(16-x)}}\right]}{\left[Na^{+}\right]^{x}\left[M^{2-}\right]^{8}}$$
 (5b)

In the experimental procedure for determining K and x in equation (5b), two important criteria were met.

First, the total 5'-GMP concentration was held constant in order to determine only the effect of the Na⁺. This

was accomplished by adding incremental amounts of $0.78\underline{M}$ Na₂5'-GMP into $0.78\underline{M}$ (TMA)₂5'-GMP. Second, care was taken to avoid changes in ionic strength. Data were collected with $0.5\underline{M}$ TMACl to keep the ionic strength nearly constant ($\mu = 2.8 \, (\pm 0.1)\underline{M}$). The NMR spectra used were provided by Bouhoutsos-Brown. 50

Table 7 lists the fraction of 5'-GMP structured as a function of the 5'-GMP to Na⁺ ratio. These data were fit to equation (5b) using KINFIT (see Experimental section for full details). This resulted in a value of $x = 4.1(\pm 0.1)$ and $K = 1.7(\pm 0.7) \times 10^{10} \, \underline{\text{M}}^{-11}$ at the 95% confidence level. This would indicate that four Na⁺ ions are required for every octamer unit.

Bouhoutsos-Brown⁵⁰ has proposed that each octamer requires six Na⁺ ions in order for the structure to be formed. The results in Table 6 were refitted using KINFIT allowing only K to vary and holding x constant at six. This calculation yields a value of K = $3.5(\pm 21.) \times 10^8 \, \text{M}^{-9}$ at the 95% confidence level. Due to the high standard deviation in the value of K when x = 6,it appears that a value of four is a more acceptable value.

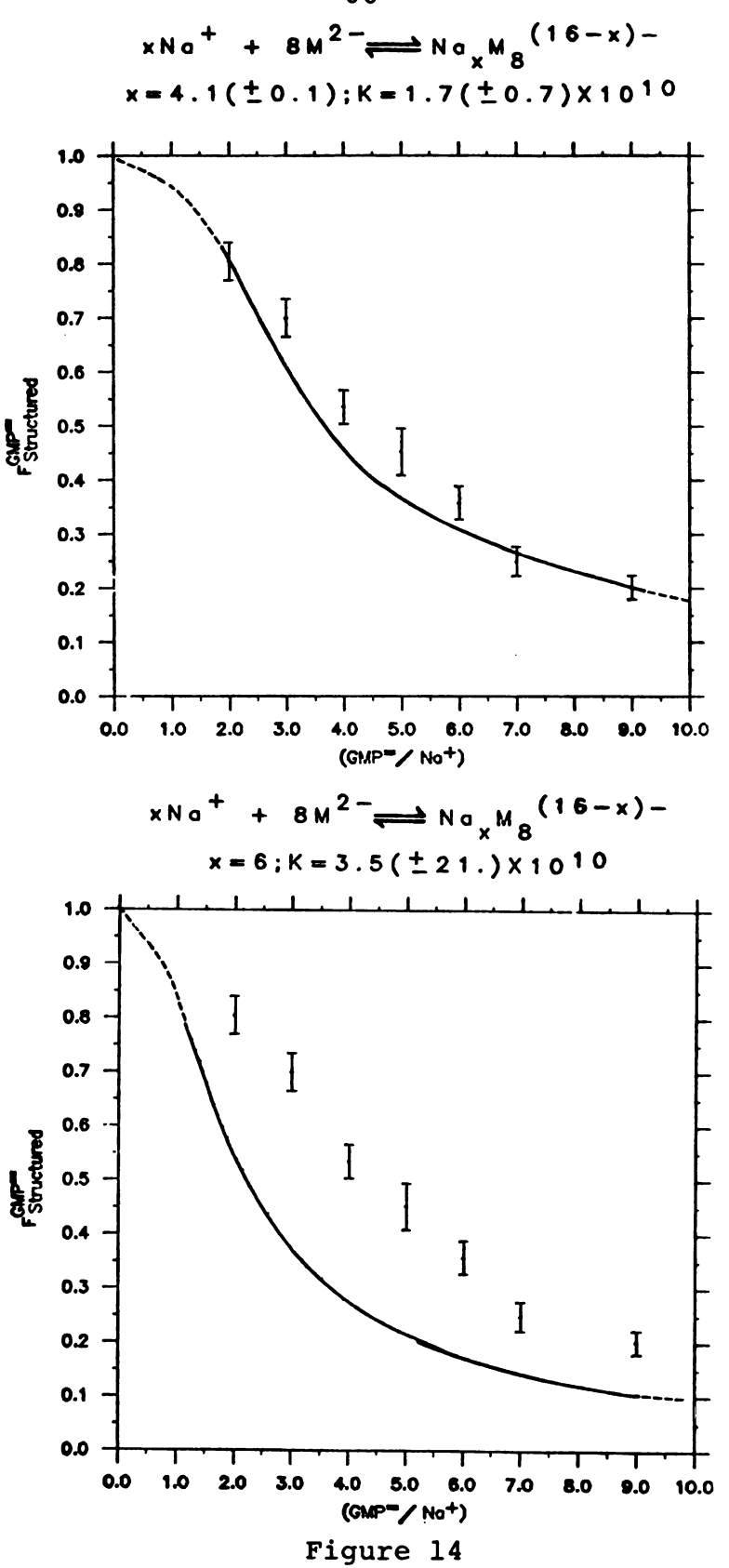
Figure 15 shows plots of the ratio of $5'-GMP^{=}/Na^{+}$ versus the fraction of $5'-GMP^{=}$ structured showing the fitted curves when x and K both are varied and when x = 6 and K is varied.

Table 7. Fraction of Structure of 5'-GMP with Changing 5'-GMP=/Na+ a

S'-GMP ⁼ Na ⁺	F _{structured}
2.0	0.805(±0.035)
3.0	0.700(±0.035)
4.0	0.535(±0.031)
5.0	0.452(±0.043)
6.0	0.358(±0.031)
7.0	0.249(±0.027)
9.0	0.202(±0.022)

a. 0.78M 5'-GMP added into 0.78M (TMA)₂5'-GMP and 0.5 M TMAC1; 0.3°C; ionic strength = 2.8(±0.1)M.

Figure 14. Plots of the best fits for equation (5a) with a) the values of x and K allowed to vary and b) x held constant at 6 and K allowed to vary. Experimental conditions are the same as in Table 7. Error bars represent the experimental points. Errors in x and K are reported at the 95% confidence level.



D. Interaction of Intercalation Compounds with Structured Na₂5'-GMP and K₂5'-GMP

Due to the fact that the stacking of hydrogen bonded tetramers of 5'-GMP is structurally similar to the polynucleotides, an attempt was made to insert intercalation compounds either between the tetramers or to bind the compounds on the external surfaces of the stacked tetramers. Studies were done on the intercalation compounds ethidium bromide (EtdBr) and platinum(II)2,2',2"-terpyridyl chloride (Pt(terpy)Cl₂) (cf. Figure 7). In addition, the disodium and dipotassium salts of the water soluble porphyrin, hematoporphyrin (Figure 15), were investigated. Measurement

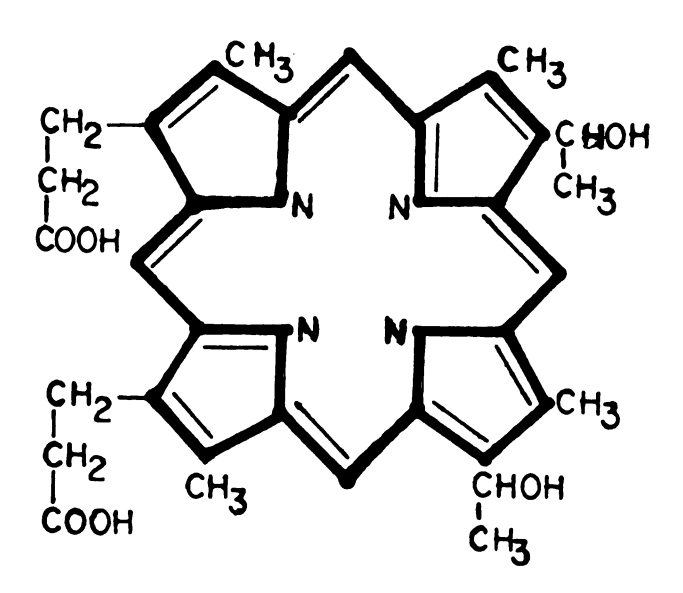


Figure 15. Structure of hematoporphyrin.

of CPK models of the tetramer and the porphyrin show that one aromatic porphyrin should be the appropriate size to overlap with one of the tetramer units. Unfortunately, the hematoporphyrin proved too insoluble in aqueous solution to give adequate NMR spectra at concentrations where 5'-GMP shows structure formation. At high concentrations of either Na₂5'-GMP or K₂5'-GMP the intensity of the chemical shifts due to the porphyrin were too weak to be observed. No change in chemical shift or intensity of either the structure or monomer H(8) resonances was observed. These observations were taken to mean that little or no interaction was occurring.

The addition of Pt(terpy)Cl₂ to structured forms of Na₂5'-GMP and K₂5'-GMP caused precipitation of all the platinum salt and some of the nucleotide. Lippard and coworkers, ⁸³ in work with Pt(terpy)Cl₂ and calf thymus DNA, have proposed that in addition to intercalation, the platinum-chloride bond is sufficiently labile to be broken in aqueous medium and a new covalent bond is formed to the DNA. They postulated that the platinum binds to nitrogen donors on the aromatic bases thereby disrupting the normal hydrogen bonding scheme. If a similar reaction is expected with 5'-GMP⁼, the platinum would be expected to bond to the N(7) position and block tetramer formation. The precipitate was therefore assumed to be a platinum-5'-GMP complex.

E. Interaction of Ethidium Bromide with Structured and Unstructured Forms of Na₂5'-GMP

The addition of the intercalation drug ethidium bromide (EtdBr) to Na₂(5'-GMP) does not cause precipitation. A preliminary investigation of the change in chemical shifts of both the drug and nucleotide resonances revealed interactions were occurring. This led to a more quantitative investigation of the interaction.

Figure 16 shows the effect of the addition of Na₂5 GMP into 0.034M EtdBr at 5°C. The top spectrum represents the spectrum of the "free" EtdBr with chemical shifts the same as previously characterized by Kreishman and Chan. Hey assigned the resonances as follows (see Figure 7 for numbering sequence): para- and meta-protons on phenyl group between 7.8 and 7.7 ppm; H(1) and H(10) at 7.69 and 7.65 ppm respectively; the ortho-position of the phenyl group, H(2), H(9), and H(4) between 7.20 and 7.06 ppm; H(7) at 6.26 ppm; methylene resonance at 4.40 ppm; and methyl resonance at 1.40 ppm. Splitting between the methyl resonance and methylene resonance (J = 8.3 Hz) is incompletely resolved at this concentration and temperature due to some base stacking of the drug with itself.

As the drug becomes intercalated, Kreishman and Chan reported a general upfield movement of the aromatic resonances along with considerable broadening. 69 H(1) and H(10) were observed to shift upfield to ~ 8.0 ppm; H(2), H(4), and H(9) shift upfield to the region of ~ 6.6 to 7.2 ppm;

Figure 16. Effect on the ¹H NMR of adding Na₂5'-GMP into 0.034<u>M</u> EtdBr at 5°C. Nucleofide H(8) resonances are denoted by shading.

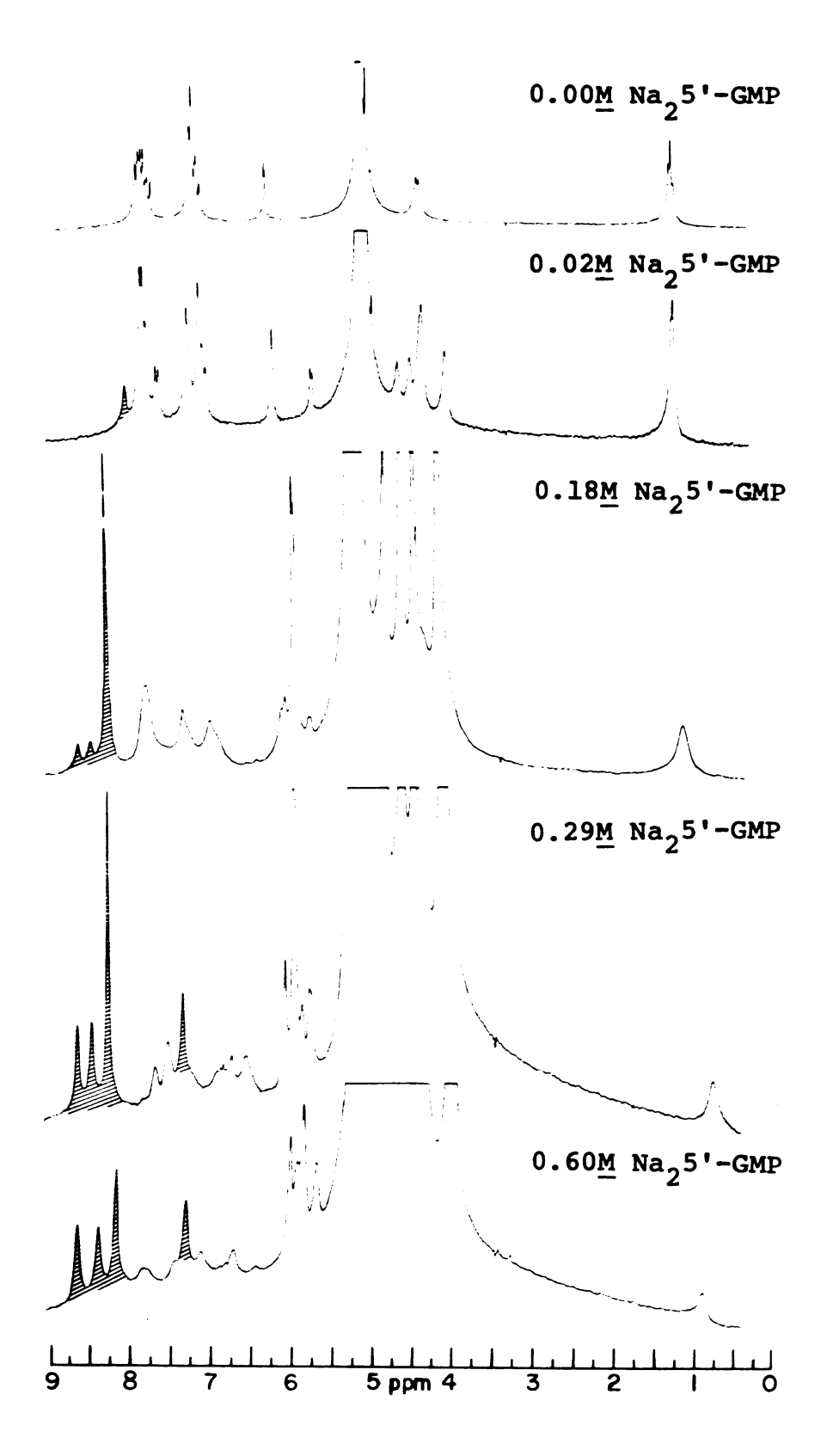


Figure 16.

and H(7) moves to a position under the nucleotide's H(1') resonance at ~ 5.9 ppm. The chemical shifts of the <u>ortho-</u>, <u>meta-</u>, and <u>para-hydrogens</u> of the phenyl group on the drug exhibit no change upon intercalation.

As a small amount $(0.02\underline{M})$ of Na_25' -GMP is added into the solution, below the concentration at which structure formation begins to occur, dramatic spectral changes can be observed. First, the aromatic region of the EtdBr spectrum broadens substantially and generally shifts upfield. This is the same general movement observed by Kreishman and Chan upon intercalation of the drug. 69 Due to overlap, most resonances cannot be assigned; however, H(7) has shifted from 6.26 to 6.13 ppm. A small upfield shift of the methyl resonance of the drug (~ 0.05 ppm) is also observed. drug methylene resonance has become obscurred by the ribose protons of the 5'-GMP ($\delta_{H(1')} = 5.63 \text{ ppm}$, $\delta_{H(2')} = 4.59$ ppm, $\delta_{H(3')} = 4.44 ppm$, $\delta_{H(4')} = 4.29 ppm$, and $\delta_{H(5')} =$ 4.00 ppm). The most dramatic change, however, is that the monomer H(8) resonance of the 5'-GMP, which in the absence of the drug has a chemical shift of 8.22 ppm at this concentration and temperature, has shifted upfield to 7.94 ppm. Since no evidence of structure formation is apparent, the shift of the H(8) line and the change in the drug resonance indicate that the EtdBr is interacting with the 5'-GMP in some manner which perturbs the chemical shift of the aromatic region of the spectrum. This is most likely due

to base stacking of the EtdBr and 5'-GMP monomer. This type of monomer nucleotide interaction with the drug has been suggested by Waring to explain the change in the extinction coefficient of EtdBr upon addition of mononucleotides or deoxymononucleotides.

As the concentration of monomer nucleotide increases, the monomer H(8) resonance moves downfield until at 0.18M it remains at 8.10 ppm, 0.07 ppm upfield of its position at the same concentration and temperature in the absence of the drug. At this concentration, structure formation of the 5'-GMP is observable. Two new H(8) resonances at 8.48 and 8.33 ppm can be observed. These are presumably the same structure lines (A and B, Figure 8) which have chemical shifts of 8.55 and 8.26 ppm in the absence of added drug. The change in their chemical shift is an indication that the drug is also interacting with the structures in some way. The highest field structure line (D, 7.25 ppm in absence of drug) appears at 7.18 ppm, partially overlapping with some of the aromatic resonances. The most notable change, however, is that the resonance associated with the methyl group on the EtdBr has moved upfield to 1.07 ppm. As the total concentration of Na₂5'-GMP in the system increases and the concentration of structure increases, the drug methyl resonance continues to move upfield. At 0.29M Na₂5'-GMP the methyl resonance has moved upfield to 0.69 ppm. Upfield shifts of the methyl resonance have been reported previously when EtdBr intercalates with dinucleoside monophosphates. $^{67-69}$ However, in these cases, the maximum change in chemical shift in the upfield direction ($\Delta\delta$) was only about 0.50 ppm. The upfield shift of the drug methyl resonance, relative to the uncomplexed state ($\Delta\delta$ = 0.71 ppm), is therefore 0.21 ppm higher field than has been observed previously.

A further increase in the total concentration of structured Na₂5'-GMP causes the drug methyl resonance to shift downfield until at 0.60M Na₂5'-GMP its chemical shift reaches 0.85 ppm. Any further increase in the total concentration of Na₂5'-GMP causes no further change in this methyl resonance. In addition, as the concentration of structure is further increased, the H(8) structure lines approach the chemical shifts that are observed in the absence of the drug.

These observations indicate that when Na₂5'-GMP is added into a solution of EtdBr, two modes of binding can be observed. The first, denoted as "monomer binding," occurs at low concentrations of Na₂5'-GMP and is characterized by the upfield shift of the H(8) monomer resonance. The second, denoted as "structure binding," is observed only at concentrations of Na₂5'-GMP which are high enough for structure formation to be observed. Structure binding of the drug to the 5'-GMP is most easily characterized by the large upfield shift of the methyl resonance of the EtdBr.

Binding of the drug to the structured nucleotide does not appear to perturb the structure to a great extent as can be noted by the small changes of chemical shift of the H(8) structure lines ($\Delta \delta \approx 0.07 \text{ ppm}$). It does however have a pronounced effect on the total amount of structure for a given concentration and temperature. Figure 17 shows the fraction of 5'-GMP structured as a function of the total 5'-GMP in solutions containing and absent of EtdBr. It is readily apparent that the fraction of structure is increased in the solution that contains EtdBr. This is especially apparent at the lower concentrations of Na₂5'-GMP. This is probably attributable to the drug acting as a template for structure formation. The tricyclic aromatic portion can most efficiently overlap with two hydrogen bonded base pairs. If this were to occur in the case of Na₂5'-GMP this could be a precursor to the formation of the tetramers and later the octamers.

Figure 18 shows the chemical shift of the EtdBr methyl resonance as a function of the ratio of the amount of structured Na₂5'-GMP to EtdBr. The upfield then downfield chemical shift changes indicate that two separate complexes are being formed between the EtdBr and the structured Na₂5'-GMP. Extrapolation of the linear portions of the curve indicates that these stoichiometries are approximately four and eight 5'-GMP⁼'s per drug molecule. If it is assumed that the octamer is the basic unit of

Fraction of Na₂GMP Structured With & Without Drug $(\Delta = Without; \Box = With)$

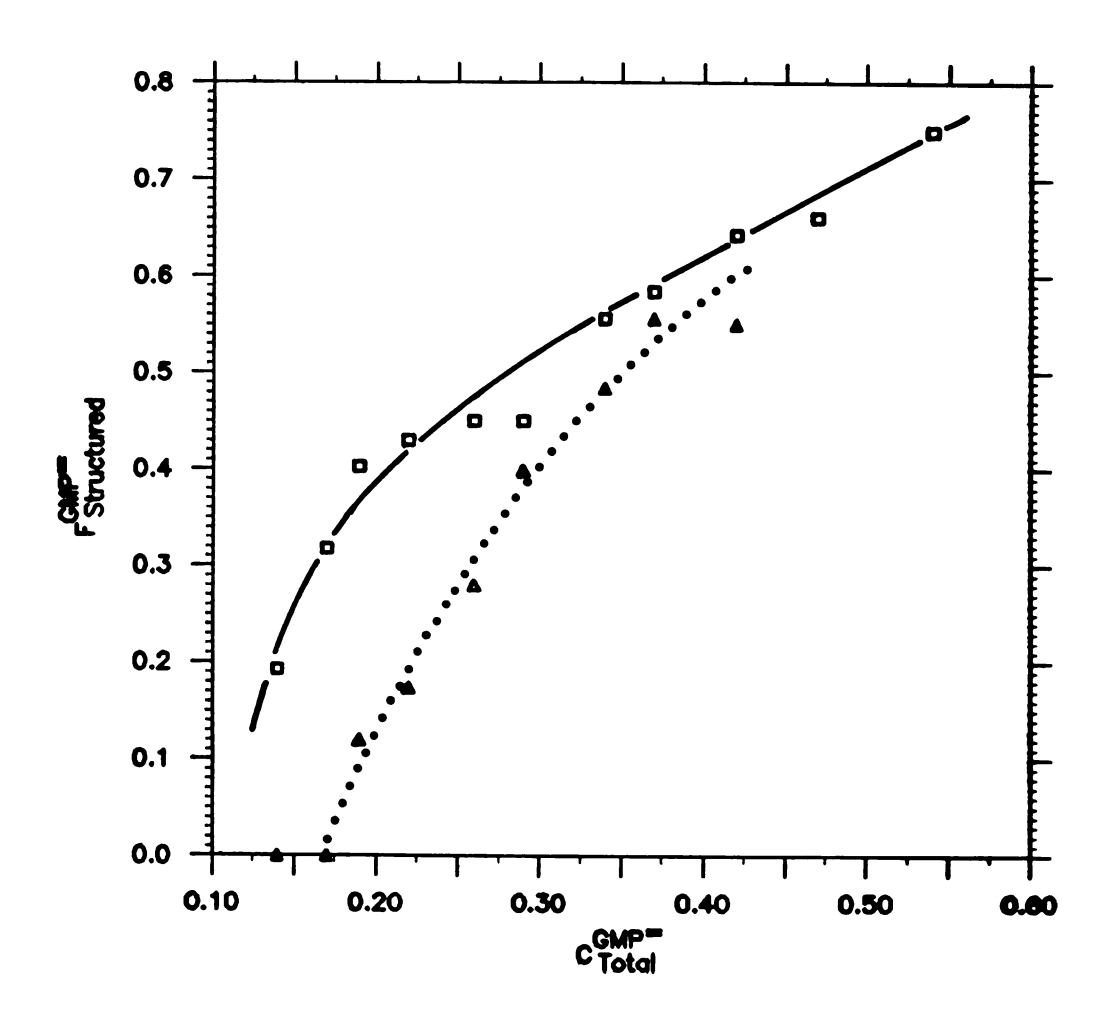


Figure 17. Effect of the fraction of Na₂5'-GMP structured in the presence (□) and in the absence (Δ) of EtdBr. Experimental conditions are the same as in Figure 16.

Structured 5'-GMP Binding to EtdBr Sodium Salt

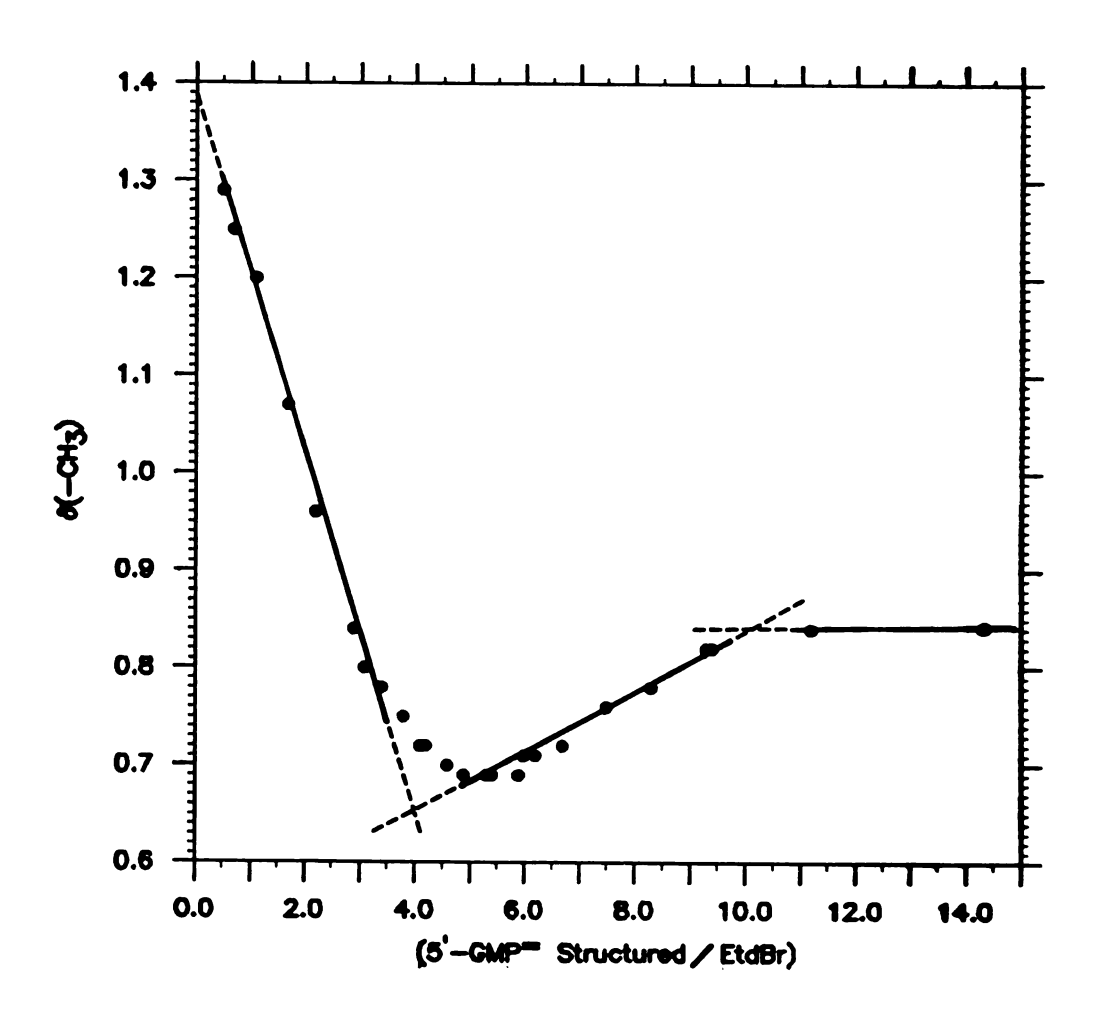


Figure 18. Plot of the chemical shift of the EtdBr methyl resonance as a function of the structured Na₂5'-GMP/Drug ratio. Extrapolation of the linear portions of the curve included.

structured Na₂5'-GMP this would indicate the binding of two and one drug molecules per structured unit respectively.

A two step equilibrium process can therefore be written for the formation of the two structure-drug complexes.

$$M_8 + 2D \stackrel{K_1}{\neq} M_8 \cdot D_2$$
 (6a)

$$M_8 \cdot D_2 + M_8 \stackrel{K_2}{\stackrel{?}{=}} 2M_8 \cdot D \tag{6c}$$

$$K_1 = \frac{\left[M_8 \cdot D_2\right]}{\left[M_8\right] \left[D\right]^2} \tag{6b}$$

$$K_2 = \frac{\left[M_8 \cdot D\right]^2}{\left[M_8 \cdot D_2\right]\left[M_8\right]} \tag{6d}$$

Popov and coworkers 75 observed a similar change in the 133 Cs chemical shift in the reaction of Cs⁺ with the macrocyclic polyether 18-crown-6 (18C6). In their work, they used KINFIT to determine the binding constants K_1 and K_2 for the complexes Cs(18C6)⁺ and Cs(18C6)⁺ respectively. In the present work, their equations have been modified (see Experimental section for details) to solve for values of K_1 , K_2 , δ_1 , the chemical shift of the drug for $M_8 \cdot D_2$,

and δ_2 , the chemical shift of the drug for $M_8 \cdot D$, using the data from Figure 18.

This curve-fitting yields values of $K_1 = 6.4 (\pm 6.4) \times 10^5 \, \text{M}^{-2}$, $K_2 = 1.1 (\pm 0.54) \times 10^3$, $\delta_1 = 0.47 (\pm 0.11)$, and $\delta_2 = 0.86 (\pm 0.01)$. Figure 19 shows this theoretical curve plotted against the experimental data. The curve seems to diverge from the data in the first part of the curve where the equilibrium defined by K_1 is very large. Its large standard deviation could be an indication that the technique is insensitive to changes in the data for large values of K. To test this hypothesis, an attempt was made to fit the data with K_1 held constant at two orders of magnitude higher and lower than the previously calculated value and only K_2 , δ_1 , and δ_2 allowed to vary.

Figure 20 shows the plots for K_1 = constant = 6.4 x 10^3 and K_1 = constant = 6.4 x 10^7 . The values obtained for the former case appear to diverge away from the experimental points even further. It should also be noted that the δ_1 value of -1.7(±0.75) appears far too low in comparison to the extrapolated value of 0.63 (cf. Figure 19). The curve obtained for K_1 = constant = 6.4 x 10^7 fits the data at low M_8 /D ratios better but the fit is unsatisfactory at the intermediate values where the equilibrium defined by K_2 becomes important. The calculated value of δ_1 = 0.67(±0.01) agrees well with the extrapolated value.

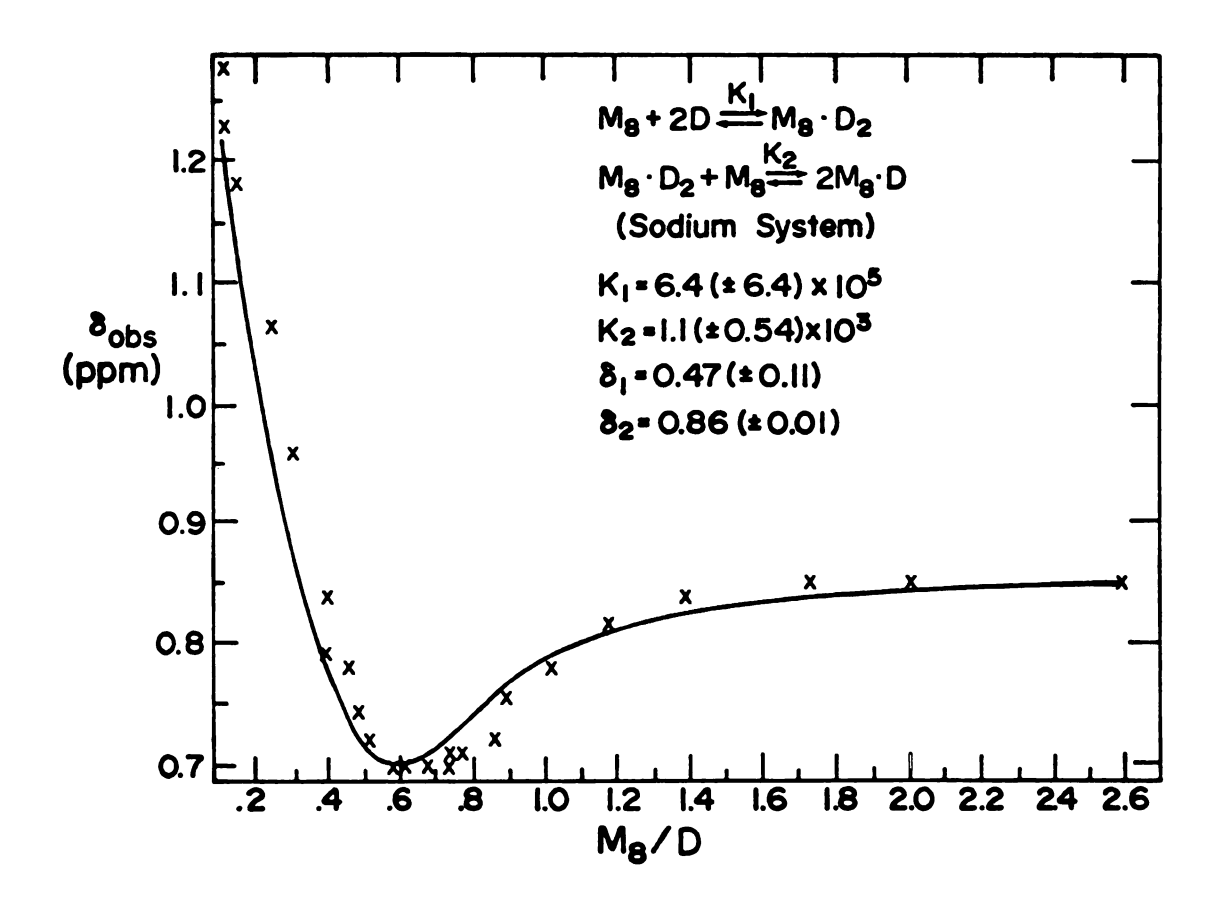


Figure 19. Plot of the best fit curve for equations (6a) and (6c). $\delta_{\rm Obs}$ is the observed chemical shift in ppm of the EtdBr methyl resonance and M₀/D is the ratio of the structured Na₂5'-GMP to total drug. X's represent experimental points. Errors in K's and δ 's are standard deviations.

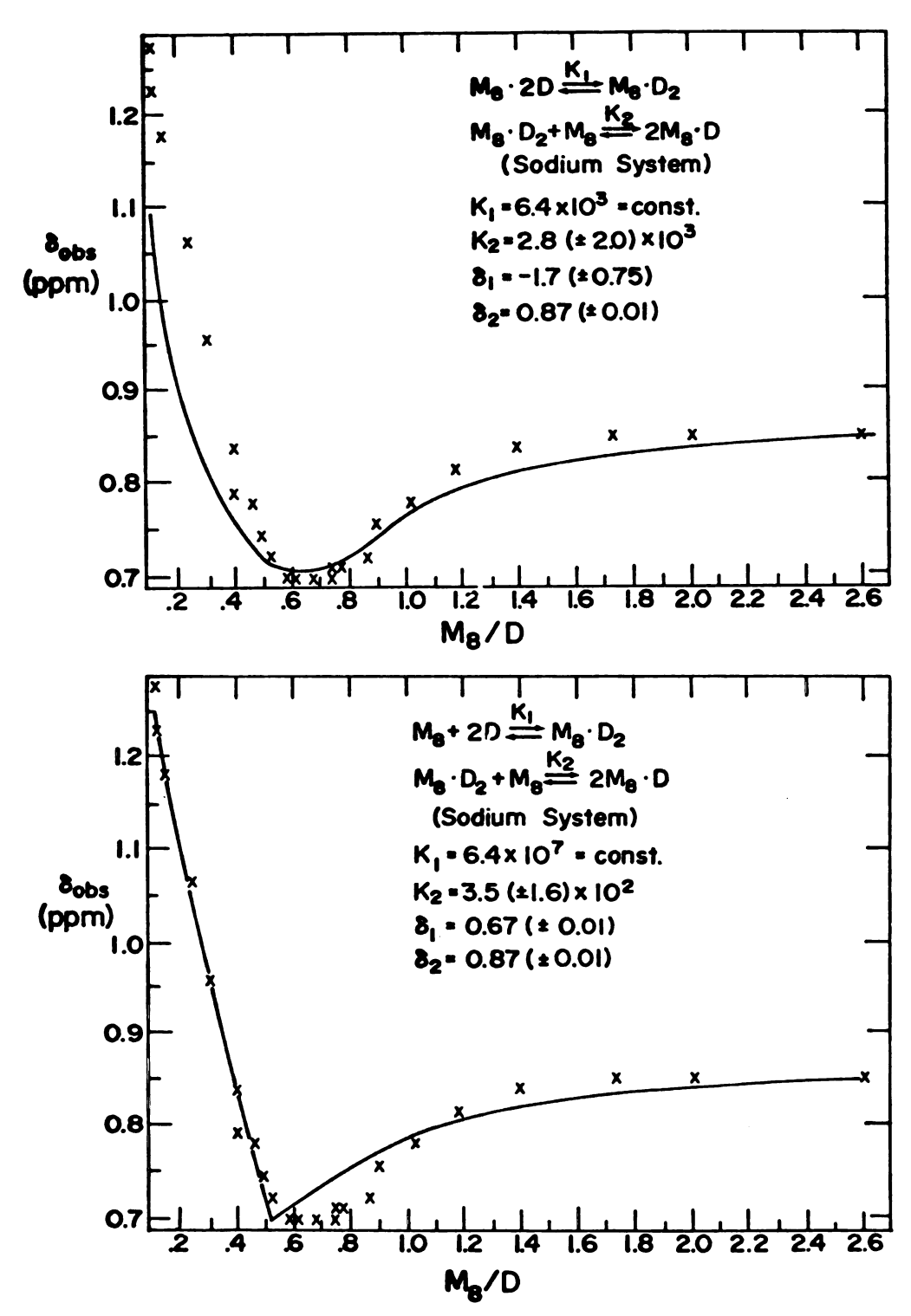


Figure 20. Plots of the best fits for equations (6a) and (6c) in which K_1 is held constant at a) 6.4 x 10^3 and b) 6.4 x 10^7 and only K_2 , δ_1 and δ_2 are allowed to vary. Legends are the same as in Figure 19. Errors in K_2 and δ 's are standard deviations.

It therefore appears that the value of K_1 for equation (6a) lies somewhere between 10^5 and 10^7 ($10^5 \le K_1 \le 10^7$). As a final check on this assumption, the data were again fitted allowing K_1 and K_2 to vary, and δ_1 and δ_2 were held constant at their extrapolated values of 0.63 and 0.87 ppm (<u>cf</u>. Figure 19). The results of this calculation are shown in Figure 21. The value of $K_1 = 5.1(\pm 1.8) \times 10^6$ lies well within the expected value. Therefore, acceptable values would be $10^5 \ \underline{\text{M}}^{-2} \le K_1 \le 10^7 \ \underline{\text{M}}^{-2}$, $K_2 = 1.1(\pm 0.54) \times 10^3$, $\delta_1 = 0.47(\pm 0.11)$, and $\delta_2 = 0.86(\pm 0.01)$.

F. Interaction of Ethidium Bromide with Structured and Unstructured Forms of K25'-GMP

Figure 22 shows the results of adding K_2^5 '-GMP into a $0.029\underline{M}$ solution of EtdBr at 5° C. As in the case of the addition of Na_2^5 '-GMP to EtdBr an interaction is apparent between the monomer and the drug. This is characterized as it was in the Na_2^5 '-GMP case by a strong upfield shift of the H(8) monomer resonance. At $0.01\underline{M}$ this resonance, which has a chemical shift of 8.22 ppm moves upfield to 7.88 ppm. As the concentration of monomer K_2^5 '-GMP is increased, the monomer H(8) resonance moves to lower field indicating that for the equilibrium

$$M + D \stackrel{\rightarrow}{\downarrow} M \cdot D \tag{9}$$

an excess of monomer (M) is being build up.

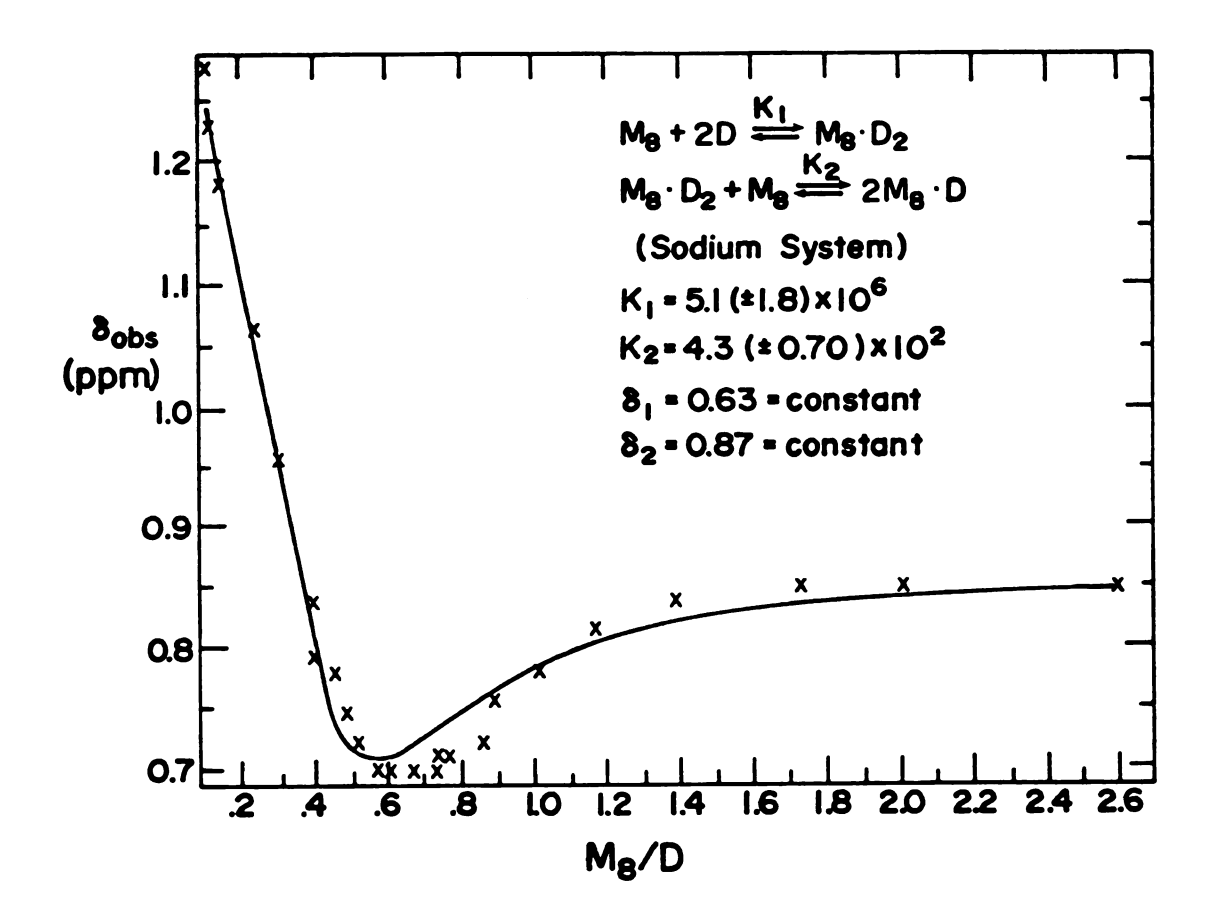


Figure 21. Plot of the best fit for equations (6a) and (6c) in which δ_1 and δ_2 are held constant at 0.63 and 0.87 ppm and K_1 and K_2 are allowed to vary. Legends the same as in Figure 19. Errors in K_1 and K_2 are standard deviations.

Figure 22. Effect on the ¹H NMR of adding K₂5'-GMP into 0.029M EtdBr at 5°C. Nucleotide H(8) resonances denoted by shading.

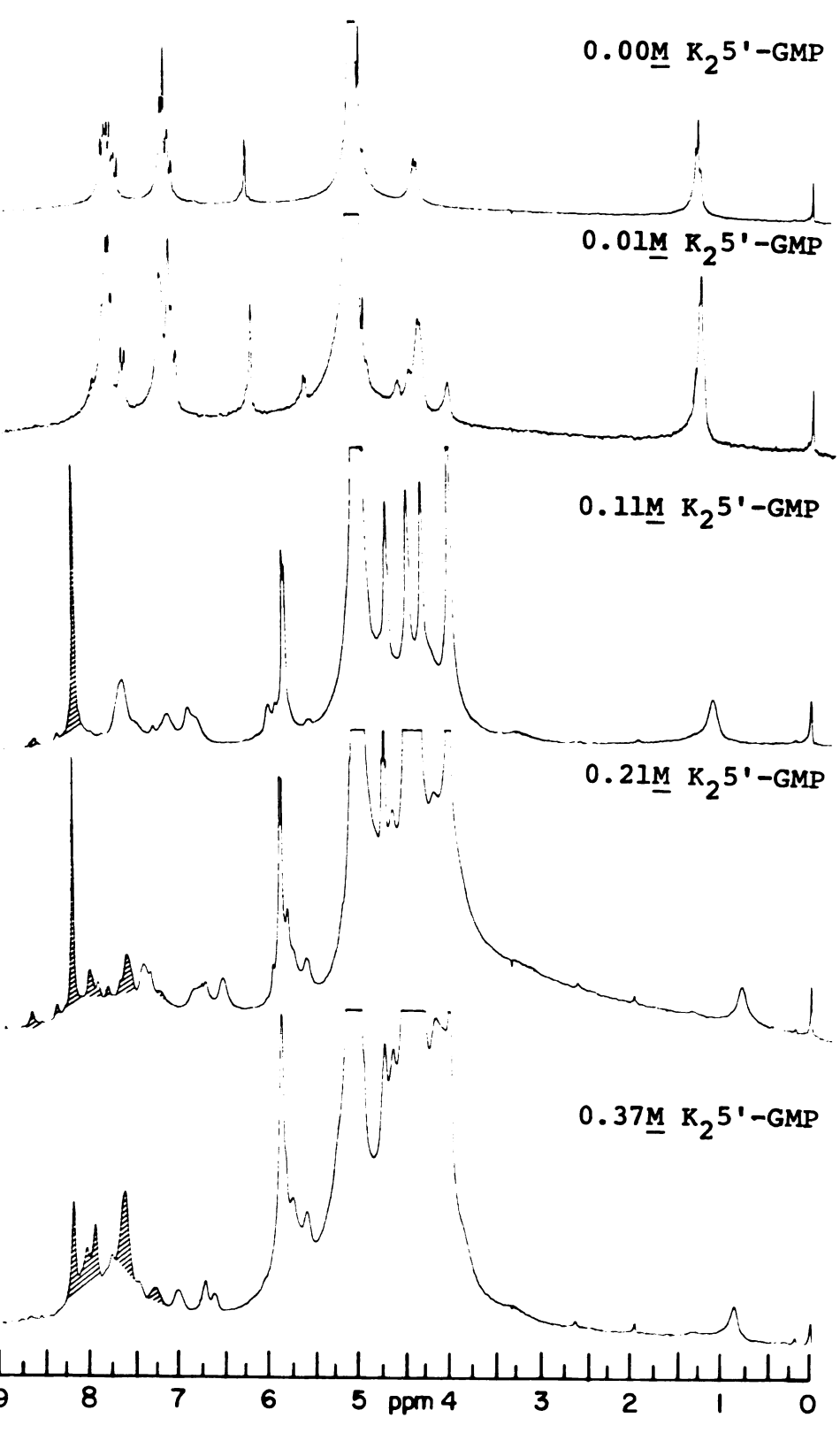


Figure 22.

At 0.11M K₂5'-GMP structure formation begins to occur as evidenced by new lines appearing in the H(8) region of the spectrum. In addition to the normal K₂5'-GMP structure lines which appear between 8.01 and 7.23 ppm, ^{42,43} two new H(8) resonances appear at 8.56 and 8.32 ppm. These lines were confirmed as H(8) resonances by recording the spectrum with deuterium selectively substituted for H(8). ⁸⁵ These lines have never been observed in spectra of structured K₂5'-GMP. Their chemical shifts, however, are very close to those of the two lowest field resonances (cf. A and B, Figure 8) in the NMR spectrum of structured Na₂5'-GMP. This would indicate that EtdBr, at least to some extent, has structure directing or structure altering abilities, similar to those of the alkali metal ions.

As was observed in the $\mathrm{Na_25'}\text{-}\mathrm{GMP}$ system, the drug's methyl resonance moves upfield with increasing concentration of structure. This indicates that EtdBr forms a "strong" complex with structured $\mathrm{K_25'}\text{-}\mathrm{GMP}$. The upfield movement of this methyl resonance continues as the total concentration and hence the structured concentration of $\mathrm{K_25'}\text{-}\mathrm{GMP}$ increase. At $0.21\underline{\mathrm{M}}$ total nucleotide concentration, the drug methyl resonance ceases moving upfield with further increases in nucleotide concentration and begins to move downfield, as was observed in the $\mathrm{Na^+}$ case. Above a total concentration of nucleotide of $0.52\underline{\mathrm{M}}$, the drug's methyl resonance has a chemical shift of 0.90 ppm

independent of nucleotide concentration. It is interesting to note that at concentrations of total nucleotide higher than required for the drug methyl resonance to be at its highest field position, the two new H(8) structure lines (8.56 and 8.32 ppm) decrease in intensity and eventually disappear altogether. This would indicate that although the EtdBr has some structure perturbing properties, the structuring ability of the K⁺ ion is far stronger. However, EtdBr also destabilizes the K⁺/5'-GMP self-structure. At 0.37M K₂5'-GMP in the presence of the drug about 25% of the nucleotide is in the monomer form (cf. Figure 22). In the absence of drug at this concentration the monomer represents less than 10% of the total 5'-GMP concentration. 42

Figure 23 shows a plot of the chemical shift of the EtdBr methyl resonance as a function of the ratio of structured K₂5'-GMP to total EtdBr. The general shape of the curve is the same as the shape observed in the case of Na₂5'-GMP/EtdBr (cf. Figure 18). Extrapolation of the linear portions provides estimates of the chemical shifts and stoichiometries of the two K₂5'-GMP/EtdBr complexes (0.72 and 0.90 ppm and 4.0 and 11.6 respectively). Due to the similarities between this system and the Na⁺ system, an attempt was made to fit this data to equations (6a) and (6c) using KINFIT. This calculation yields values of K₁ = 3.1(±1.5) x 10^4 $\underline{\text{M}}^{-2}$, K₂ = 2.7(±0.86) x 10^3 $\underline{\text{M}}^{-2}$, δ_1 = -0.29(±0.32) ppm, and δ_2 = 0.91(±0.01) ppm. A plot of

Structured 5'-GMP Binding to EtdBr Potassium Salt

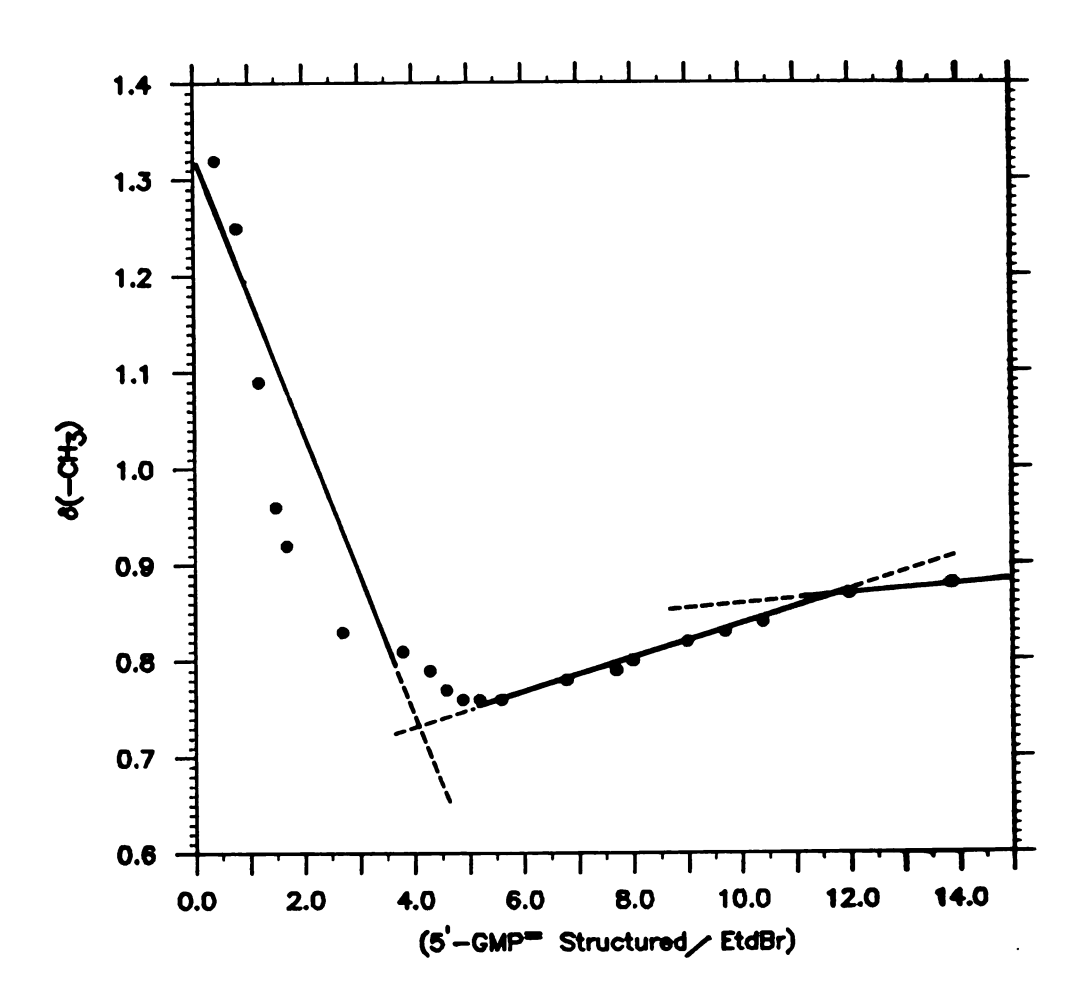


Figure 23. Plot of the chemical shift of the EtdBr methyl resonance as a function of the structured K25'-GMP/Drug ratio. Extrapolation of the linear portions of the curve included.

the best fit to the experimental data points is shown in Figure 24a. The curve appears to fit the data very well. The only questionable result is the chemical shift of the $M_8 \cdot D_2$ species, δ_1 , which at -0.29 ppm would be an enormous upfield shift ($\Delta \delta = 1.69$ ppm versus the free drug). This led to the search for an alternative model.

It has been proposed by Bouhoutsos-Brown that the predominant species in solution for a structured $K_2^{5'}$ -GMP system is a hexadecamer. Therefore an attempt was made to fit the two step equilibrium

$$M_{16} + 2D \stackrel{?}{=} M_{16} \cdot D_2$$
 (10)

$$^{M}_{16} \cdot ^{D}_{2} + ^{M}_{16} \stackrel{?}{\leftarrow} ^{2M}_{16} \cdot ^{D}$$
 (11)

Figure 24b shows the result of fitting equations (10) and (11).

It appears obvious from a comparison of the fit of the curve to the experimental points and also the high standard deviations for three of the four parameters that a hexadecamer interacting with the drug molecules does not fit nearly as well as an octamer interacting with the drug in the case of K_25' -GMP.

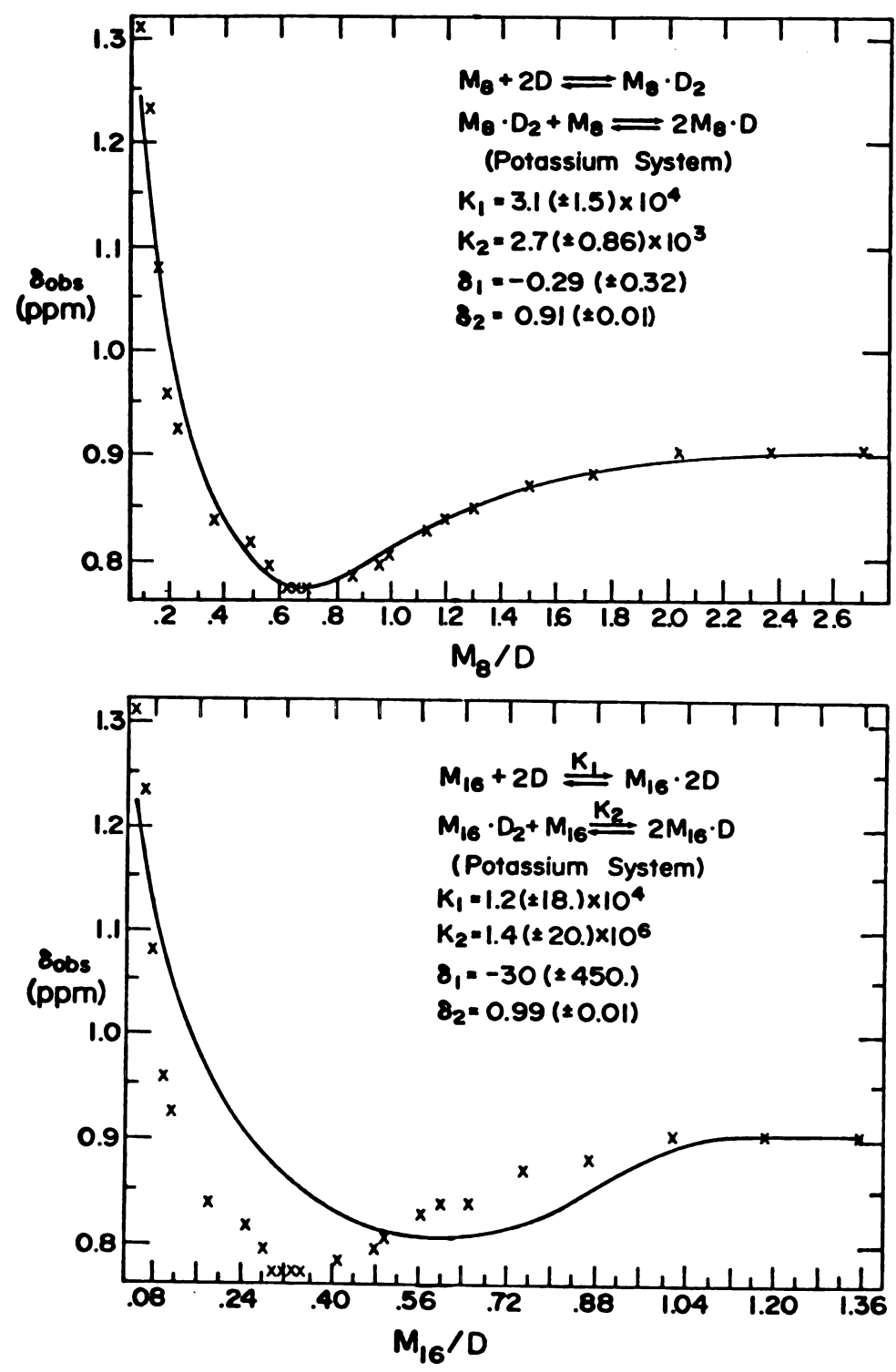


Figure 24. Plots of the best fits for a) equations (6a) and (6c) and b) equations (10) and (11). $\delta_{\rm Obs}$ is the observed chemical shift in ppm of the EtdBr methyl resonance and a) Mg/D or b) M16/D is the ratio of structured K25'-GMP to total drug. Errors are standard deviations.

DISCUSSION

A. Present Study

The results of the curve-fitting for the 5'-GMP stoichiometry in the presence of excess Na indicate that upon structure formation, two tetramers are brought together to form an octamer. The fits for both the monomer to n-mer and monomer to stack tetramer equilbria (equations (la) and (2a) respectively) indicate the requirement of two tetramers. Although the standard deviations in the values of n are fairly large (25% and 22% respectively at 95% confidence) they provide a range of values from which to make a logical In contrast, the standard deviations of the values of K' are extremely high (337% for (la) and 237% for (2a) at 95% confidence). Two features of the experimental technique may help to explain the large errors encountered. First, although the total concentration of Na remains a constant throughout the experiment, its ratio with respect to the total 5'-GMP concentration decreases. At the beginning, the ratio $\left[Na^{+}\right]_{tot}/\left[5'-GMP^{-}\right]_{tot}=6.5$; whereas in the final measurement, the ratio = 3.7. This lowering of the over-all ratio is probably not an important factor due to the fact that the ratio of $[Na^+]_{tot}/[5'-GMP^=]_{struct}$.

which goes from 84 to 11 is far larger than the expected stoichiometry of Na⁺. Even if the ratio of bound Na⁺ to structured 5'-GMP⁼ was 1:1, the amount of Na⁺ in the final solution is still in a ten-fold excess.

A more serious drawback is the limited concentration range over which structure formation could be observed. For the concentration of NaCl employed (0.85M), structure formation does not occur at 15°C until the concentration of (TMA)₂5'-GMP reaches ~ 0.13M. Above the highest concentration studied ([5'-GMP] = 0.23M), precipitation occurs, yielding unusable data. Therefore, the range of usable 5'-GMP concentrations is only 0.10M. Extrapolation of the curve in Figure 9a shows it to be sigmoid shaped. The data used only provide information about slope and position of the middle portion of the curve and provide no information in the region where the [5'-GMP]_{structured} versus [5'-GMP]_{total} curve is horizontal. This leads to uncertainties in the K' and n values.

Lowering the Na⁺ concentration to $0.72\underline{M}$ still did not permit observation of a large concentration range for structure formation. Precipitation occurred at the same fraction of 5'-GMP⁼.

An examination of Table 2 shows that the tetramer to stacked tetramer equilibrium (equation (4a)) yields errors in n and K' that are comparable with those of either the monomer-n-mer or monomer-stacked tetramer equilibria

(equations (la) and (2a) respectively). Within the reported error limits of the values of n for equation (4a) there are between five and eight tetramers per structured unit. This would yield a minimum of three (n = 5 or 6, intensity ratio)2:2:1 or 1:1:1 respectively) or four (n = 7 or 8) H(8)structure lines for the most symmetric stacking pattern. If one considers the second highest H(8) resonance (line C, Figure 8) as being due to monomer (which is what was assumed in the data treatment) then only three structure lines are observed. Thus the stacking of seven or eight tetramer units can be eliminated on the basis of the number of lines observed. The highest and lowest field structure lines (A and D) have been reported 40 to arise from the same structure, which is different from that giving rise to the second lowest field line (B). A single structure with five or six stacked tetramer units would be inconsistent with these observations, thereby eliminating the results of equation (4a).

Chantot and Guschlbauer ⁷⁶ and Yee and Chan ⁷⁷ found strong formation constants for tetramer formation in slightly acidic (pH = 5) aqueous solution. The lack of an adequate fit for the monomer-tetramer-stacked tetramer equilibria (equations (3a) and (3b)) and the tetramer-stacked tetramer equilibrium (equation (4a)) indicates that at the pH value studied (~8) the amount of free tetramer in solution is apparently small. Thus, the results of Chantot and

Guschlbauer 76 and Yee and Chan 77 at acidic pH values do not appear to be applicable in the present case. The major difference between their work and the present work appears to be the size of the charge on the monomer unit. In the pH \approx 5 form the monomer nucleotide unit is monoprotonated and has a -1 charge, which would give a -4 total charge to the tetramer. At pH \approx 8 the monomer has a -2 charge, yielding a -8 charge to the tetramer. Thus, tetramer formation should be less favorable at pH \approx 8 than at pH \approx 5 because of increased electrostatic repulsion. As further indication of the importance of charge on tetramer formation, the uncharged nucleoside guanosine gels in very dilute ($\sim 10^{-2} \underline{\text{M}}$) solutions in the presence of an alkali metal salt. The indicate as the tetramers are stacked.

The principal equilibrium in the structuring of Na₂5'-GMP is believed to be

$$8M^{2-} \stackrel{?}{\downarrow} (M_4)_2^{16-}$$
 (12)

In regard to the stoichiometry of the Na⁺ in the octamers, the data presented in Figure 14a support a value of $x = 4.0(\pm 0.1)$ and $K' = 1.7(\pm 0.7) \times 10^{10} \, \text{M}^{-11}$. In contrast to the large errors encountered in the determination of n and K' for 5'-GMP⁼ aggregation, the standard deviations of x and K' at the 95% confidence level are reasonable with

respect to this case. The salt concentration employed allowed investigation over a larger concentration range and allowed better definition of the data at extreme concentrations of 5'-GMP by the curve fitting program. The more complete data set provides lower deviations and supports the suggestions made earlier for the sources of the errors in the determination of n and K' for the stoichiometry of 5'-GMP aggregation.

These data, along with those obtained for 5'-GMP aggregation, support the following equilibrium:

$$4Na^{+} + 8GMP^{-} \stackrel{?}{\leftarrow} Na_{4} (GMP_{4})_{2}^{12-}$$
 (13)

Model building studies make it possible to propose reasonable solution structures. In order to do this, however, a firmer understanding of the type of binding between the Na⁺ and the structured nucleotide is required.

Investigations of the effects of cationic binding to polyanions have revealed three states in which the cation may exist. 86-88 These can be classified as "site bound," "territorial bound," and "free" counterions. Manning 89 has recently reviewed work on the theory of polyelectrolyte binding. He defines site binding as direct contact between the counterion and the polyion without intervening solvent molecules. This would be analogous to "inner

sphere complexation in coordination chemistry or contact ion pairing. Bound counterions which are not site bound are therefore considered to be territorially bound. As defined by Manning, a territorially bound ion has at least its first hydration sphere intact (i.e., solvent separated ion pairing). For territorial binding the cation and its hydration sphere will be strongly pulled to the polyanion, but it will be free to wander the length of the polymer chain. In territorial binding, the number of bound cations is dependent only on the charge on the cation and the charge density of the polyanion. Territorial binding is therefore independent of both the ionic strength of the solution and the specific cation. For example, K⁺ and Na⁺ should give the same amount of binding per phosphate charge irrespective of the ionic strength of the solution. Thus, a mass-action formulation does not hold for territorial binding.

As stated earlier, changing the ionic strength, through changing the total concentration of NaCl, has a pronounced effect on the amount of structure and hence the amount of sodium bound. This ionic strength effect implies that the mode of alkali binding is mass action. Furthermore, the stability and types of structures formed are highly dependent upon the specific cation employed. 41-43,44-47,50

The cation specificity for structure formation indicates that Na^+ coordinates to $(5'-GMP)_8^{16-}$ via site binding.

Clearly, the tetramer hole defined by four O(6) oxygens defines a unique site for complexation of the alkali metal ion which should be quite specific. The metal ion size dependence of aggregation should be based upon the unhydrated metal ion to ligand bond length.

It has been proposed previously that Na occupies the central hole in the tetramer due to a size selective coordination mechanism (cf. Figure 5a). 42,43 The stacking of two tetramers to form an octamer would account for two of the four required sodium ions. Bouhoutsos-Brown bas proposed that the required ions not in the "ion specific hole" are chelated between the octamer plates by a pair of negatively charged phosphate groups. This proposal is based on the fact that addition of excess salt to a structured system does not stabilize, but destabilizes the structures. It was proposed that an excess of metal ion causes ion pairing with the phosphate which would decrease the number of phosphates available for chelation, thereby destabilizing the structures. The requirement is to determine which of the stacking patterns proposed (cf. Table 6) would allow the best alkali metal ion chelation.

In the case of normal stacking, the two diastereomers $(C_4(CW,CW,+30^\circ))$ and $C_4(CW,CW,-30^\circ)$ have identical overlap patterns and nearly identical interplate hydrogen bonding schemes (four OH(3')-OP bonds in the former and four OH(2')-OP bonds in the latter). Consequently, their

energies should be nearly equal, with little preference to be shown for either in solution. As stated previously, the highest and lowest field lines (\underline{A} and \underline{D}) probably arise from isomerization of C_4 (CW, CW, $+30^{\circ}$) and C_4 (CW, CW, -30°). This requires that the two remaining Na^+ ions, which are chelated to phosphates in this stacking pattern, should have equal probabilities of being found on either of the two diastereomers.

The reversed stacking modes for the $\mathrm{D_4}\left(\mathrm{CCW},\mathrm{CW},\mathrm{\Theta}\right)$ and D_4 (CW,CCW, Θ) isomers have markedly different interplate hydrogen bonding schemes (Table 6). Each D_A (CCW,CW, Θ) isomer is capable of forming eight hydrogen bonds between a phosphate group on one plate and an N(2) position on the plate above or below it. In the $D_A(CW,CCW,\Theta)$ isomers, only four interplate hydrogen bonds (four OH(2')-O(3') hydrogen bonds for the $D_A(CW,CCW,+60^{\circ})$ isomer and four OH(2')-OP hydrogen bonds for the $D_4(CW,CCW,+30^{\circ})$ isomer) are expected per octamer (Table 6). Therefore, the D_4 (CCW,CW, Θ) isomers are expected to be more stable than the D_4 (CW,CCW, Θ) isomers. In addition, model building studies show that the average phosphate oxygen-phosphate oxygen distance is ~ 4.2 $^{\text{A}}$ in both D₄(CCW,CW, Θ) isomers, ~ 6.5 $^{\circ}$ in the D₄(CW,CCW,+30 $^{\circ}$) isomer, and ~ 8.8 $^{\circ}$ in the D_4 (CCW,CW,+60°). The phosphate oxygens are ~ 4.8 $\stackrel{\circ}{A}$ apart for the $C_4(CW,CW,+30^{\circ})$ isomer and ~ 7.8 $^{\circ}$ apart for the C_4 (CW, CW, -30°) isomer. Crystallographic Na-O bond

distances have been reported for Na_2ATP (2.3Å), ⁹¹ NaGpC (2.3-2.4Å), ⁹² and NaApU (2.3-2.4Å). ⁹³ These distances indicate that the best chelation of a sodium ion by two phosphate groups occurs when the ioninzed oxygens are ~ 4.6-4.8Å apart as they are in the C_4 (CCW,CW, Θ) isomers.

Consequently, the second lowest field structure line (\underline{B}) is believed to arise from the D_4 (CCW,CW,-30°) and D_4 (CCW,CW,-60°) isomers, which are being interconverted on the nmr time scale by rapid segmental twisting between $\Theta = -30^\circ$ and $\Theta = -60^\circ$ about the C_4 axis.

In summary, the two octameric structures which appear in concentrated solutions of Na₂5'-GMP are assigned to C_4 (CW,CW, Θ) and D_4 (CCW,CW, Θ) stacking patterns with rapid isomerization of $+30^{\circ}$ and -30° (or -30° and -60°) of the twist angle (0). The structure directing Na + ions coordinated to four O(6) donors are believed to be situated slightly above the plane of the top tetramer and slightly below the plane of the bottom tetramer. Since Na ions bound to donor atoms in nucleic acids are always found coordinated to water 94 a water molecule probably occupies a fifth coordination site. In addition, in order to reduce the coulombic repulsions between these two sodium ions, it is proposed that a water molecule intercalates between the tetramer plates by hydrogen bonding to the O(6) donors. Assuming a 3.5A stacking distance and an OH-O hydrogen bond distance of 2.7A, 95 an intercalated water can hydrogen bond

to an O(6) donor on one tetramer plate and to an O(6) on the second plate which is twisted by $\theta=60^{\circ}$ with respect to the first. The remaining two Na⁺ ions per octamer unit are chelated between a phosphate group on the top tetramer and a phosphate group on the bottom tetramer. The lifetime of the metal ion at a specific site is small on the NMR time scale (correlation time, $\tau_{\rm C}=5-8{\rm ns}^{96}$). Therefore, the symmetry as observed by ¹H NMR is unaffected by the site specificity of the Na⁺ binding. On the NMR time scale, each phosphate will chelate an Na⁺ part of the time. In addition to metal ion coordination, each of the two structures is expected to have either four $(C_4(CW,CW,\theta))$ or eight $(D_4(CCW,CW,\theta))$ interplate hydrogen bonds increasing the stability (Table 6).

A schematic representation of the structures proposed is illustrated in Figure 25.

B. Other Proposed Structures

In the past five years, several papers have proposed structures for the self-assembled form of Na₂5'-GMP. A discussion of these in relation to the structures proposed here should be informative with respect to the validity of any or all of them.

Laszlo and coworkers have presented several different models to explain the metal ion specific binding to 5'-GMP by Na⁺. Their first model ⁹⁶ assumed the structures to be micelles. Based on ²³Na NMR lineshape analysis, they

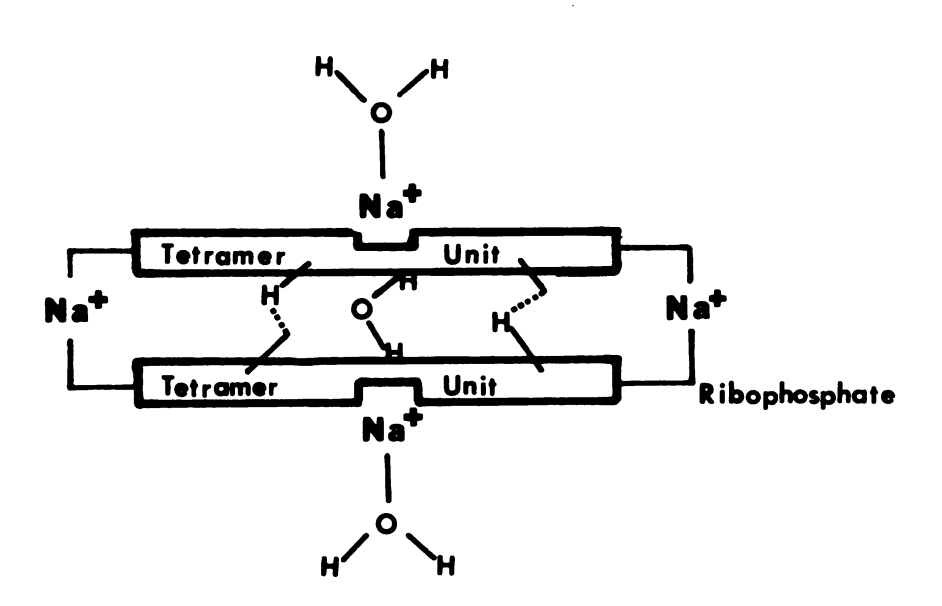


Figure 25. Schematic diagram of the proposed structure for the self-assembled forms of Na₂5'-GMP.

proposed that the structures contain between 12 and 20 monomer units. A preference for a structure based upon 16 monomer units was stated but not substantiated. No information concerning the nature of the structures was presented. In 1978, they proposed the coordination of the Na ion into the central cavity of the tetramer plate. 44 A week later they proposed the coordination of K⁺ at the same position on the tetramer. 45 Their model for the K+ structure was based on the observation that when KCl is added to a dilute solution of Na₂5'-GMP (0.1M, 31°C) the 23 Na linewidth shows a dramatic increase ($\Delta v_{1} \approx 150 \text{ Hz}$) indicative of structure formation. An analogous change in the 39 K linewidth ($\Delta v_{1} \simeq 50$ Hz) was taken as indication that K⁺ and Na⁺ structure in the same position. The addition of LiCl, NaCl, RbCl, or CsCl had no effect on the Na linewidth under the same conditions. No explanation was provided with regards to how the same coordination site can accommodate both the K⁺ and the Na⁺ ions and no proposals of nucleotide stoichiometry were advanced.

Based on 1 H and 31 P NMR of Na $_2$ 5'-GMP, Borzo and Laszlo 46 accepted the proposal made by Pinnavaia, et al. 40 that the Na $_2$ 5'-GMP self-structure contains two distinctly different structures in solution. The structures they proposed are illustrated on Figure 26. The structure labelled $\underline{\mathbf{A}}$ on Figure 26 was presumed by Borzo and Laszlo 46 to represent the structure which gives rise to the highest

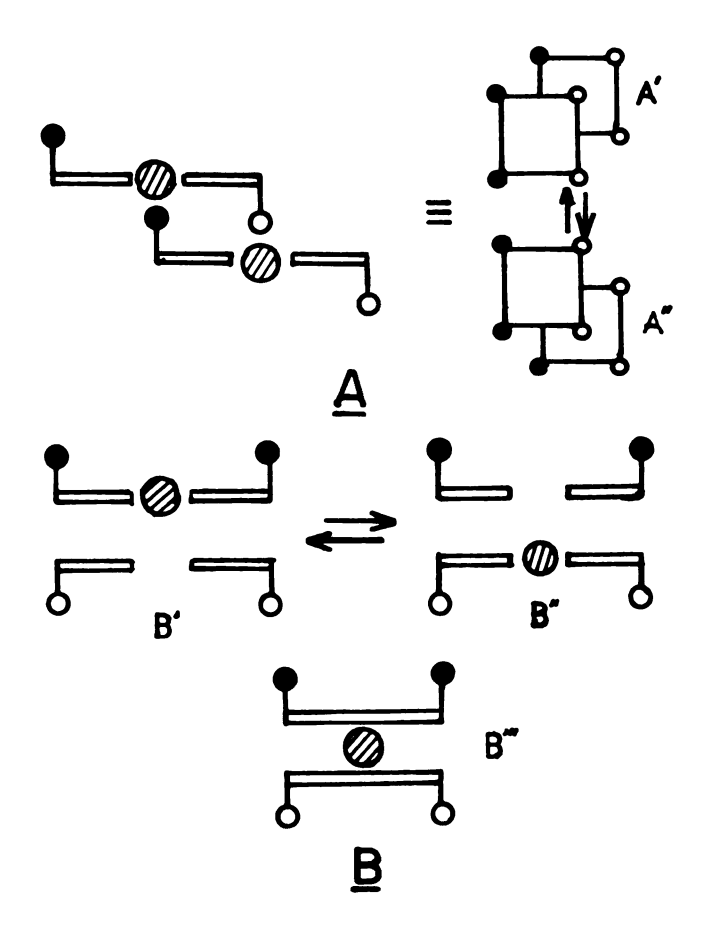


Figure 26. Structures proposed by Borzo and Laszlo⁴⁶ to explain the ¹H NMR spectrum of the self-assembled forms of Na₂5'-GMP. Open circles represent phosphate groups pointing down while closed circles represent phosphate groups pointing up. Na⁺ ions represented by striped circles (from ref. 46).

and lowest field H(8) resonances (\underline{A} and \underline{D} , \underline{cf} . Figure 8). The highest and lowest field lines observed in the ^{31}p spectrum were also assigned to structure \underline{A} . The Na⁺ ion was presumed to be coordinated in the core position of the tetramer with a fifth coordination site occupied by a phosphate group on the adjacent tetramer unit. The rapid equilibrium between states \underline{A} ' and \underline{A} " (Figure 26) was presumed to impart two-fold symmetry to the octamer units with the open and shaded circles representing phosphate groups pointing down and up respectively. The rapid equilibrium of \underline{B} ' and \underline{B} " would give the time averaged structure \underline{B} " which was assumed to give rise to the second lowest field structure line (\underline{B} , Figure 8).

Species <u>A</u> (Figure 26) can be ignored on several grounds. First, the authors completely ignore the hydrogen bond directionality of the tetramers. It is clear from previous arguments that in order for a C_2 axis to exist between the tetramer plates, the tetramers have to be stacked in one of the reversed modes. Second, back and forth slippage of the tetramer plates along only one direction requires a rigid glycosidic ($\chi = C(9)-C(1')$) conformation, in which half of the nucleotide units in the octamer are in a <u>syn</u> conformation ($\chi = 215^{\circ}$) and half are in an <u>anti</u> conformation ($\chi = 35^{\circ}$). Even if this unlikely conformation existed, the absence of a mirror plane in both the normal and reverse stacking modes would cause this

motion to give rise to more than two lines. The model also permits very little overlap of the purine bases, which is an essential contributor to the stability of the structures. 14,17 Finally, model building studies show that the phosphates not chelated to the central Na⁺ ions are too far apart (>12Å) to allow chelation of additional metal ions.

The model could have some merit, however, if facile rotation between <u>syn</u> and <u>anti</u> conformations is allowed and if segmental slippage is allowed along two directions to permit migration of one tetramer unit around the periphery of the other. Such a motion would result in a two-line spectrum for normal stacking. Each of the two diastereomers resulting from reversed stacking would give a one-line H(8) spectrum.

In addition, no explanation was provided as to how the \underline{B} structure would give rise to only one H(8) resonance. It is clear, however, from previous arguments, that the tetramers would have to be stacked in a reversed stacking mode.

Again using 23 Na NMR lineshape analysis, Deville, Detellier, and Laszlo 47 predicted structures for the $K_2^{5'}$ -GMP self-structures in solution. This paper proposed the same structure for the potassium self-structure as they postulated previously for the sodium system (Figure 26). 46 The structure labelled A (Figure 26) was changed to include K^+ in the two core positions of the tetramer. This time, the A' $\stackrel{?}{\downarrow}$ A" equilibrium was not considered and the single

"staircase" model was assumed to have C_{2h} symmetry. The authors state that this model gives rise to three of the H(8) nmr resonances observed for the potassium salt with an integral intensity of 1:2:1. They also state, with no apparent justification, that structure \underline{A} is energetically more favorable than structure \underline{B} . If, however, the hydrophobicity of the base stacking is such an important stabilizing factor in structure formation, 14,17 structure \underline{B} should be the more favorable species. Model studies have shown only limited overlap of two of the eight guanine bases for structure \underline{A} . The overlap patterns of \underline{B} should be nearly the same as in Figures 11, 12, and 13.

In the two most recent papers presented by Laszlo and coworkers, 97,98 the model A proposed previously 46,47 (Figure 26) is entirely abandoned without explanation. In these two papers, ^{1}H , ^{23}Na , ^{31}P , ^{39}K , and ^{87}Rb NMR were used to determine the size of the structures and the sites of binding. Again using ^{23}Na lineshape analysis, they examined the mixed $K^{+}/Na^{+}-5'-GMP^{-}$ structured system. In their model, they proposed that the tetrameric species is by far the predominant form of the monomer. They infer that this tetramer formation requires no metal ion interaction. This assumption is in conflict with the findings of Chantot and Guschlbauer 76 that the nucleoside guanosine does not gel without the presence of an alkali metal salt.

Laszlo, et al., 98 attempted to fit a three step equilibrium for a mixed Na⁺/K⁺-5'-GMP⁼ system.

$$G_4 + K^+ \stackrel{K_1}{\not=} G_4, K^+$$
 (14)

$$G_4, K^+ + G_4 \stackrel{K_2}{\stackrel{?}{\downarrow}} G_8, K^+$$
 (15)

$$G_8, K^+ + nNa^+ \stackrel{K_3}{\stackrel{?}{=}} G_8, K^+, nNa^+$$
 (16)

where G = 5'-GMP monomer unit.

From the linear dependence of $p_B \chi^2$ against K^+ (p_B = fraction of Na⁺ bound, χ = 23 Na quadrupole coupling constant) they found 2.1 < n < 5.6. They reasoned that due to the four-fold symmetry of the tetramer a value of n = 4 was the most reasonable. Their proposed structure for the $K^+/Na^+-5'-GMP^-$ structure is shown on Figure 27.

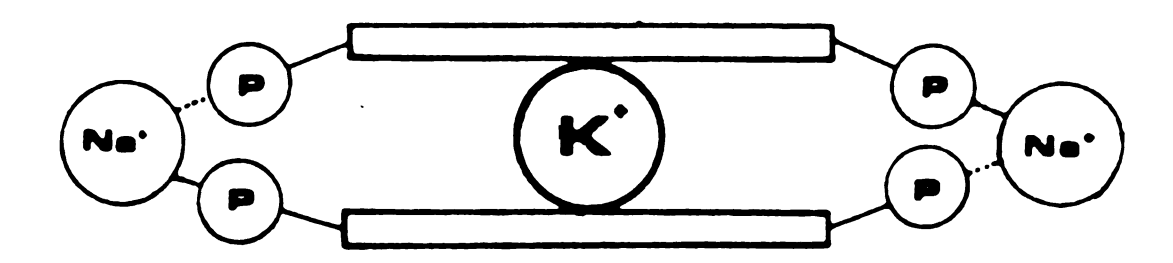


Figure 27. Structure proposed by Detellier and Laszlo 98 to explain the NMR results for the K⁺/Na⁺-5'-GMP⁼ self-structure. Only two of the four chelated Na⁺ ions are illustrated (from ref. 98).

The value of n arrived at for the metal stoichiometry in the K⁺/Na⁺-5'-GMP⁼ was then applied to the structured system with no added K⁺. ⁹⁷ Here, by using what they termed a "phase separation model," they calculated thermodynamic parameters based upon a stoichiometry of Na₅(5'-GMP)¹¹⁻₈ in which it was assumed that four Na⁺ ions were chelated between phosphates and the fifth occupied the central core position. Although claiming to have abandoned the micellular model of a previous paper ⁹⁶ the "phenomenological equations" used were based on those used for micelle formation. ⁹⁷ In addition, the equations used were for a massaction process and not a phase separation process as they claimed. ⁹⁹

With the basic Na_5 (5'-GMP) $_8^{11-}$ stoichiometry, Laszlo and coworkers proceeded to propose a series of structures to explain the spectra. They favored one in which two major equilibria exist

$$2G_4 \stackrel{?}{\leftarrow} G_8 \tag{16}$$

$$2G_8 \stackrel{?}{\downarrow} G_{16} \tag{17}$$

The G_8 species was presumed to give rise to the second lowest field H(8) structure line (\underline{B} , Figure 8) in which top and bottom H(8) positions are equivalent. This would correspond to a reversed stacking mode in the present study

(cf. Figures 12 and 13). Laszlo and coworkers state that this type of stacking for the octamer has either C_{4h} or S₈ symmetry. However, these point groups are meaningless because they ignore the directionality of the hydrogen bonding in the tetramer units and the presence of the chiral ribose-phosphate. The two outer lines (A and D, Figure 8) are claimed to be due to dimerization of the G_{Q} species to form the G_{16} species. They presumed that G_{16} could lead to a species with two-fold symmetry; the two "outer" tetramers would be equivalent, and the two "inner" tetramers would be equivalent. This would be equivalent to the reversed stacking of a pair of reversed octamer stacks (e.g., CW,CCW,CW,CCW) or reversed stacking of a pair of normal octamer stacks with opposite hydrogen bond directionality (e.g., CW,CW,CCW,CCW). No explanation was offered as to why other G_{16} and G_{8} stacking patterns were not observed. They also stated that the B line (Figure 8) could arise from free tetramer and the A and D lines could arise from octamer.

In summary, the models that have been proposed by

Laszlo and coworkers are of only limited value due to their

total neglect of both the hydrogen bond directionality and

the ribose-phosphate chirality.

Fisk 100 has recently investigated the 13 C NMR of structured Na $_2$ 5'-GMP. In her work, she determined the longitudinal and transverse relaxation rates (T $_1$ and T $_2$)

and the Nuclear Overhauser Enhancement (NOE) for the carbons in the structured form. Using Woessner's 101 treatment for determining the relaxation rates and NOE's of nuclei in a rotating spheroid, she then calculated T_1 , T_2 , and NOE values for a series of stacked tetramers between n=4 and n=64. She found that four models would yield the same values as were obtained experimentally. These were

- i) a hydrated octamer; $\eta = 0.074$
- ii) an unhydrated 44-mer; $\eta = 0.074$
- iii) a hydrated 52-mer; $\eta = 0.019$
 - iv) an unhydrated 64-mer; $\eta = 0.019$

where η is the solution viscosity ($\eta=0.019$ is the viscosity of D_2O at 5^OC ; $\eta=0.074$ is the viscosity of the solution of Na_25' -GMP at 5^OC). From this she supported the hydrated octamer. The remaining structures could not explain the three H(8) structure lines observed.

has proposed a Na⁺/5'-GMP⁼ structure with six Na⁺ ions for every octameric structured unit. Each octamer was presumed to have a sodium ion in the center of each tetramer. In addition, four other sodium ions were presumed to be chelated between phosphate groups on the top and bottom plates. The fact that Li⁺ tended to decrease structure formation was taken to mean that the strong lithium phosphate bond would break up chelation and cause the formation of "free" tetramers in the solution. The observation of a

fifth structure line (δ = 7.6 ppm) was taken as the chemical shift of the tetramer in solution. The same solution showed a very strong "monomer" resonance indicating that only under certain special conditions can a sizable amount of tetramer be observed in solution, an assumption that the present study supports.

Finally, a structurally similar polynucleotide, polyinosine, has recently been shown to have a melting temperature which is highly dependent upon the alkali metal salt which is added into the solution. 48 Inosine differs from quanosine in only having a hydrogen at position 2 of the base (cf. Figure 3). This means that poly(I) can still form stacked tetramers of the bases from the tetramerization of four strands, 102,103 however, only one hydrogen bond is expected per base unit. The metal ion dependence of the melting profiles implies the size selective coordination of the alkali metal ions to either the center of the tetrameric plates or to octahedral holes between the plates. The stability of the ordered polynucleotide was a direct function of the fit of the ion into the coordination site. This is analogous to the size selective coordination proposed here for the 5'-GMP self-structure.

C. Stability of the Base Overlap

With the stacking patterns proposed, the question of stability of the overlap of the bases must be addressed. Gupta and Sasisekharan 104 have done theoretical calculations

to determine the stability of various overlap patterns of the free bases. These calculations were based on monopolemonopole interactions of a pair of overlapping bases. 105 Their results indicated that the reversed stacking mode is energetically more favorable than the normal stacking mode. In addition, the enantiomeric pairs, D_A (CW,CCW,+30 $^{\rm O}$) and $D_A(CCW,CW,-30^{\circ})$, are very close in overlap to the lowest energy structure. This structure is proposed to be 12.0 kcal/2 moles more stable than the free bases. These calculations do not rule out the normal stacking pattern, however. A stacking pattern similar to the normal stacking pattern proposed here would still be lower in energy than the two free base units. It must be pointed out, moreover, that the utility of using these calculated numbers is extremely limited due to the fact that contributions from the bulky ribose-phosphate groups have not been considered in their work.

Table 6 lists the expected upfield shifts of the H(8) protons from Giessner-Prettre and Pullman's theoretical calculations considering only ring current and atomic diamagnetic susceptibility effects. 82 The expected upfield shift of a proton depending on its position is shown on Figure 28. A comparison of Table 6 with the spectra on Figure 8 shows no correlation between the calculated shifts and the observed shifts. However, the theoretical curves (Figure 28) also would predict no downfield shift of

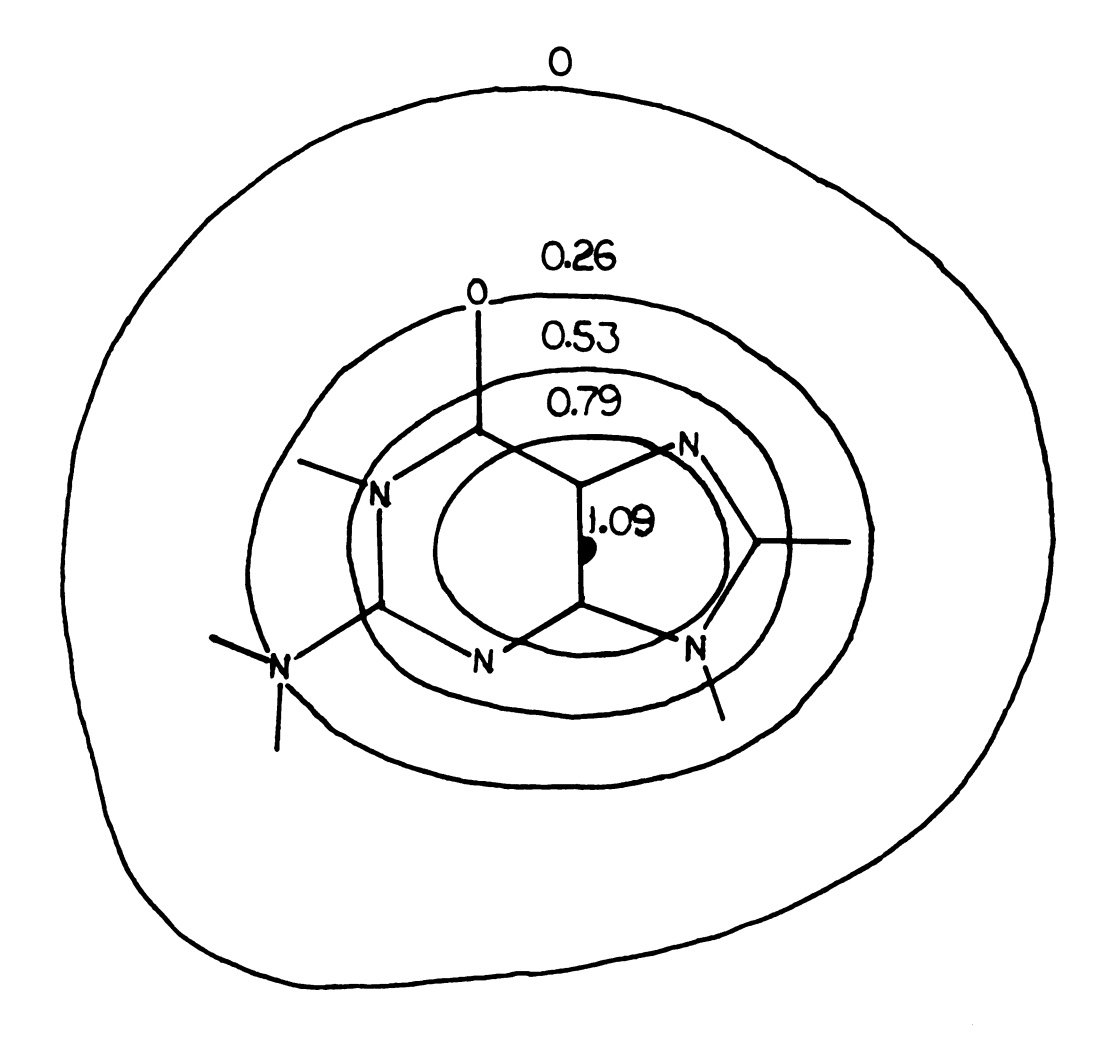


Figure 28. Expected upfield shift (in ppm) of a nucleus 3.5 Å above or below the aromatic plane due to the ring current and diamagnetic susceptibility effects (from ref. 82).

structured protons as observed for peaks \underline{A} and \underline{B} (\underline{cf} . Figure 8). This indicates that other effects (e.g., proximity to phosphate charge, electron withdrawal upon hydrogen bonding to N(7)) not taken into account in the theoretical calculation 82 are also effecting the chemical shifts of H(8).

D. Drug Intercalation

It has been clearly shown that EtdBr interacts with both monomeric and structured forms of Na $_2$ 5'-GMP and K $_2$ 5'-GMP. Binding to the monomer is characterized by a large ($\Delta\delta \approx 0.3$ ppm) upfield shift of the H(8) monomer resonance along with corresponding upfield shifts (~ 0.2 ppm) of the aromatic protons of the drug. This interaction is most likely due to the base stacking of monomer 5'-GMP and monomer drug.

The spectral changes assigned to the structure-drug complex on the other hand are observed only at concentrations of nucleotide sufficiently large for the observation of structure formation. At this point a large upfield shift ($\Delta\delta \ge 0.50$ ppm) is observed for the methyl resonance of the drug molecule. Due to the fact that only small changes in the chemical shifts of the structured H(8) resonances ($\Delta\delta < 0.05$ ppm) are observed, it is assumed that the mode of binding is for the drug molecules to stack on the outside of the octamer units. If the mode of binding were intercalation, the symmetries of the stacking modes

would be expected to undergo dramatic changes with correspondingly dramatic changes in the H(8) chemical shifts. The changes in the aromatic drug resonances would indicate that the mode of binding occurs through aromatic base stacking of the drug with the octamer. Simple ion pairing of the anionic octamer with the cationic drug would not be expected to induce the large shifts observed for the drug's aromatic protons.

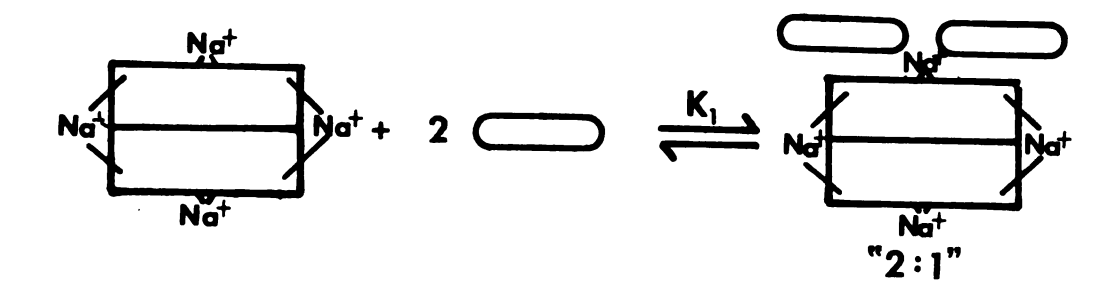
This mode of structure binding would add further evidence to the belief that the \underline{C} resonance (Figure 8) is monomer and not tetramer. If the mode of structure-drug binding is through aromatic overlap to the outside of the octamers, the surfaces available to the drug should be nearly identical in the free tetramer. As such, a large upfield shift of the drug's methyl resonance would be expected. Since only small perturbations of this methyl resonance are observed at concentrations where only the \underline{C} resonance is observed, this resonance is assumed to be due to free monomer.

The success in fitting the equilibria for the binding of two drug molecules and then one drug molecule to the octamer of Na₂5'-GMP (equations (6a) and (6c) respectively) indicates two important points. First, the fit of these two equations supports the evidence that an octamer is the predominant species for structured Na₂5'-GMP. Second, when the binding of the drug to the structured form occurs, it

takes place via a two step process. First, two drug molecules bind to the outside of the octamer. As more octamer is built up, it then competes for some of the drug already bound, allowing only a 1:1 (drug:structure) species to remain. In addition, this binding is to the monomeric drug molecule and not a stacked dimer. At the concentrations of drug employed, the EtdBr is predominantly in the monomeric form (>90%). 106

The 2:1 (drug:structure) complex is expected to be binding of both drug molecules to the same aromatic face of the octamer unit. If binding of the two drugs were to opposite faces of the octamer, when the 1:1 complex is formed, little change would be expected in the orientation of the remaining drug on the octamer due to the lack of any direct interactions. The lack of direct interaction should invoke no change in the chemical shift of the drug's methyl resonance in going from the 2:1 to the 1:1 species, which is not observed. Figure 29 shows schematically the type of binding expected for the two complexes.

The case of the binding of the drug to structured forms of K_2^5 '-GMP is quite different from the sodium case. With the potassium self-structure, a dramatic change in the structure lines is observed. Most noteworthy is the appearance of two new H(8) structure resonances (δ = 8.56 and 8.32 ppm) downfield from the monomer resonance. This indicates that EtdBr has some structure directing abilities



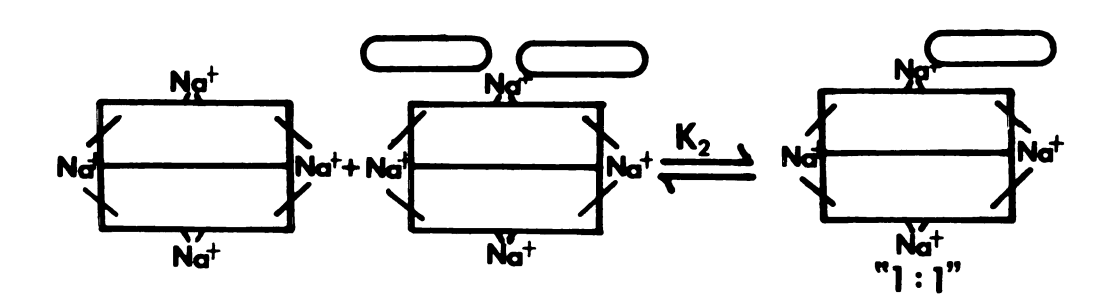


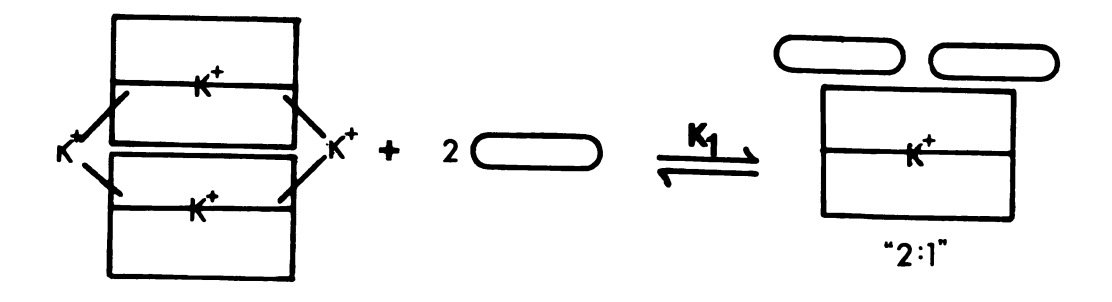
Figure 29. Schematic diagram of the proposed equilibrium involved in the formation of a 2:1 and 1:1 complex between the intercalation drug EtdBr and the octameric forms of Na₂5'-GMP.

of its own. The fact that the equations for the binding of the drug molecules to octameric species (equations (6a) and (6c)) provide a better fit to the experimental data than the equations for the drug binding to a hexadecamer (equations (10) and (11)) supports the same binding mode for K_25' -GMP as was proposed for Na_25' -GMP (Figure 29). As further evidence of the octameric form of the structured potassium-drug complexes, the new structured H(8) resonances observed have nearly the same chemical shift as those observed in the sodium case (δ = 8.56 and 8.32 ppm for K_25' -GMP-EtdBr and δ = 8.48 and 8.33 ppm for Na_25' -GMP-EtdBr) which is proposed as having an octameric structure.

Bouhoutsos-Brown⁵⁰ has proposed a structure for what she terms the "complex" potassium structure as arising from dimerization of octamers to form a hexadecamer. In her model, a K^+ ion occupies the core position of each octamer coordinated to the eight O(6) positions of the two tetramers. The dimerization of the two octamers is facilitated by chelation of K^+ ions between phosphate groups of each octamer.

It is proposed in this case that the drug, ethidium bromide, is capable of disrupting the hexadecameric forms of K_2^5 '-GMP in favor of an octameric form when the concentration of the structured form is low. The mode of action suggested is one in which the drug molecule attempts to intercalate between the two octamers of the hexadecamer.

In separating the two octamers, the chelation of K^+ ions which holds them together is no longer possible. The newly formed octamer-drug complex gives rise to the additional H(8) structure lines ($\delta=8.56$ and 8.32 ppm). As the concentration of structure increases, however, the hexadecameric structure becomes the predominant species and the equilibrium favors the binding of the drug to the other surface of the hexadecamer. A concomitant disappearance of the two new H(8) resonances assigned to octamer occurs as the equilibrium is shifted back towards the hexadecamer. In addition, the chemical shifts of the H(8) structure resonances approach those observed in the absence of added drug. 42,43,50 A schematic representation of the proposed binding modes is shown in Figure 30.



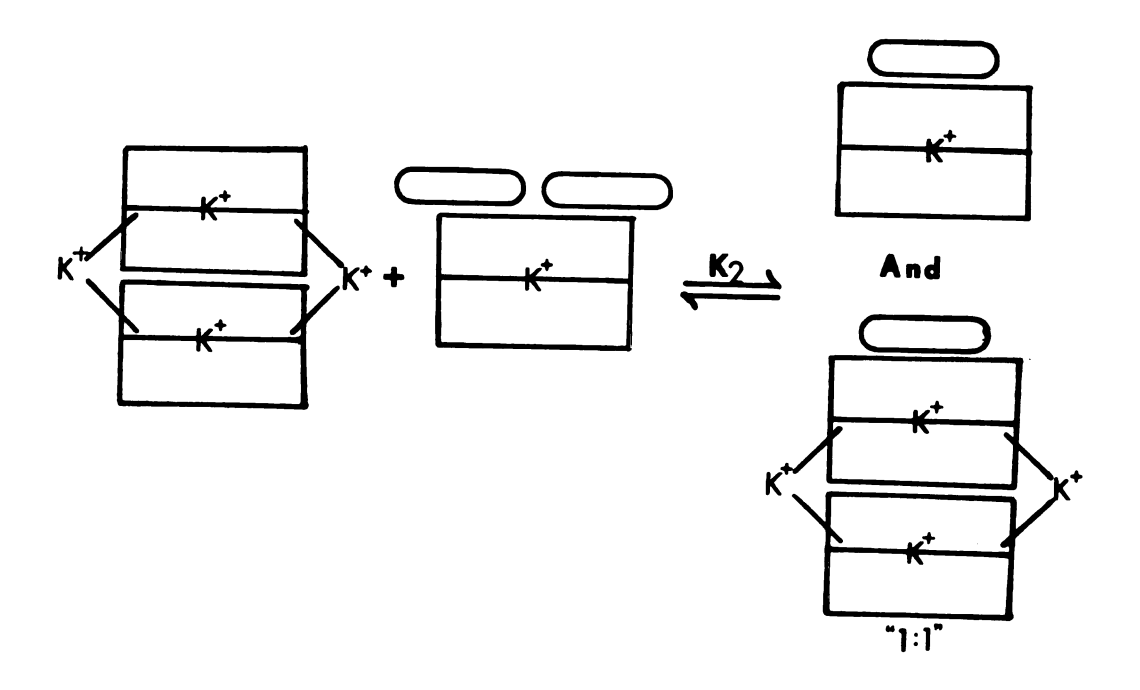


Figure 30. Schematic diagram of the proposed equilibrium involved in the formation of a 2:1 and 1:1 complex between the intercalation drug EtdBr and structured forms of K₂5'-GMP.

CONCLUSION

The work presented in this thesis has shown evidence that structure formation by $Na_2^{5'}$ -GMP can best be described in terms of the stacking of two hydrogen bonded tetramer units to form an octamer. The most likely structures are of two types. One type, which gives rise to the outer set of H(8) structure lines, arises from the normal stacking of two tetramers to form a unit with C₄ symmetry. A second structure, which is responsible for the inner H(8) structure line, has D_A symmetry due to the reversed stacking mode in which the top tetramer has hydrogen bonds in a counterclockwise fashion and clockwise on the bottom In both cases, twisting of the tetramer plates is rapid on the NMR time scale while stack separation is considered slow. The amount of free tetramer in solution is believed to be small, based on both the inability to fit the data to equations which allow a large tetramer build up and the fact that no evidence of any tetramer-drug interaction was found.

Stabilization of the octamers is possible through two mechanisms. First, sodium ions are site bound to two positions of the octamer. Two sodiums are coordinated to four carbonyl oxygens in the center of each tetrameric face. A

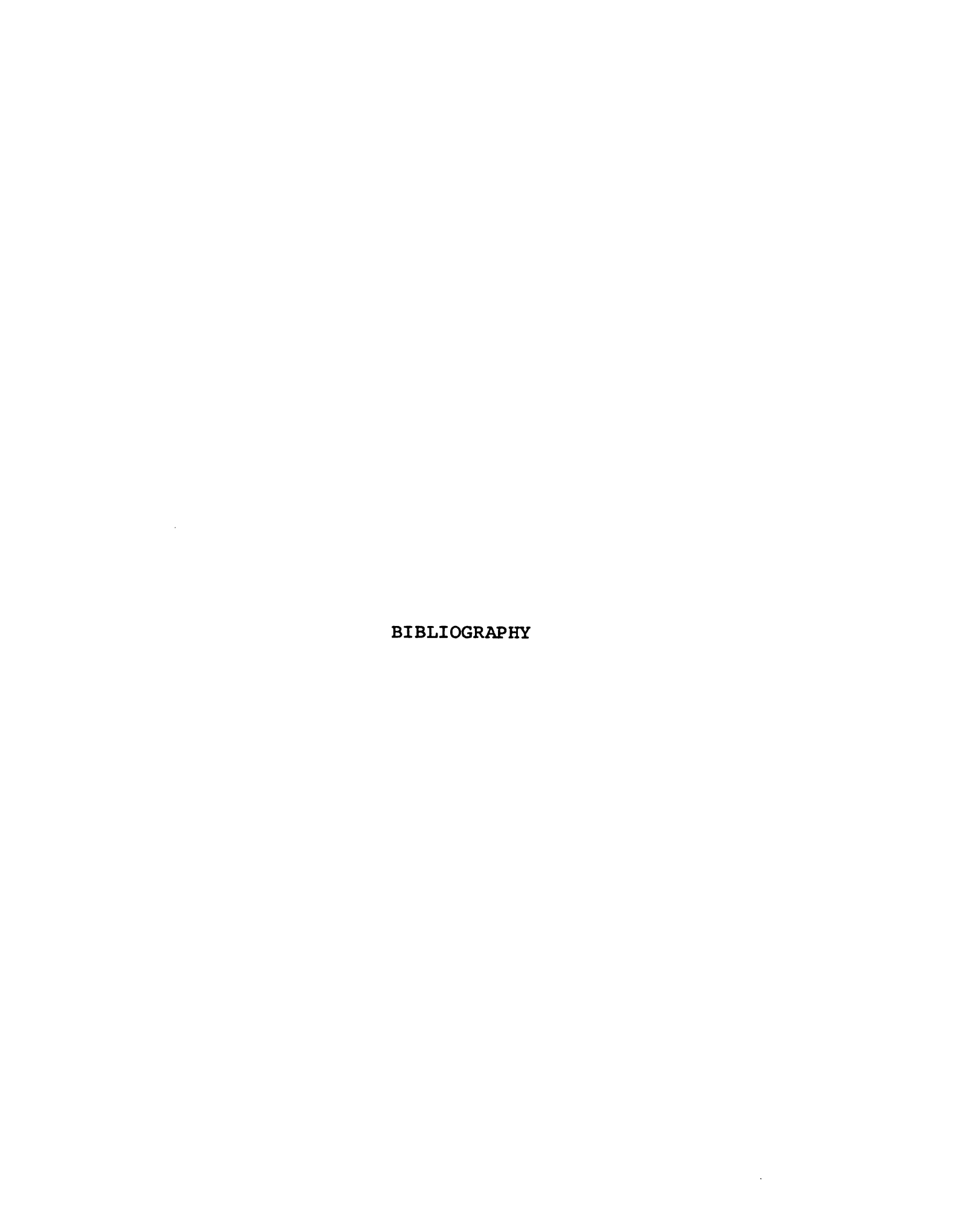
water molecule intercalated between the plates, is proposed to decrease coulombic repulsions between these two ions. The remaining two Na⁺ ions are chelated between a pair of phosphate groups on opposite tetrameric plates. The lifetime of a given sodium ion at a given site is considered short on the NMR time scale. The second form of stabilization is through interplate hydrogen bonding. Model building studies predict a minimum of four and up to eight hydrogen bonds per octamer unit.

Finally, the present study has shown that the structured forms of Na_2^5 '-GMP and K_2^5 '-GMP interact very strongly with the intercalation drug, ethidium bromide.

In the sodium case, evidence has been shown for the strong binding of two drug molecules to the octamer unit and the less strong binding of a 1:1 (octamer:drug molecule) complex. The binding is presumed to be to the exterior aromatic faces of the octamer since only slight changes in the chemical shifts of the H(8) structure lines are observed.

The potassium self-structures, however, show dramatic changes for the H(8) structure lines upon the addition of the drug. It is presumed that this is evidence that the drug molecules are able to disrupt the hexadecameric structures of K_25 '-GMP. The drug then forms a strong 2:1 complex with the octamer and weaker 1:1 complex. A build up in solution of the hexadecameric K_25 '-GMP

structure shifts the equilibrium towards binding of the drug to the hexadecamer.



BIBLIOGRAPHY

- 1. "Die Histochemischen und Physiologischen Arbeiten von Friedrich Miescher," <u>l and 2</u>, F.C.W. Vogel, Leipzig (1897).
- 2. Sci. Cit. Index, Perm. Subj. Index, 11, 42635(1978).
- 3. A. L. Lehninger, "Biochemistry: The Moelcular Basis of Cell Structure and Function," World Publishers, Inc., N.Y., 1970, Ch. 12, 25, and 28.
- 4. J. D. Watson and F. H. C. Crick, <u>Nature</u>, <u>171</u>, 737 (1953).
- 5. J. D. Watson and F. H. C. Crick, <u>Nature</u>, <u>171</u>, 964 (1953).
- J. Pitha, R. N. Jones, and P. Pithova, <u>Can. J. Chem.</u>, 44, 1045(1966).
- 7. Y. Kyogoku, R. Lord, and A. Rich, <u>Science</u>, <u>154</u>, 518 (1966).
- 8. E. Kuchler and J. Derkosch, Z. Naturforsch., 21, 209 (1966).
- 9. R. M. Hamlin, Jr., R. C. Lord, and A. Rich, <u>Science</u>, 148, 1734(1965).
- 10. R. R. Shoup, H. T. Miles, and E. D. Becker, Biochem. Biophys. Res. Comm., 2, 194(1966).
- 11. L. Katz and S. Penman, J. Mol. Biol., 15, 220(1966).
- 12. S. M. Wang and N. C. Li, <u>J. Am. Chem. Soc.</u>, <u>90</u>, 5069(1968).
- 13. M. Raszka and N. O. Kaplan, <u>Proc. Nat. Acad. Sci. USA</u>, 69, 2025 (1972).
- 14. P. O. P. Ts'o, in "Basic Principles in Nucleic Acid Chemistry," P. O. P. Ts'o, Ed., Academic Press, New York, 1974, Vol. 1, pp. 454-577.

- 15. W. Schimmack, H. Sapper, and W. Lohmann, <u>Biophys.</u>
 <u>Struct. Mechanism</u>, <u>1</u>, 311(1975).
- 16. E. Plesiewicz, E. Stepien, K. Krystyna, and K. L. Wierzchowski, Nucl. Acids Res., 3, 1295(1976).
- 17. P. O. P. Ts'o, in "Basic Principles in Nucleic Acid Chemistry," P. O. P. Ts'o, Ed., Academic Press, New York, 1974, Vol. 1, p. 561.
- 18. D. M. Crothers and D. I. Ratner, <u>Biochem.</u>, <u>7</u>, 1823 (1968).
- S. I. Chan, M. P. Schweizer, P. O. P. Ts'o, and
 G. K. Helmkamp, J. Am. Chem. Soc., 86, 4182 (1964).
- M. P. Schweizer, S. I. Chan, and P. O. P. Ts'o,
 J. Am. Chem. Soc., 87, 5241(1965).
- 21. A. D. Broom, M. P. Schweizer, and P. O. P. Ts'o, J. Am. Chem. Soc., 89, 3612(1967).
- M. P. Schweizer, A. D. Broom, P. O. P. Ts'o, and
 D. P. Hollis, J. Am. Chem. Soc., 90, 1042(1968).
- 23. I. Bang, Bioch.Z., 26, 293(1910).
- 24. H. T. Miles and J. Frazier, Biochim. Biophys. Acta, 79, 216 (1964).
- 25. F. B. Howard and H. T. Miles, <u>J. Biol. Chem.</u>, <u>240</u>, 801(1965).
- 26. J. P.-Leicknam, C. Chavelier, J. F. Chantot, and W. Guschlbauer, Biophys. Chem., 1, 134(1973).
- 27. J. F. Chantot and W. Guschlbauer, FEBS Lett., 4, 173(1969).
- 28. J. F. Chantot, M. T. Sarocchi, and W. Guschlbauer, Biochimie, 53, 347(1971).
- 29. E. W. Small and W. Peticolas, <u>Biopolymers</u>, <u>10</u>, 1377 (1971).
- 30. V. Gramlich, H. Klump, R. Herbeck, and E. D. Schmid, FEBS Lett., 69, 15(1976).
- 31. J. M. Delabar and W. Guschlbauer, <u>Biopolymers</u>, <u>18</u>, 2073(1979).

- 32. C. Becker and T. Ackerman, Ber. Bunsenges Phys. Chem., 77, 203(1973).
- 33. M. Gellert, M. N. Lipsett, and D. R. Davies, Proc. Nat. Acad. Sci. USA, 48, 2013(1962).
- 34. J. Iball, C. H. Morgan, and H. R. Wilson, <u>Nature</u>, <u>199</u>, 688(1969).
- 35. P. Tougard, J. F. Chantot, W. Guschlbauer, Biochim. Biophys. Acta, 308, 9(1973).
- S. B. Zimmerman, G. H. Cohen, and D. R. Davies,
 J. Mol. Biol., 92, 171(1975).
- 37. S. B. Zimmerman, <u>J. Mol. Biol.</u>, <u>100</u>, 663(1976).
- 38. H. T. Miles and J. Frazier, Biochem. Biophys. Res. Comm., 49, 199(1972).
- 39. R. M. Bock, N. S. Ling, S. A. Morell, and S. H. Lipton, Arch. Biochem. Biophys., 62, 253(1956).
- 40. T. J. Pinnavaia, H. T. Miles, and E. D. Becker, J. Am. Chem. Soc., 97, 7198 (1975).
- 41. C. M. Mettler, M. S. Thesis, Michigan State University, East Lansing, Michigan, 1977.
- 42. C. L. Marshall, M. S. Thesis, Michigan State University, East Lansing, Michigan, 1977.
- 43. T. J. Pinnavaia, C. L. Marshall, C. M. Mettler, C. L. Fisk, H. T. Miles, and E. D. Becker, J. Am. Chem. Soc., 100, 3625(1978).
- 44. A. Paris and P. Laszlo, <u>C. R. Hebd. Seances Acad.</u> Sci., Ser. D, <u>286</u>, 717(1978).
- 45. C. Detellier, A. Paris, and P. Laszlo, C. R. Hebd. Seances Acad. Sci., Ser. D, 286, 781(1978).
- 46. M. Borzo and P. Laszlo, C. R. Hebd. Seances Acad. Sci., Ser. C, 287, 475(1978).
- 47. A. Delville, C. Detellier, and P. Laszlo, <u>J. Mag.</u>
 <u>Reson.</u>, <u>34</u>, 301(1979).
- 48. H. T. Miles and J. Frazier, <u>J. Am. Chem. Soc.</u>, <u>100</u>, 8037(1978).

- 49. K. B. Roy, J. Frazier, and H. T. Miles, Biopolymers, 18, 3077 (1979).
- 50. E. Bouhoutsos-Brown, Ph.D. Thesis, Michigan State University, East Lansing, Michigan, 1980.
- 51. J. E. Huheey, "Inorganic Chemistry: Principles of Structure and Reactivity," Second Edition, Harper and Row, N.Y., 1978, pp. 72-73.
- 52. E. F. Gale, E. F. Cundliff, P. E. Reynolds, M. H. Richmonds, and M. J. Waring, "The Molecular Biology of Antiobiotic Action," Wiley, New York, 1972.
- 53. L. S. Lerman, J. Mol. Biol., 3, 18(1961).
- 54. T. R. Krugh and M. E. Nuss in "Biological Applications of Magnetic Resonance," R. G. Shulman, Ed., Academic Press, New York, 1979, pp. 113-175.
- 55. B. A. Newton in "Advances in Chemotherapy," A. Goldin and F. Hawking, Eds., Academic Press, New York, Vol. 1, 1964, p. 35.
- 56. L. Dickinson, D. H. Chantrill, G. W. Inkley, and M. J. Thompson, Brit. J. Pharmacol., 8, 139(1953).
- 57. J. F. Henderson, Cancer Res., 23, 491(1963).
- 58. W. H. Elliot, Biochem. J., 86, 562 (1963).
- 59. M. J. Waring, <u>Biochim. Biophys. Acta</u>, <u>87</u>, 358(1964).
- 60. J.-B. LePecq and C. Paoletti, <u>C. R. Acad. Sci. Paris</u>, <u>260</u>, 7033(1965).
- 61. J.-B. LePecq and C. Paoletti, <u>J. Mol. Biol.</u>, <u>27</u>, 87(1967).
- 62. V. W. F. Burns, Arch. Biochem. Biophys., 133, 420 (1969).
- 63. J. Vinograd and W. R. Bauer, <u>J. Mol. Biol.</u>, <u>33</u>, 141 (1968).
- 64. J. Vinograd and W. R. Bauer, <u>J. Mol. Biol.</u>, <u>54</u>, 281(1970).
- 65. J.-B. LePecq in "Methods of Biochemical Analysis," D. Glick, Ed., Wiley Interscience, New York, Vol. 20, pp. 42-86, 1971.

- 66. L. P. G. Wakelin and M. J. Waring, Mol. Pharm., 9, 544(1974).
- 67. T. R. Krugh, F. N. Wittlin, and S. P. Cramer, Biopolymers, 14, 197(1975).
- 68. T. R. Krugh and C. G. Reinhardt, <u>J. Mol. Biol.</u>, <u>97</u>, 133(1975).
- 69. G. P. Kreishman, S. I. Chan, and W. Bauer, <u>J. Mol.</u> Biol., 61, 45(1971).
- 70. G. M. Intille, Ph.D. Thesis, Syracuse University, Syracuse, New York, 1970.
- 71 D. A. Skoog and D. M. West, "Analytical Chemistry, An Introduction," Third Edition, Holt, Rhinehart, and Winston, Inc., New York, 1979, p. 438.
- 72. E. Volkin and W. E. Cohn in "Methods of Biochemical Analysis," D. Glick, Ed., Interscience, New York, 1954, p. 304.
- 73. J. L. Dye and V. A. Nicely, <u>J. Chem. Educ.</u>, <u>48</u>, 443(1971).
- 74. W. E. Wentworth, J. Chem. Educ., 42, 96(1965).
- 75. E. Mei, J. L. Dye, and A. I. Popov, <u>J. Am. Chem. Soc.</u>, <u>99</u>, 5308(1977).
- 76. J. F. Chantot and W. Guschlbauer, Jerusalem Symp. Quant. Chem. Biochem., 4, 205(1972).
- 77. G. C. Yee and S. I. Chan, <u>J. Am. Chem. Soc.</u>, <u>94</u>, 3218(1972).
- 78. M. Borzo, C. Detellier, P. Laszlo, and A. Paris, J. Am. Chem. Soc., 102, 1124 (1980).
- 79. M. Sundaralingam, Biopolymers, 7, 821(1969).
- 80. M. Sundaralingam, <u>Jerusalem Symp. Quant. Chem.</u> Biochem., 5, 417(1973).
- 81. M. Sundaralingam, <u>Int. J. Quant. Biol. Symp.</u>, <u>1</u>, 81 (1974).
- 82. C. Giessner-Prettre and B. Pullman, <u>Biochem. Biophys.</u> Res. Comm., 70, 578 (1976).

- 83. K. W. Jennette, S. J. Lippard, G. A. Vassiliades, and W. R. Bauer, Proc. Nat. Acad. Sci. USA, 71, 3839(1974).
- 84. M. J. Waring, Biochim. Biophys. Acta, 114, 234(1966).
- 85. F. J. Bullock and O. Jardetsky, <u>J. Org. Chem.</u>, <u>29</u>, 1988(1964).
- 86. R. Zana and C. Tondre, Biophys. Chem., 1, 367(1974).
- 87. P. Spegt and G. Weill, Biophys. Chem., 4, 143(1976).
- 88. P. C. Karenzi, B. Meurer, P. Spegt, and G. Weill, Biophys. Chem., 9, 181(1979).
- 89. G. S. Manning. Acc. Chem. Res., 12, 443(1979).
- 90. F. Basolo and R. G. Pearson, "Mechanisms of Inorganic Reactions, A Study of Metal Complexes in Solution," Second Edition, John Wiley and Sons, Inc., New York, 1967, pp. 34-35.
- 91. O. Kennard, N. W. Isaacs, W. D. S. Motherwell, J. C. Coppola, D. L. Wampler, A. C. Larson, and D. G. Watson, Proc. R. Soc. London Ser. A., 325, 401 (1971).
- 92. J. M. Roseberg, N. C. Seeman, R. O. Day, and A. Rich, J. Mol. Biol., 104, 145(1976).
- N. C. Seeman, J. M. Rosenberg, F. L. Suddath, J. J.
 P. Kim, and A. Rich, J. Mol. Biol., 104, 109(1976).
- 94. V. Swaminthan and M. Sundaralingam, Crit. Rev. Biochem., 6, 245(1979).
- 95. J. E. Huheey, "Inorganic Chemistry: Principles of Structure and Reactivity," Harper and Row, New York, 1972, p. 194.
- 96. A. Paris and P. Laszlo, Am. Chem. Soc. Symp. Ser., 34, 418(1976).
- 97. M. Borzo, C. Detellier, P. Laszlo, A. Paris, <u>J. Am.</u> <u>Chem. Soc.</u>, <u>102</u>, 1124(1980).
- 98. C. Detellier and P. Laszlo, <u>J. Am. Chem. Soc.</u>, <u>102</u>, 1135(1980).
- 99. L. R. Fisher and D. G. Oakenfull, Quart. Rev. Chem. Soc., 1977, 25(1977).

- 100. C. L. Fisk, personal communication.
- 101. D. E. Woessner, J. Chem. Phys., 37, 647(1962).
- 102. S. B. Zimmerman, G. H. Cohen, and D. R. Davies,
 J. Mol. Biol., 92, 181(1975).
- 103. S. Arnott, R. Chandrasekaran, and C. M. Marttila, Biochem. J., 141, 537(1974).
- 104. G. Gupta and V. Sasisekharan, Nucl. Acids Res., 5, 1639(1978).
- 105. A. Pullman and B. Pullman, <u>Adv. Quant. Chem.</u>, <u>4</u>, 267 (1968).
- 106. D. H. Turner, R. Yuan, G. W. Flynn, and N. Sutin, Biophys. Chem., 2, 385(1974).